

THE NONLINEAR TRANSIENT RESPONSE
OF THIN RECTANGULAR PLATES

By

GANESH RAJAGOPAL
"

Bachelor of Technology
Indian Institute of Technology
Madras, India
1964

Master of Engineering
Indian Institute of Science
Bangalore, India
1966

Submitted to the Faculty of the
Graduate College of the
Oklahoma State University
in partial fulfillment of
the requirements of
the Degree of
DOCTOR OF PHILOSOPHY
July 1972

AUG 16 1973

THE NONLINEAR TRANSIENT RESPONSE
OF THIN RECTANGULAR PLATES

Thesis Approved:

R. L. Lowery

Thesis Adviser

A. H. Jami

Ronald E. Boyd

W. P. Dawkins

N. Hurham

Dean of the Graduate College

ACKNOWLEDGMENTS

During the course of this study, I received guidance, help and encouragement from many persons and organizations, and I thank them all. To some I owe a special word of gratitude.

I am indebted to Dr. R. L. Lowery, my thesis adviser, for his able counsel and understanding which made this study possible. It has been a rewarding experience to have taken part in his research and teaching programs.

My thanks to Drs. D. E. Boyd, W. B. Brooks, W. P. Dawkins, and A. H. Soni for serving on my doctoral committee and for editing this thesis.

The author received financial assistance from Oklahoma State University and NASA, Langley Research Center (NGR-37-002-051), during the course of this work. The Watumull Foundation provided a grant for the preparation of this thesis. My thanks to them for their support.

The very thin glass plates used in this study were generously supplied by the Lustron Corporation, a subsidiary of ASG Industries Inc.

As a graduate student, I have done a good amount of learning from my colleagues in the laboratory. My thanks are due to Jack

Bayles, Curtis Ikard, Stan Taylor, and Bob Maffeo for their many hours of advice and assistance during this study and to Grady Cook, Bill Smith, C. P. Rao and B. N. Murali for the many useful and stimulating discussions I have had with them.

I am especially grateful to my parents and my sister for their faith and encouragement.

My thanks to Mr. Eldon Hardy for his drafting and to Mrs. Judy Lambert for typing the manuscript.

TABLE OF CONTENTS

Chapter	Page
I. INTRODUCTION	1
II. LITERATURE REVIEW	4
Large Deflections of Plates	4
Dynamic Loading of Plates	7
Whole Field Experimental Techniques	7
Window-Room-Door Response	9
III. EXPERIMENTAL METHOD	10
The Plate	10
The Pressure Load	12
Moiré Method of Determining Whole Field Response	18
Pressure, Deflection and Strain Measurements	23
Simulation of a Window-Room-Door System . . .	24
IV. THEORETICAL SOLUTION	26
Finite-Difference Method	26
Lumped Parameter Solution	29
V. EXPERIMENTAL RESULTS	34
Moiré Fringe Data	34
Strain Data	43
Deflection Response	57
Window-Room-Door Simulation	57
VI. SUMMARY, CONCLUSIONS AND RECOMMENDATIONS	65

Chapter	Page
BIBLIOGRAPHY	72
APPENDIX A	75
APPENDIX B	90
APPENDIX C	95

LIST OF TABLES

Table	Page
I. Maximum Pulse Pressure as a Function of of Tank Pressure	15

LIST OF FIGURES

Figure	Page
1. Layout of Equipment Used in Tests	11
2. Details of Plate Support and Location of Pickups	13
3. Pulse Generator	14
4. Operating Principle of Pulse Generator	16
5. Pressures at the Center and 1 in. From the Corner on a 3/4 in. Plywood Plate (1 cm = 0.005 sec.)	17
6. Pressure at the Surface of Thin Glass Plate (1 cm. = 0.005 sec.)	17
7. Principle of Moiré Method	19
8. Model of Window-Room-Door System	25
9. Moiré Fringes in the y Direction of a Rectangular Plate Subjected to Static Pressure	35
10. Moiré Fringes in the x Direction of a Rectangular Plate Subjected to Static Pressure	35
11. Static and Dynamic Deflection Profiles of the y Center- line of the Plate by Moiré and Finite-Difference Methods	36
12. Static and Dynamic Deflection Profiles of the x Center- line of the Plate by Moiré and Finite-Difference Methods	37
13. Moiré Fringes in y Direction at 0.0025 sec.	39
14. Moiré Fringes in x Direction at 0.0025 sec.	39

Figure	Page
15. Moiré Fringes in x Direction at 0.0040 sec.	40
16. Moiré Fringes in x Direction at 0.0044 sec.	40
17. Moiré Fringes in y Direction at 0.0094 sec.	41
18. Moiré Fringes in x Direction at 0.0094 sec.	41
19. Moiré Fringes in y Direction at 0.010 sec.	42
20. Moiré Fringes in x Direction at 0.010 sec.	42
21. Deflected Surface of Plate at 0.0025 sec.	44
22. Deflected Surface of Plate at 0.0040 sec.	45
23. Oscilloscope Traces for Response Corresponding to Max. Center Displacement to Thickness Ratio of 5.6 (1 cm. = 0.002 sec.)	46
24. Oscilloscope Traces for Response Corresponding to Max. Center Displacement to Thickness Ratio of 2.6 (1 cm. = 0.002 sec.)	46
25. Strain at the Center of the Front Surface in the y Direction for Max. Displacement to Thickness Ratio of 5.6	47
26. Strain at the Center of the Front Surface in the y Direction for Max. Displacement to Thickness Ratio of 5.6 (Galerkin model, M = N = 3, J = K = 4)	47
27. Strain at the Center of the Front Surface in the y Direction for Max. Displacement to Thickness Ratio of 2.6	48
28. Strain at the Center of the Front Surface in the y Direction for Max. Displacement to Thickness Ratio of 2.6 (Galerkin model, M = N = 3, J = K = 4)	48

Figure	Page
29. Strain at the Center of the Front Surface in the y Direction for Max. Displacement to Thickness Ratio of 0.85	49
30. Strain at the Center of the Front Surface in the y Direction for Max. Displacement to Thickness Ratio of 0.85 (Galerkin model, $M = N = 3$, $J = K = 4$)	49
31. Strain at the Center of the Back Surface in the x Direction for Max. Displacement to Thickness Ratio of 5.6	51
32. Strain at the Center of the Back Surface in the x Direction for Max. Displacement to Thickness Ratio of 5.6 (Galerkin model, $M = N = 3$, $J = K = 4$)	51
33. Strain at the Quarter Diagonal Point of the Back Surface in the x Direction for Max. Displacement to Thickness Ratio of 5.6	52
34. Strain at the Quarter Diagonal Point of the Back Surface in the x Direction for Max. Displacement to Thickness Ratio of 5.6 (Galerkin model, $M = N = 3$, $J = K = 4$)	52
35. Strain at the Quarter Diagonal Point of the Back Surface in the y Direction for Max. Displacement to Thickness Ratio of 5.6	53
36. Strain at the Quarter Diagonal Point of the Back Surface in the y Direction for Max. Displacement to Thickness Ratio of 5.6 (Galerkin model, $M = N = 3$, $J = K = 4$)	53
37. Total Strain in the y Direction on the Front Surface of the Plate at 0.0065 sec.	54
38. Plate Center Displacement for Maximum Displacement to Thickness Ratio of 5.6	58

Figure	Page
39. Plate Center Displacement for Maximum Displacement to Thickness Ratio of 5.6 (Galerkin model, $M = N = 3$, $J = K = 4$)	58
40. Plate Center Displacement for Maximum Displacement to Thickness Ratio of 2.6	59
41. Plate Center Displacement for Maximum Displacement to Thickness Ratio of 2.6 (Galerkin model, $M = N = 3$, $J = K = 4$)	59
42. Plate Center Displacement for Maximum Displacement to Thickness Ratio of 0.85	60
43. Plate Center Displacement for Maximum Displacement to Thickness Ratio of 0.85 (Galerkin model, $M = N = 3$, $J = K = 4$)	60
44. Oscilloscope Traces of Test on Window-Room-Door Model With Small Room (1 cm = 0.005 sec.)	62
45. Oscilloscope Traces of Test on Window-Room-Door Model With Large Room (1 cm = 0.005 sec.)	62
46. Strain in y Direction at Center of Front Surface of Plate in Window-Room-Door System (Small Room, Volume = 1.8 cu.ft.)	63
47. Strain in y Direction at Center of Front Surface of Plate in Window-Room-Door System (Large Room, Volume = 3.66 cu.ft.)	63
48. Plate Center Displacement for Window-Room-Door Model With Small Room	64
49. Plate Center Displacement for Window-Room-Door Model With Large Room	64

CHAPTER I

INTRODUCTION

Large amplitude vibrations in plates occur in practice in large glass windows, in skin panels of aircraft, in flexible roof structures, and in the walls of containers and cartons of various types. The present study is mainly concerned with the response of large glass windows to pressure pulses such as sonic booms. During the last seven years there have been several studies made at Oklahoma State University, on various aspects of structural response to the sonic boom. The latest study dealt with a finite-difference solution to the nonlinear Von Kármán plate equations for the transient response of thin, rectangular, elastic plates with various boundary conditions. There are no known exact solutions to the Von Kármán equations with which the finite-difference solutions may be compared. A major purpose of the experiments described in this report was to compare the experimentally observed response with that predicted by the finite-difference solution. Thin glass plates with simply supported edges were used to model the response of large glass windows. A plate is generally considered to be loaded into its nonlinear range when its center deflection exceeds half the plate thickness. The maximum

center deflection recorded during the present tests was of the order of five and a half times the plate thickness.

The response of a continuous structure like a plate should ideally be measured over its entire surface. The reflected Moiré technique was applied to measure the deflection of the plate over its whole area at several instants during its transient response. A continuous record of the surface strains and the deflection at the center was also obtained experimentally.

In some of the previous studies on the linear response of glass windows, it has been pointed out that the response of a window set in a room with an open door can be larger than that of a glass window alone. This important practical case was simulated experimentally by coupling a thin glass plate to a Helmholtz resonator and subjecting it to pressure pulses such that large amplitudes were excited. The finite-difference program was suitably modified to accommodate this type of loading.

Another objective of this study was to compare the measured response of thin plates with the response predicted by lumped-parameter models for the plate. Lumped-parameter models are described by ordinary differential equations which are generally less costly to integrate than partial differential equations. In this report several models for the plate derived by Galerkin's method and involving both single and multiple plate modes are compared with

the experimental data and the finite-difference results. The single mode model is also applied to the case of a plate coupled to a Helmholtz resonator. In the determination of the critical response of such systems, the finite-difference solution is prohibitively costly and the use of a reasonably accurate single mode model is necessary.

The objectives of this study are as follows:

- (1) To design and construct apparatus to subject thin, simply supported elastic plates to pressure pulses such that large amplitudes result.
- (2) To develop an experimental technique for obtaining the dynamic response of a plate over its whole surface.
- (3) To compare the experimentally observed plate response with the theoretical response predicted by the finite-difference solution of the Von Kármán equations.
- (4) To compare the experimental response with the theoretical nonlinear response obtained from lumped parameter models.
- (5) To determine, experimentally, the transient response of a plate coupled to a Helmholtz resonator and compare the results with the theoretical response predicted by finite-difference and lumped parameter solutions.

CHAPTER II

LITERATURE REVIEW

The scope of the present study indicated that a literature survey in the following areas was required: (1) theoretical and experimental work on plates undergoing large deflections with special reference to dynamic response studies, (2) experimental methods of subjecting plates to transient pressure pulses, (3) whole field, experimental techniques for determining the dynamic response of plates, (4) dynamics of mechano-acoustical systems with special reference to window-room-door interactions.

Large Deflections of Plates

The equations most commonly used to describe the large deflections of thin, elastic plates were derived by Th. Von Kármán (1) in 1910 and are named after him. The maximum relative deflection for which these equations are valid has not been established. Tadjbakhsh and Saibel (2) have derived a more general set of equations for a thin plate which include the effect of rotatory and in-plane inertias and transverse shear. However, no solution is available for these equations.

R. L. Penning (3) has reviewed the theoretical and experimental work done up to 1970 on the static, large deflection behavior of plates. The theoretical methods used to solve the nonlinear partial differential equations fall under the general categories of finite-difference methods, perturbation, finite elements and Fourier series solutions. The experimental methods generally made use of deflection transducers for point by point deflection measurements and standard strain gages.

The pertinent literature on the large deflection dynamic response of plates has been reviewed by D. J. Bayles (4) for the period up to 1969. The theoretical solutions up to that time were based on a lumped-parameter representation of the plate which was derived by various approximate methods and which was based on assuming that the plate deflected in its fundamental, linear mode shape. Bayles solves the Von Kármán equations by the finite-difference method for rectangular plates with different types of boundary conditions and compared his results with those obtained from lumped-parameter models derived by Yamaki (5). He found that the lumped-parameter model and the finite-difference solution were in good agreement at relatively small nonlinear deflections but differed considerably from each other at larger deflections. The finite-difference solution appears to be the most accurate theoretical solution that is available at present.

Since 1969 several papers have appeared that deal with the dynamics of plates undergoing large deflections. Ventres and

Dowell (6) used Galerkin's method on the Von Kármán equations to study the nonlinear flutter of clamped rectangular plates subjected to a static pressure differential. For the case of zero in-plane edge restraint, they assumed a series of functions for the deflection and for the stress function and reduced Von Kármán's equations to a set of ordinary differential equations. The assumed functions satisfied all the boundary conditions. They obtained good correlation between experimental and theoretical flutter boundaries for plates exposed to a static pressure differential. It was found that four to six modes must be used in the modal expansion for the deflection to obtain accurate results. A similar approach has been taken by Farnsworth and Evan-Iwanowski (7) in determining the resonance response of nonlinear circular plates subjected to a uniform static load. Bennett (8) has recently extended this method to the study of nonlinear vibration of simply supported, angle ply, laminated plates. It is apparent, from a study of the literature, that Galerkin's method is widely used in solving nonlinear plate vibration problems. This approach has not yet been applied to transient response problems. A comparison of the solutions obtained by Galerkin's method with finite-difference solutions should yield some insight into their relative accuracies, ease of application, and cost.

Dynamic Loading of Plates

Edge and Hubbard (9) have recently reviewed various sonic-boom simulation methods. Most of the methods described by them are specifically for generating a sonic boom type of pressure signal. One of the devices, described by Tombouliau (10), permits a wide variety of pulse shapes to be generated in a diverging tube. The test objects are placed directly inside the diverging tube, or, as in the case of glass panels, on one of the walls of the tube. The reflections from the end of the tube were reduced by means of a special absorber. Some of the basic features of Tombouliau's design have been incorporated in the pulse generator used in the present study.

Whole Field Experimental Techniques

Since a plate is a continuous structure, an adequate experimental measurement of the plate response should ideally yield continuous data on a significant variable over the whole surface of the plate. A brief review of the methods reported in the literature for determining whole field response of plates is next given.

Photoelastic methods for plates have been studied by Goodier (11), Mindlin (12), Drucker (13) and Bednar (14). The methods suggested involve either bonding of two birefringent materials of different stress optic coefficients, or initially freezing a direct stress in the plate, or sandwiching a reflecting aluminum foil between two sheets of

birefringent material. These methods have not been applied to vibrating thin plates.

Several Moiré grid methods have been developed for measuring plate deflections. Ligtenberg (15) has described a method in which the reflection on the plate surface, of a coarse grid of straight lines is photographed and contours of equal partial slope are obtained by superposing the images of the grid before and after loading the plate. This method has been applied by Nickola (16) to determine the dynamic response of thin membranes. A Moiré grid method, using finer grids, in which the shadow of a reference grid on the deflected surface of the plate interferes with the reference grid to produce fringes which directly indicate the deflection contours of the plate has been applied by Hazell (17) to vibrating plates. Some other techniques are described in the books on the Moiré method written by Theocaris (18) and Durelli and Parks (19).

Photogrammetric methods have been used by Merchant et al (20) to measure the dynamic displacements of plates. Holographic techniques were applied, for the first time, to obtain the deflection contours in steady state vibration by Powell and Stetson (21). Since then there have been several papers on this method. For the case of transient motion, pulsed lasers have been used. The principal disadvantage of the holographic method, in the context of the present study, is that its application is limited to very small motions (of the order of microinches).

For the experiments described in this report, the Moiré grid method used by Nickola (16) was chosen because it was simple, applicable to large deflections, required nothing in close proximity to the plate (so that the pressure field near the plate was not affected), and it did not require a perfectly flat plate.

Window-Room-Door Response

Previous studies at Oklahoma State University (22, 23) have indicated that the maximum center deflection of a window subjected to a N wave type of pressure pulse is larger when it is coupled to a room and an open doorway than when it is by itself. This is the case whether the deflections are in the linear or in the nonlinear range. In the analysis of such coupled systems, it is essential that the simplest analytical models be used to represent the distributed physical systems. Not much experimental work has been done in this area to verify the validity of the models used. Clarkson and Mayes (24) have recently reviewed the literature on building structure response to sonic booms. Usually windows are coupled to other windows and to several rooms and doorways. It was decided to confine the present study to the case of one window coupled to a room and an open doorway.

CHAPTER III

EXPERIMENTAL METHOD

Figure 1 shows the general layout of the equipment used in the tests. A pressure pulse was produced at the pulse generator, sent down the plane wave tube and reflected off the simply supported glass plate mounted at the other end of the tube. The plate was instrumented to record the Moiré pattern of the deflected plate, strains at the surface of the plate, center deflection and pressure acting on the surface of the plate. Details regarding each of the elements in the test are given below.

The Plate

The plate used in the experiments had the following properties and dimensions:

Size	14 in. x 9.35 in.	$\pm 1/32$ in.
Thickness	0.037 \pm 0.001 in.	
Material	Glass plate*	
Modulus of elasticity	9.0×10^6	$\pm 0.2 \times 10^6$ psi

*Supplied by the American Saint Gobain Corp., Kingsport, Tennessee.

OVERALL VIEW OF PLANE WAVE TUBE

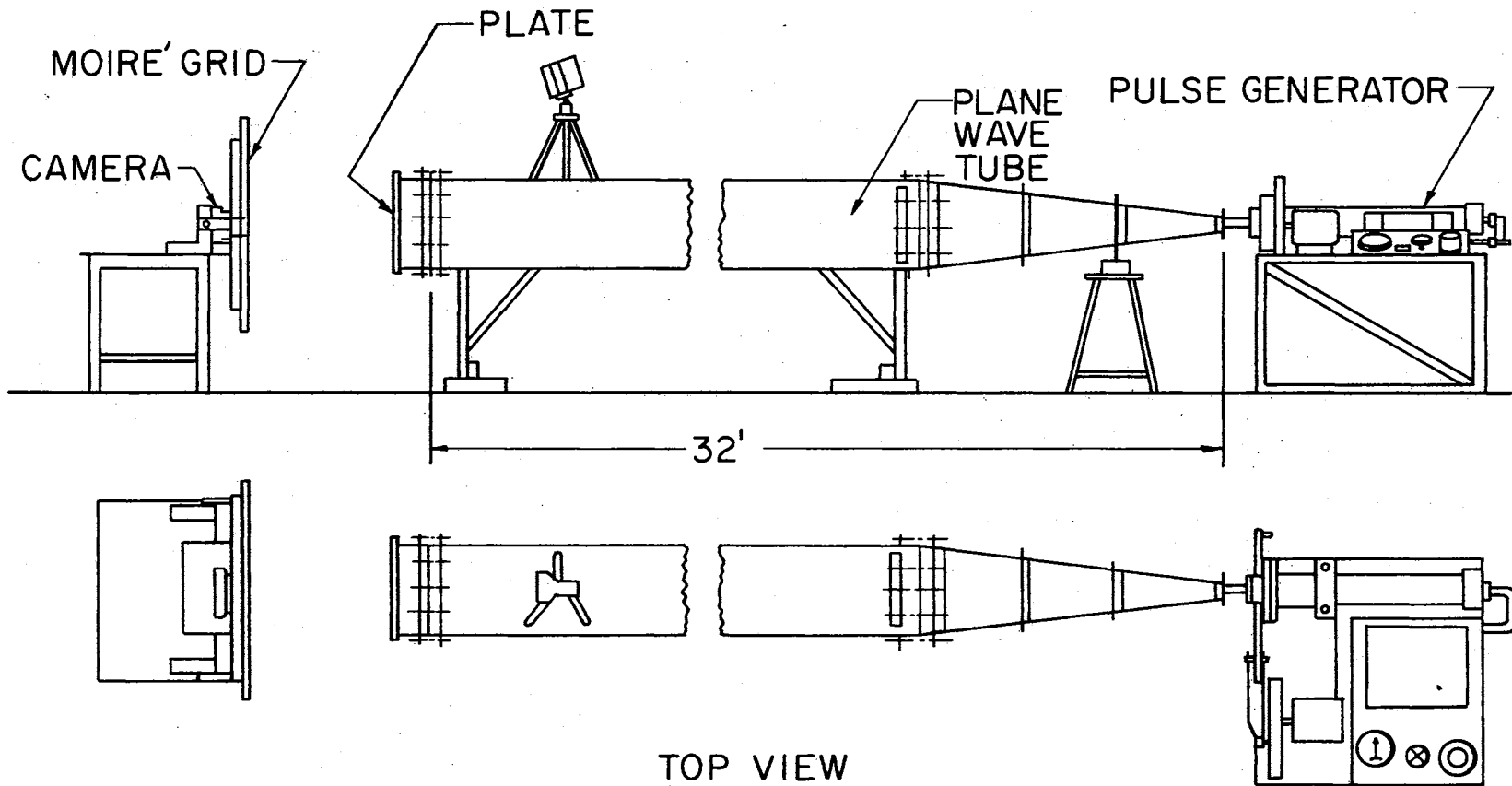


Figure 1. Layout of Equipment Used in Tests

Poisson's ratio	0.220	± 0.004
Density	153.0	± 0.5 lbm/cu ft

The plate was mounted in an aluminum box whose supporting edges had been beveled to approximate a simply supported boundary condition. (Figure 2) The box was designed to accommodate various sizes of plates ranging from a maximum size of 14 in. x 14 in. to 14 in. x 7 in.

The Pressure Load

The plate was subjected to an uniform, transient pressure load which approximated an N wave. The actual shape of the load was not critical for the tests so long as it was accurately known for use as input for the theoretical methods. However, a pulse with its fundamental frequency component close to that of the plate was desirable so that larger plate deflections could be excited for a given amplitude of the pressure pulse.

The pressure load was produced by a pulse generator based on a basic design due to Tombouljian (10). Figure 3 gives some details of the pulse generator. This is based on the principle that the pressure at a given radius from an ideal compressible fluid flow source is proportional to the rate of change of the mass rate of fluid flow. In the pulse generator, the mass rate of flow is controlled by varying the exit area of a converging nozzle through which choked

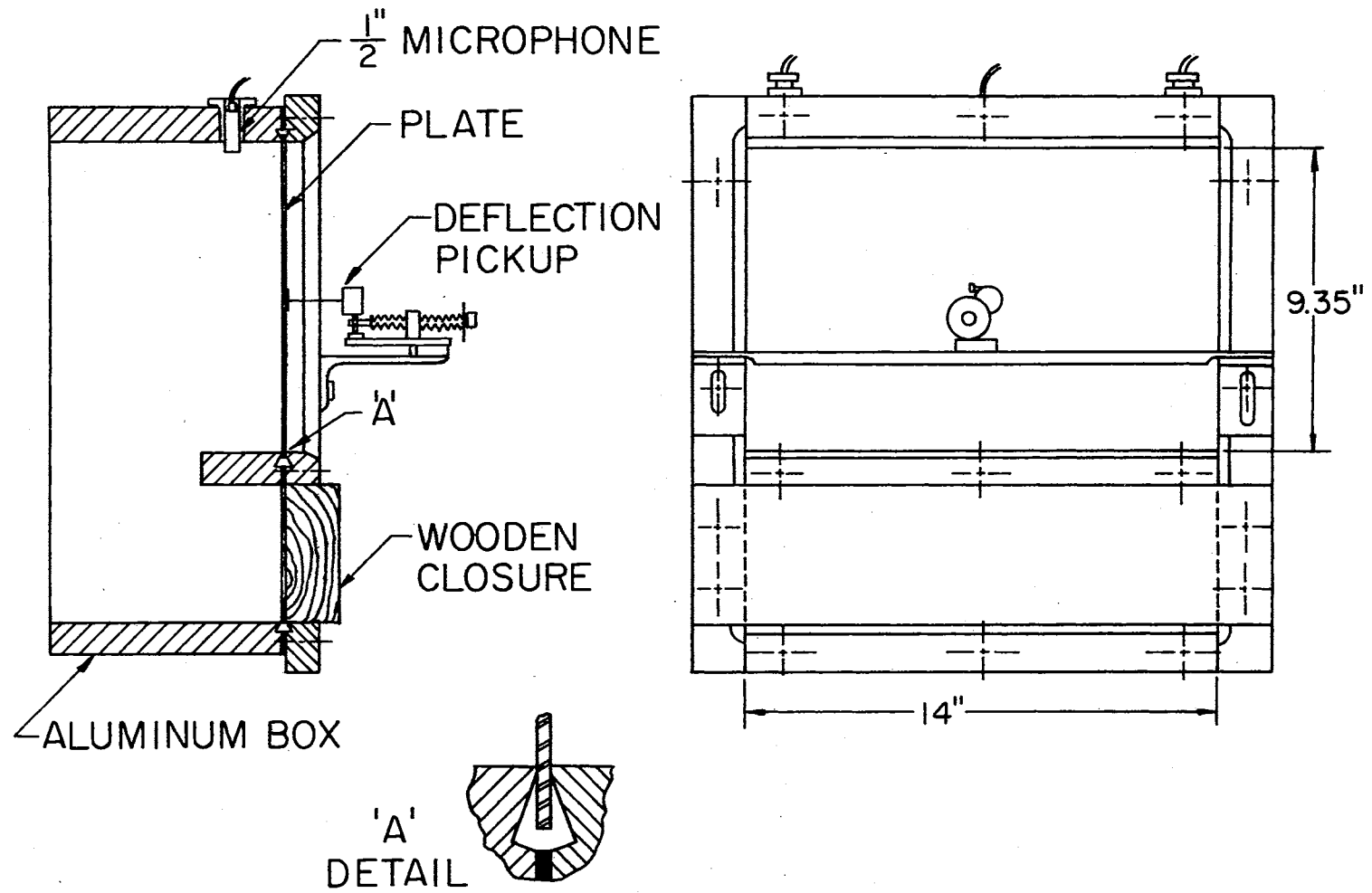


Figure 2. Details of Plate Support and Location of Pickups

PULSE GENERATOR

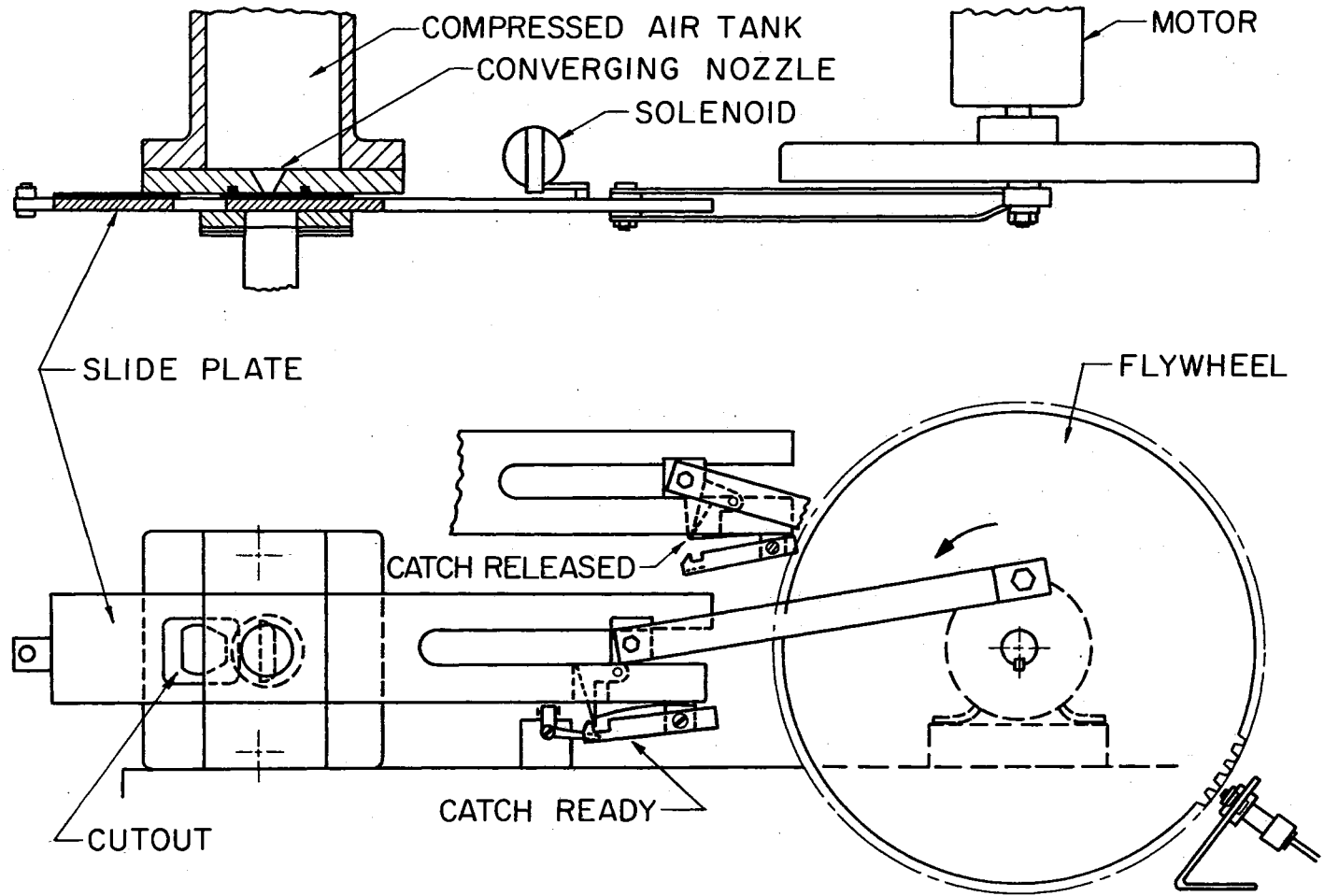


Figure 3. Pulse Generator

flow is taking place. The exit area is varied by pulling a sliding orifice plate across a fixed orifice. A slider crank mechanism is used to pull the sliding orifice plate at approximately constant velocity. The orifice in the sliding plate was shaped to nominally produce an N wave. In Figure 4, the idealized variation of nozzle exit area (and hence, mass rate of flow) with time and the corresponding variation of pressure with time are shown. Figure 5 shows the pressures measured using B & K 1/4 in. microphones at two different points at the surface of a 3/4 in. plywood plate at the end of the plane wave tube. The pressure measured using a Photocon 514-3997 microphone with the thin plate in position is shown in Figure 6. The maximum pulse pressure was varied both by using different sliding orifice plates and by varying the tank pressure. The possible variation in pressures is shown in Table I for one sliding orifice plate. The pulse duration is varied by changing the speed of the motor driving the slider mechanism.

TABLE I

MAXIMUM PULSE PRESSURE AS A
FUNCTION OF TANK PRESSURE

<u>Tank Pressure [psig]</u>	<u>Max. Pulse Pressure [psf]</u>
20.0	18.0
30.0	30.0
40.0	36.0
60.0	45.0
80.0	54.0

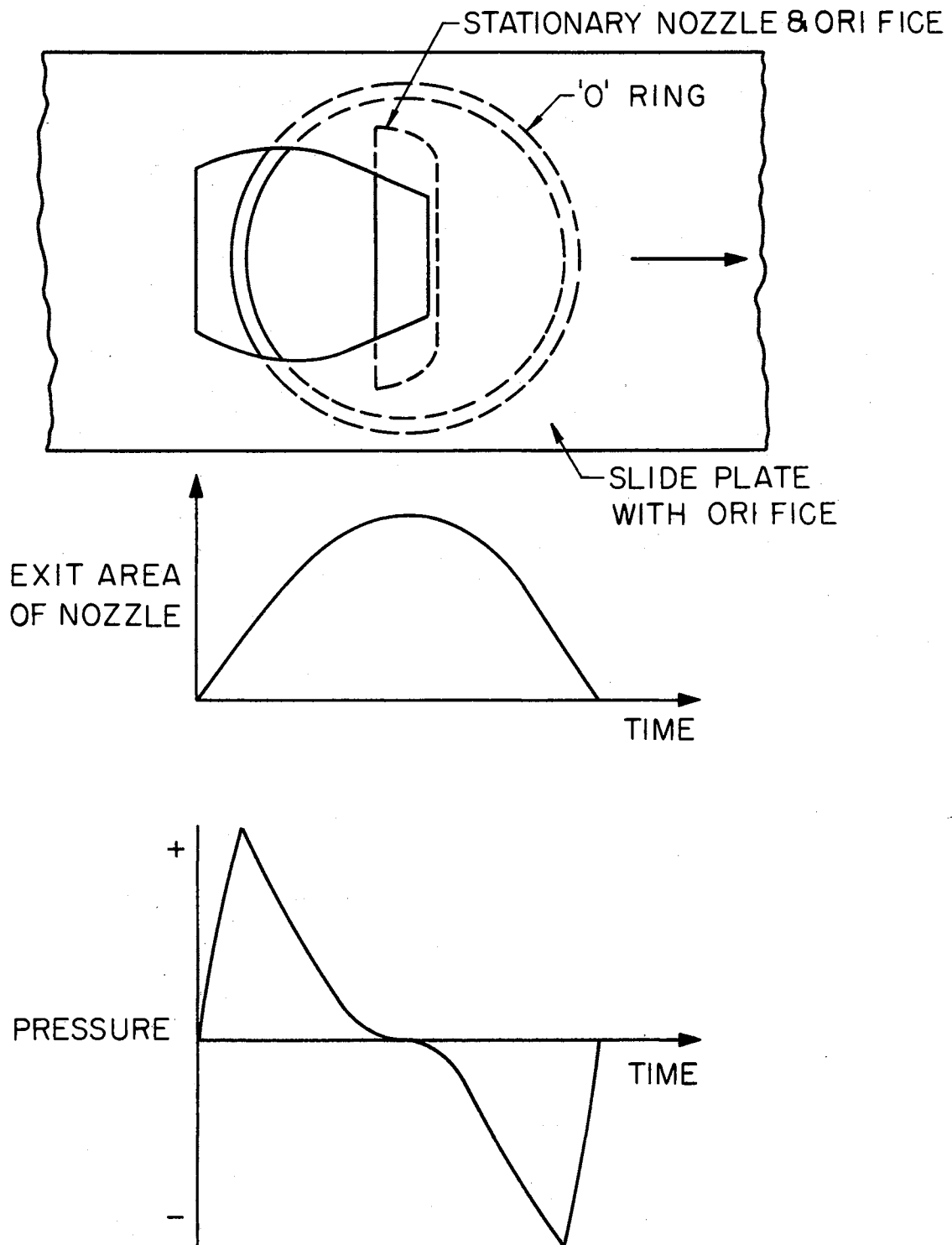


Figure 4. Operating Principle of Pulse Generator

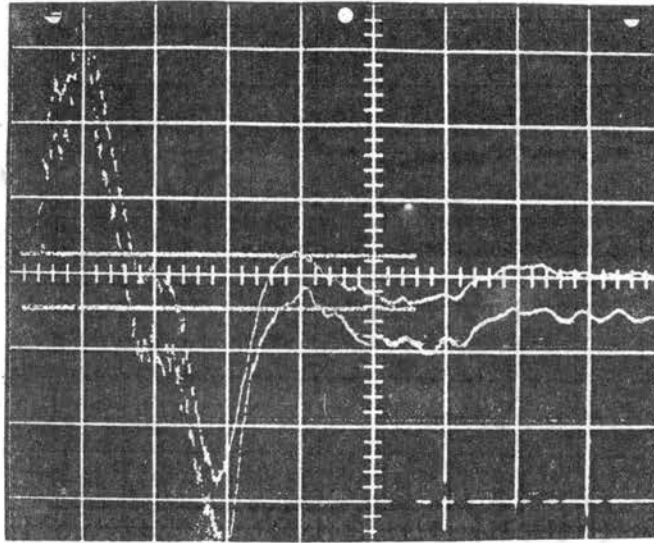


Figure 5. Pressures at the Center and
1 in. From the Corner on
a 3/4 in. Plywood Plate
(1 cm. = 0.005 sec.)

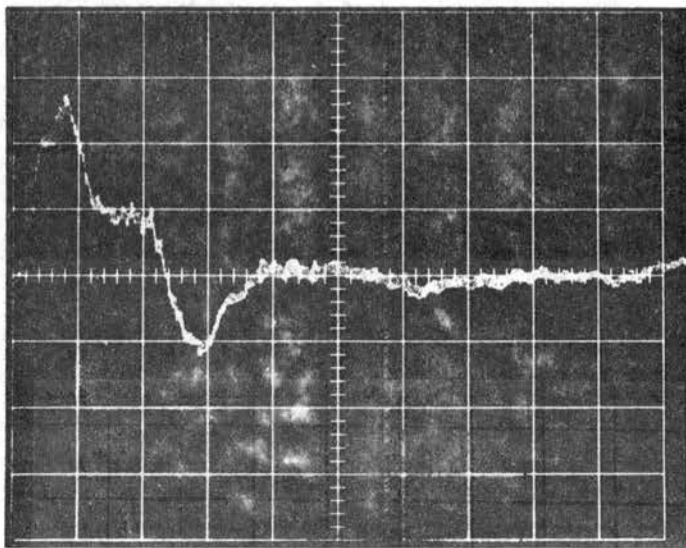


Figure 6. Pressure at the Surface of Thin
Glass Plate (1 cm. =
0.005 sec.)

A pulse effect is created by mounting the plate to be tested at one end of a 32 ft. long, 14 in. x 14 in. square, plane wave tube and, the pulse generator, at the other end. The plate thus experiences a single pulse and then almost no pressure during the time the pulse takes to retrace its path. The uniformity of the pressure pulse was checked and the variation of the pressure between different points on the surface of the plate was less than 7%.

Moiré Method of Determining Whole Field Response

The arrangement for the reflected Moiré method used in the tests described here is shown in Figures 1 and 7. It consists of a plane grid of alternate black and white lines of equal width in front of the plate under test and a 35 mm. camera facing the plate. One side of the plate is silvered so that the camera sees the reflection of the plane grid on the surface of the plate. The fringe patterns were obtained by taking one exposure of the reflected grid with the plate undeflected and then taking a second exposure at a specific deflection of the plate during its response to the pressure pulse. The second exposure was controlled by small, flexible contacts at the center of the plate. Distinct black and white fringes are formed on the film in the camera wherever black and white lines during the second exposure are superposed on black and white lines from the first exposure. To

PRINCIPLE OF METHOD

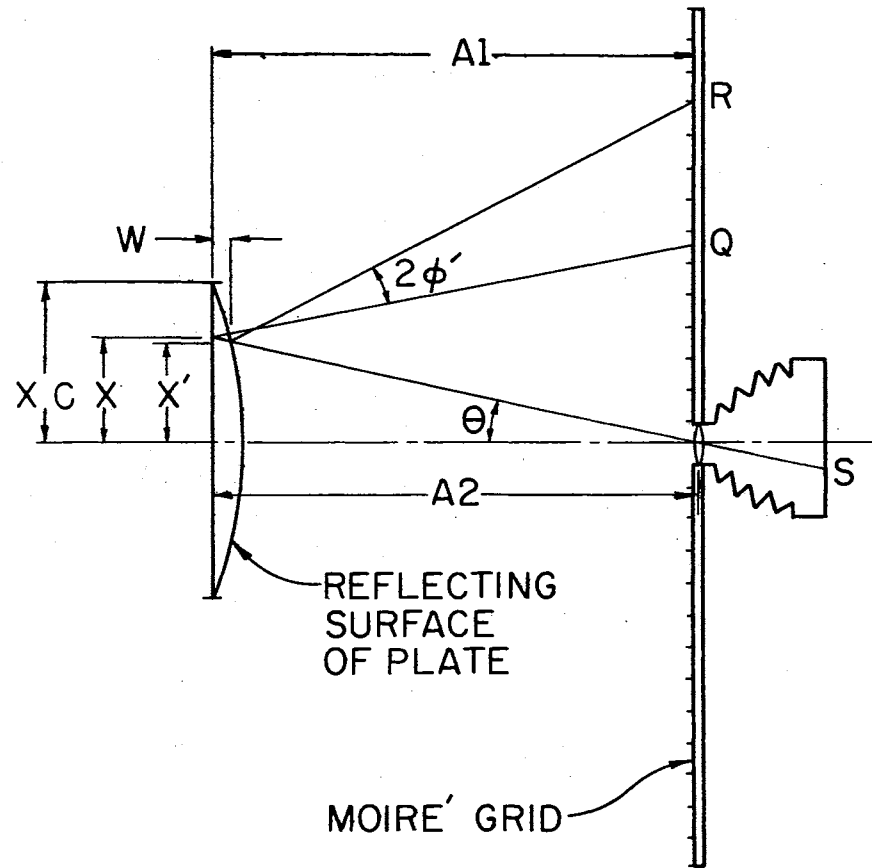


Figure 7. Principle of Moiré Method

a first approximation, the fringes obtained by this method represent lines of constant partial slope with respect to a chosen direction on the plate. For example, this direction can be either along the x or y reference axis for the plate depending on whether the grid lines are perpendicular to the x or y axis.

The relationship between plate deflection, slope and fringe order are derived next. In Figure 7, let S be a particular point on the film in the camera. With the plate in its undeflected state, the image of a point Q on the plane grid is formed at the point S. When the plate deflects, and the film is exposed a second time, the image of a point R on the plane grid is formed at the same point S on the film. A distinct fringe occurs at the point S when the distance RQ on the grid is an integral multiple of the pitch of the grid. Thus the fringe order N may be obtained from

$$N = \frac{QR}{P} \quad (1)$$

where P is the pitch of the grid. From Figure 7,

$$\begin{aligned} QR &= OR - OQ \\ &= X' + (A1 - W(X')) \tan(\theta + 2\phi') - (X + A1 \tan \theta) \end{aligned} \quad (2)$$

where ϕ' is the slope $\partial W / \partial X$ at X' and $W(X')$ is the deflection of the plate at X' .

The other symbols are defined in Figure 7. In order to get a tractable expression for QR, the following approximations are made. $W(X')$ is neglected in comparison with A1, ϕ' is taken to be the same

as ϕ which is the slope of the plate at the point X. Also, 2ϕ is assumed to be sufficiently small to allow the approximation,

$$\tan 2\phi \approx 2\phi \quad (3)$$

It may also be noted from Figure 7 that

$$\tan \theta = X/A2 \quad (4)$$

The fringe order N is then given by

$$N = \frac{1}{P} \left[2A1 \phi \frac{\left(1 + \frac{X^2}{A2^2}\right)}{\left(1 - \frac{X}{A2} 2\phi\right)} \right] \quad (5)$$

This equation may be solved for ϕ as a function of N and X.

$$\phi = \frac{\partial W}{\partial X} = \frac{N}{(2 A1/P) + 2 A1(X/A2)^2 + 2XN/A2} \quad (6)$$

In order to get the deflection of the plate surface, equation (6) is integrated numerically when the fringe order is known as a function of X. The starting point for the integration is taken at the edge of the plate where the deflection is known to be zero. The relation between N and ϕ may be linearized by dropping the nonlinear terms, $X/A2$ and $2X\phi/A2$, from Equation (5). For $(X/A2)$ equal to 0.25 the linearized equation gives a slope ϕ that is about 6% larger than the actual value. The data presented in this study were all obtained by integrating the complete Equation (6).

The reflected Moiré method gives information only on the deflection of the plate, W, and its derivatives. One of the main considerations in design is the stress distribution in the structure. The

second spatial derivatives of W may be used to determine the bending moments and, hence, the bending stresses. However, in a large deflection problem, membrane stresses are also present and the maximum stresses have to be determined by adding the membrane and bending stresses. The reflected Moiré method does not yield any information on the in-plane deformations of the center plane of the plate. Except for the case of bonded plates, the center plane is inaccessible. One possible approach to this problem is to use the standard Moiré method for determining surface strains to determine the strains on the two faces of the plate. This method has been applied by Durelli (19) to statically loaded plates. A 1000 lines/in. grating was printed on the surface of a plexiglass plate. The master grating of 1000 lines/in. was placed in contact with the printed surface of the plate using a thin layer of paraffin oil between the two surfaces to ensure uniform contact. This method, as described above, is not suitable for dynamic studies because of the added mass of the master grating and the shear layer of paraffin oil. If it is possible to make a double exposure of the printed grating on the plate surface, this method can be used in conjunction with the reflected Moiré technique to determine the complete state of strain in the plate at large deformations.

The pitch of the grid used in this study was 0.0960 in. with a standard deviation of 0.0023 in. The distances A_1 and A_2 were 30.0 in. and 31.5 in. respectively. The grid was illuminated by a

single Chadwick-Helmuth Strobex strobe light with an approximate flash duration of 50 micro sec. The strobe was placed at a distance of 6 ft. from the grid. The film used was Kodak Tri-X. The 35 mm. camera was set at f8. The exact instant at which the second exposure of the film occurred was recorded on the storage oscilloscope by means of a photocell. A modified Brashear process was used to silver one side of the thin glass plates. The silver coating added an average value of 0.25 lbm/cu. ft. to the density of the glass plate and thus was negligibly small.

Pressure, Deflection and Strain Measurements

The pressure at the surface of the plate was measured by a Dynasciences Photocon 514-3996 microphone. It was calibrated before tests by means of a piston phone over a frequency range of 3 to 30 Hz and at an amplitude of 23.7 psf. The output at 3 Hz was 3% below that at 30 Hz.

The deflection of the center of the plate was measured by a DCDT with flat response from DC to a first order corner frequency of 170 Hz. Its output was not entirely linear at the maximum plate amplitudes. The DCDT was calibrated before and after each test by means of a micrometer attachment. The DCDT data was corrected for both its nonlinearity and lack of high frequency response by

computational methods. The DCDT core assembly attached to the plate weighed 3.5 gms. Tests run with and without the DCDT affixed to the plate showed no significant difference either in the period or in the amplitude of strain at the center of the plate.

The strains were measured on the front and back surfaces of the plate in the x and y directions at the center of the plate and at a point on the diagonal midway between the center and the corner. Standard foil gages were used with Ellis BAM-1 strain meters. All data were recorded on a Tektronix 564 storage oscilloscope with four channels. The scope traces were photographed and then enlarged for data processing.

Simulation of a Window-Room-Door System

The response of a window set in a room with an open doorway subjected to a pressure pulse was simulated experimentally by means of the arrangement shown in Figure 8. This is basically the same arrangement as for the plate tests except that a rigid wooden box has been added to form a "room" and the wooden closure in Figure 2 has been removed to form a "door." Two room sizes were used in the tests. The test arrangement is such that the same pressure acts on both the plate and on the open door. The physical parameters of this system are given below:

Room sizes:	1.80 cu. ft. and 3.66 cu. ft.
Area of door:	0.357 sq. ft.
Length of door:	0.25 ft.

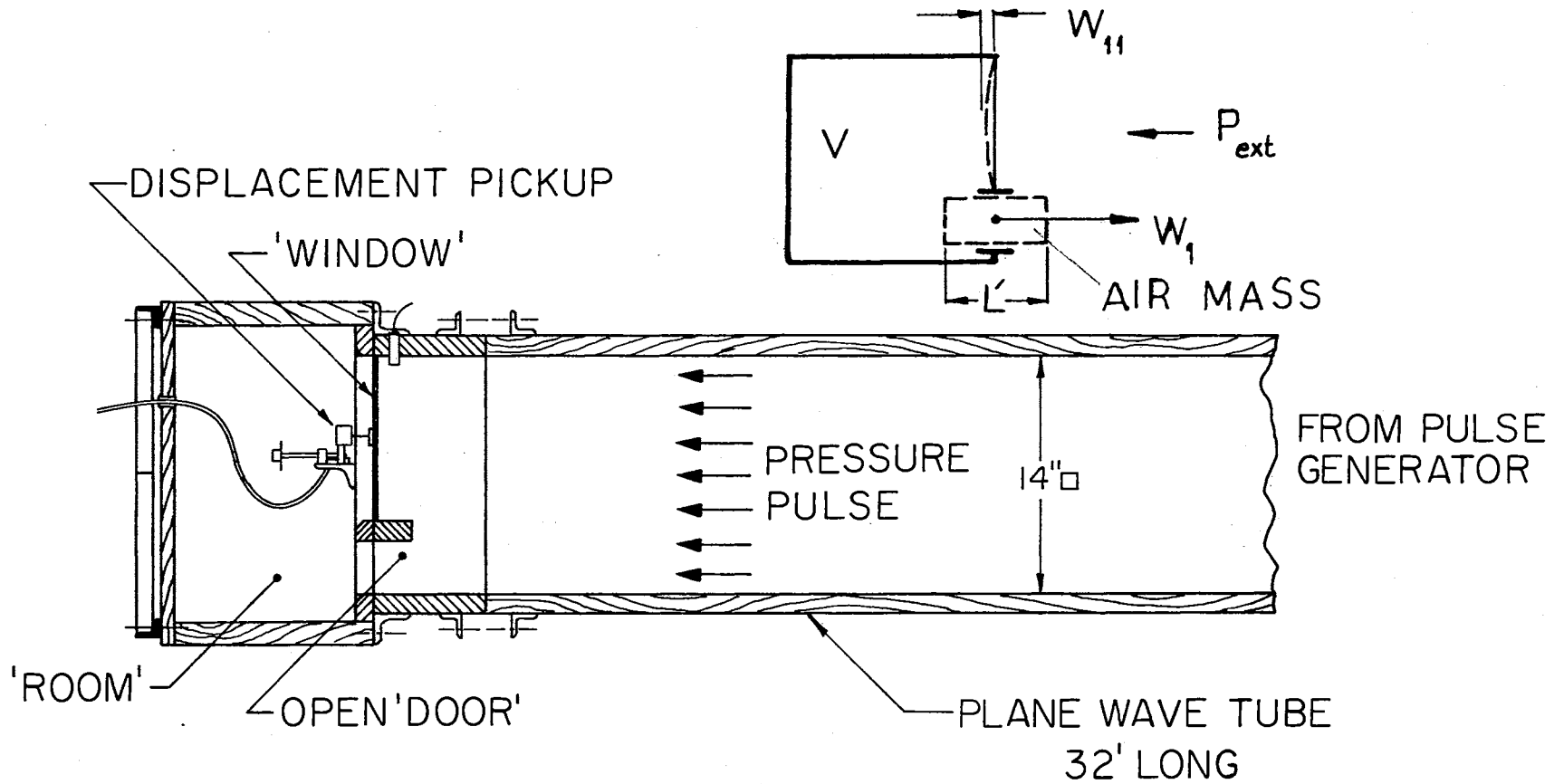


Figure 8. Model of Window-Room-Door System

CHAPTER IV

THEORETICAL SOLUTION

Finite-Difference Method

The observed experimental data is compared with solutions to the Von Kármán plate equations which describe large deflection response of elastic, isotropic, thin plates. These equations are of the form:

$$\nabla^4 F = E[W_{,xy}^2 - W_{,xx} W_{,yy}] \quad (7)$$

$$D\nabla^4 W + \rho h W_{,tt} = P(t) + h[F_{,yy} W_{,xx} + F_{,xx} W_{,yy} - 2F_{,xy} W_{,xy}] \quad (8)$$

where F = Airy stress function

W = deflection of plate. The commas stand for differentiation with respect to the subscripts which follow them.

$D = Eh^3/12(1 - \nu^2)$ plate stiffness

E = Young's modulus

h = plate thickness

ν = Poisson's ratio

ρ = plate density

$P(t)$ = pressure acting on plate

∇^4 = biharmonic operator

The above equations do not include damping, in-plane and rotatory inertia and transverse shear effects. The boundary conditions for a simply supported plate with stress-free edges, with the origin of the coordinate system at one corner of the plate, are

$$\begin{aligned} X = 0, a & \quad W = 0, & \quad W_{,xx} = 0, & \quad F_{,xy} = 0, & \quad F_{,yy} = 0 \\ Y = 0, b & \quad W = 0, & \quad W_{,yy} = 0, & \quad F_{,xy} = 0, & \quad F_{,xx} = 0 \end{aligned} \quad (9)$$

Equations (7) and (8) have been solved by the method of finite-differences by Bayles (4) for uniform transient pressure loads and for several boundary conditions. He also established the conditions to be satisfied by the spatial step size and by the time step in order to obtain a stable solution. A listing of the finite-difference program is given in Appendix A. For the particular plate used in the experiments described in this report, a grid of 9 x 6 was used for one quarter of the plate. The integration step time was chosen as 0.000018 (sec). The measured pressure at the surface of the plate was used as input to the program.

The response of the plate in the simulated window-room-door system was calculated by the finite-difference method by modifying the net pressure acting on the plate. The pressure acting on the plate for this case is (refer to Figure 8).

$$P(t) = P_{\text{ext}}(t) - K_{\text{vol}} \cdot \left(\iint_S W \, dx dy - A_d W_1 \right) \quad (10)$$

where $P(t)$ = net pressure acting on the plate and on the air mass in the door.

$P_{\text{ext}}(t)$ = External pressure acting on the outside surface of the plate and door.

K_{vol} = stiffness factor of room = $\rho_0 C^2 / V$

ρ_0 = density of air

C = speed of sound

V = volume of room

A_d = area of door

W_1 = displacement of air mass in door. (Displacement into the room is negative.)

Equation (10) is based on lumping the stiffness of the room and the inertance of the air mass (22). An additional equation for the displacement, W_1 , has to be solved simultaneously with Equations (7), (8), and (10):

$$\rho_0 L' A_d \ddot{W}_1 = -2\xi\omega \rho_0 L' A_d \dot{W}_1 - A_d P(t) \quad (11)$$

L' = effective length of door

ξ = effective damping factor at door

ω = natural frequency of room-door system

The finite-difference program listed in Appendix A has the window-room-door case built in as an option.

Lumped Parameter Solution

The lumped parameter models used in this study are a single mode model derived by Yamaki (5) and a multimode model that is derived in this section.

Bayles (25) has also developed a lumped parameter model of a rectangular plate by assuming fundamental mode solutions and using Hamilton's principle to set up the differential equation of motion for the system. The functions assumed by him are

$$F = F_{11}(t) \sin^2 \frac{\pi x}{a} \sin^2 \frac{\pi y}{b}$$

$$W = W_{11}(t) \sin \frac{\pi x}{a} \sin \frac{\pi y}{b}$$

These satisfy all the boundary conditions (9). The resulting differential equation is then of the form

$$M_{eq} \ddot{W}_{11} + K_{eq} W_{11} + \epsilon K_{eq} W_{11}^3 = A_{eq} \cdot P(t) \quad (12)$$

where W_{11} = plate center displacement

$$M_{eq} = \rho abh/4$$

a, b = plate length and width

h = plate thickness

$$K_{eq} = \frac{\pi^4 D}{4ab} \left(\beta^2 + \frac{1}{\beta^2} + 2 \right)$$

$$A_{eq} = \frac{4}{\pi^2} ab$$

$$e = \frac{3(1 - \nu)}{8h^2 \left(\beta^2 - \frac{1}{\beta} + 2 \right)} \left[2 \left(\frac{\pi^2}{3} + 2 \right) - \frac{C_1^2}{C_2} \right]$$

$$C_1 = \left(\beta^2 + \frac{1}{\beta^2} \right) \left(\frac{\pi^2}{3} + 4 \right) - 4\nu$$

$$C_2 = 3(1 - \nu) \left(\beta^2 + \frac{1}{\beta^2} \right) + \left(\frac{\pi^2}{3} + \frac{5}{2} \right) \left(\beta^4 + \frac{1}{\beta^4} \right) - 2\nu + 9$$

$$\beta = a/b$$

The stress function coefficient F_{11} is determined from

$$F_{11} = \frac{-C_1 E}{8C_2} W_{11}^2$$

The lumped parameter model derived by Yamaki (5) has been found to be more accurate than that due to Bayles. A computer program for integrating Equation (12) using either Bayles' or Yamaki's model is listed in Appendix B.

As the amplitude of the response becomes relatively larger, it has been found that there is very poor agreement between the finite-difference and the fundamental mode, lumped parameter solutions. It was surmised that the inclusion of higher modes in the lumped parameter solution would increase its accuracy. The approach followed here in deriving this lumped parameter model is to assume suitable functions for the deflection and the stress function and then to determine the differential equations for the unknown coefficients by Galerkin's method.

The following functions, which satisfy all the boundary conditions (9), are assumed for the deflection W and the stress function F :

$$W = \sum_{\substack{m=1 \\ m, n \text{ odd}}}^M \sum_{n=1}^N W_{mn}(t) \sin \frac{m\pi x}{a} \sin \frac{n\pi y}{b} \quad (13)$$

$$F = \sum_{j=1}^J \sum_{k=1}^K F_{jk}(t) \sin^2 \frac{j\pi x}{a} \sin^2 \frac{k\pi y}{b} \quad (14)$$

Only odd values of m and n are used in the assumed functions for W since a uniform pressure is assumed.

The assumed functions (13) and (14) are first substituted into Equation (7). Following Galerkin's procedure, weighted residuals are obtained by multiplying the resulting equation by each of the terms in the assumed function for F and integrating over the entire area of the plate. The residuals are then set equal to zero. This results in $J \times K$ simultaneous, linear, algebraic equations for F_{jk} in terms of $W_{pq} \cdot W_{rs}$. These equations may be written as

$$[FF] \{F_{jk}\} = [COEF] \{W_{pq} \cdot W_{rs}\}$$

where $[FF]$ is a $J \times K$ by $J \times K$ matrix of coefficients, $\{F_{jk}\}$ is a column matrix of $J \times K$ elements from Equation (14), $[COEF]$ is a $J \times K$ by $(M+1) \times (N+1)/4$ matrix of coefficients of the products $W_{pq} \cdot W_{rs}$ with W_{pq} and W_{rs} as defined in Equation (13).

The above equations may be solved to obtain the coefficients F_{jk} if the values of the deflection components are known.

$$\begin{aligned}
\{F_{jk}\} &= [FF]^{-1} [FCOEF] \{W_{pq} \cdot W_{rs}\} \\
&= [FCOEFF] \{W_{pq} \cdot W_{rs}\}
\end{aligned} \tag{15}$$

The functions for W and F are next substituted into Equation (8) and the Galerkin method is again applied, this time using the elements of W as the weighting functions. Finally, the coefficients of F_{jk} are expressed in terms of W using Equation (15) and the resulting ordinary differential equations take the form

$$\begin{aligned}
\frac{\rho abh}{4} \ddot{W}_{mn} + D \left[\left(\frac{m\pi}{a} \right)^4 + 2 \left(\frac{mn\pi^2}{ab} \right)^2 + \left(\frac{n\pi}{b} \right)^4 \right] W_{mn} \\
+ \frac{2\pi^4 h}{a^2 b^2} \sum_p^M \sum_q^N \sum_r^M \sum_s^N \sum_t^M \sum_u^N (\text{Coefw})_{mn}^{pqrst} W_{pq} \cdot W_{rs} \cdot W_{tu} \\
= \frac{4ab}{mn\pi^2} P(t)
\end{aligned} \tag{16}$$

These equations reduce to the exact linear case when the coefficients $(\text{Coefw})_{mn}^{pqrst}$ are set equal to zero. The coefficients have to be generated only once for a given plate. It is possible to obtain a simple expression for ϵ in Equation (12) by this method when only W_{11} and F_{11} are used. The results for this fundamental mode case are given below.

$$\begin{aligned}
\epsilon &= \frac{1}{h^2} \frac{12(1 - \nu^2)}{\left(\frac{1}{\beta^2} + 2 + \beta^2 \right) \left(\frac{6}{\beta^2} + r + 6\beta^2 \right)} \\
F_{11} &= - \frac{E}{\left(\frac{6}{\beta^2} + 4 + 6\beta^2 \right)} \cdot W_{11}^2
\end{aligned}$$

For comparison, the value of ϵh^2 obtained by the various methods for $\beta = 1.5$ and $\nu = 0.22$ are: above formula = 0.1207, Yamaki = 0.1252, and Bayles = 0.1755.

The ordinary differential equations of the lumped parameter models are integrated numerically using a standard predictor-corrector method. Subroutine DHPCG in the IBM Scientific Subroutine Package was used for this purpose. The computer program for the multimode model is listed in Appendix C.

The fundamental mode model was also used on the window-room-door system. The equations to be solved for this case are (refer to Figure 8)

$$\begin{aligned} \frac{\rho abh}{4} \ddot{W}_{11} + K_{eq} W_{11} + \epsilon K_{eq} W_{11}^3 \\ = \frac{4ab}{\pi^2} \left[P_{ext}(t) + \frac{\rho_0 C^2}{V} \left(A_d W_1 - \frac{4ab}{\pi^2} W_{11} \right) \right] \end{aligned} \quad (17)$$

$$\begin{aligned} \rho_0 L' A_d \ddot{W}_1 + 2\xi \rho_0 L' A_d \dot{W}_1 + \frac{\rho_0 C^2}{V} A_d^2 W_1 \\ - \frac{4ab}{\pi^2} \frac{\rho_0 C^2}{V} A_d W_{11} = -A_d P_{ext}(t) \end{aligned} \quad (18)$$

W_{11} is the center deflection of the plate and W_1 is the deflection of the air mass in the door. The other symbols have already been defined.

CHAPTER V

EXPERIMENTAL RESULTS

The plate was instrumented to obtain Moiré fringe data, strains in the x and y directions at the surface of the plate and the deflection at the center.

Moiré Fringe Data

The support conditions at the boundary were first checked for symmetry and for free rotation by taking Moiré fringe photographs of the surface of the plate when it was subjected to a static pressure. Figures 9 and 10 show the static Moiré fringes in the x and y directions for a plate center deflection of 0.039 in. The fringe lines represent contours of points which have, approximately, the same partial slope ($\partial W/\partial X$ in the x direction and $\partial W/\partial Y$ in the y direction). The static deflection profiles along the center lines of the plate are shown in Figures 11 and 12. These were obtained by integrating Equation (6) numerically using the measured fringe data. The fringe photographs indicated in a graphic manner that the boundary conditions of the plate were acceptable.

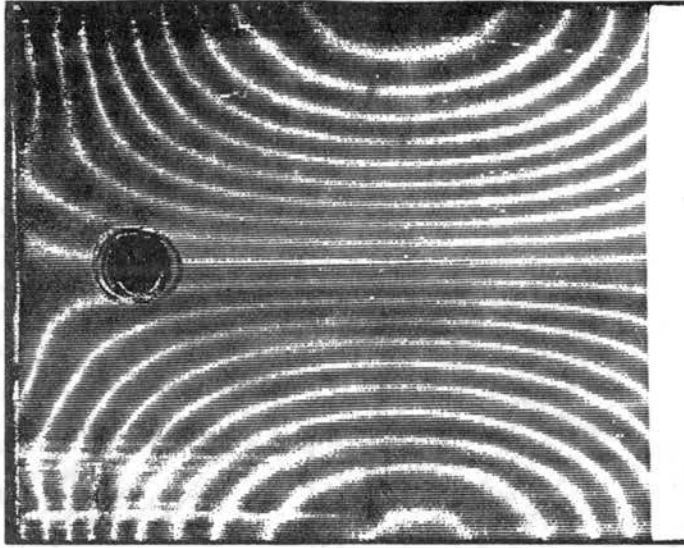


Figure 9. Moiré Fringes in the y
Direction of a Rectangular
Plate Subjected to Static
Pressure

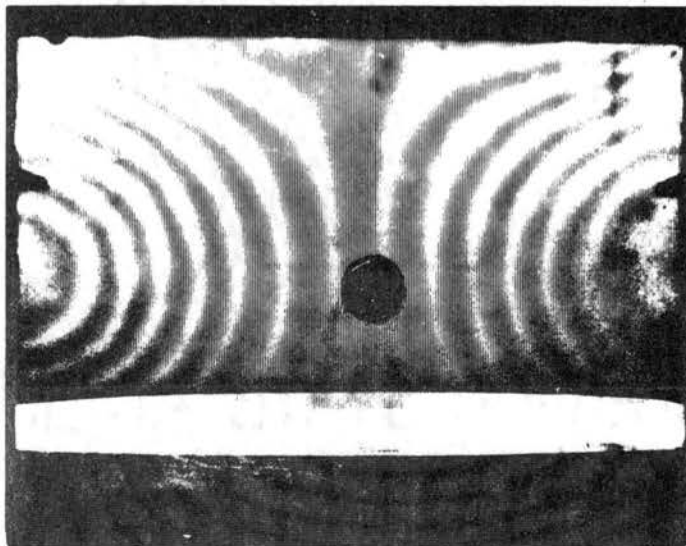


Figure 10. Moiré Fringes in the x
Direction of a Rectangular
Plate Subjected to Static
Pressure

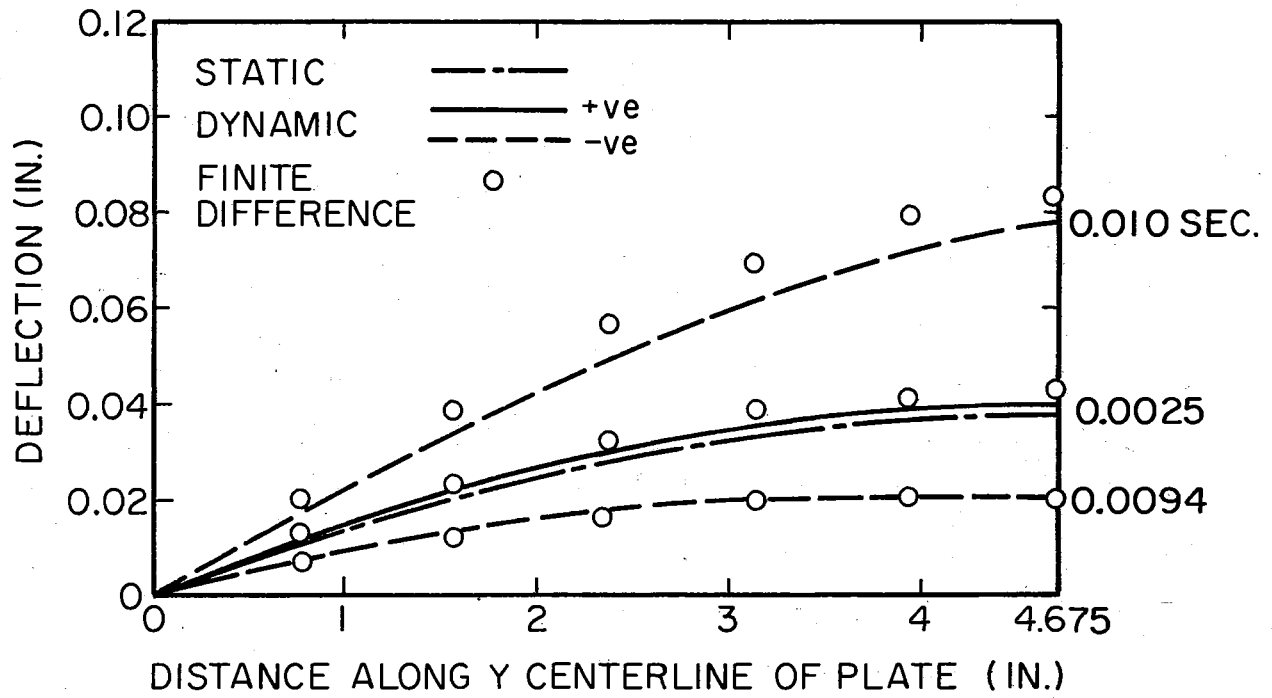


Figure 11. Static and Dynamic Deflection Profiles of the y Centerline of the Plate by Moiré and Finite-Difference Methods

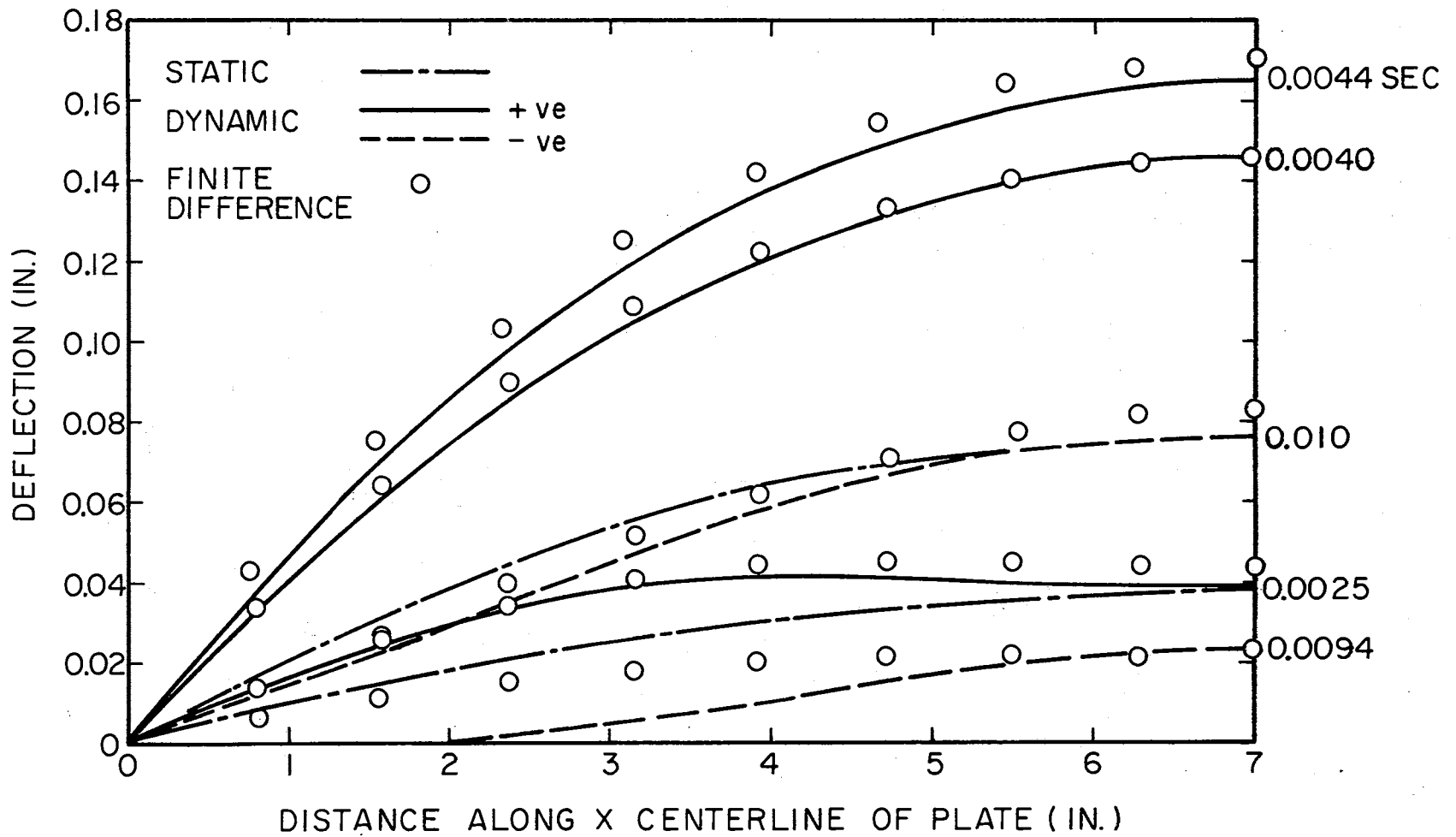


Figure 12. Static and Dynamic Deflection Profiles of the x Centerline of the Plate by Moiré and Finite-Difference Methods

A sequence of Moiré fringe photographs taken at different instants during the response of the plate when it is hit by a pressure pulse is shown in Figures 13 to 20. At smaller values of center deflection, fringes in both x and y directions are shown. For the larger deflection values (Figures 15 and 16) the fringes in the y direction were too close together to be resolved. This problem can be alleviated to a certain extent by moving the Moiré screen closer to the plate. The experimentally observed deflection profiles along the centerlines of the plate obtained by integrating the data from the fringe photographs are shown in Figures 11 and 12. The corresponding values obtained from the finite-difference solution are also shown in the same figures. The sequence of photographs was obtained by using separate pulses for each photograph. The pressure pulse was closely reproduced each time. The finite-difference data was obtained for only one pressure pulse which was characteristic of this series of tests (Figure 23). Generally, the same deflection magnitude was not obtained by the Moiré method and the finite-difference solution at the same instant of time. The profiles were obtained by matching the experimental and theoretical center deflections. The value of a whole field method of visualizing the deflection response of the plate is best brought out in Figures 13 and 14 where the effect of the third

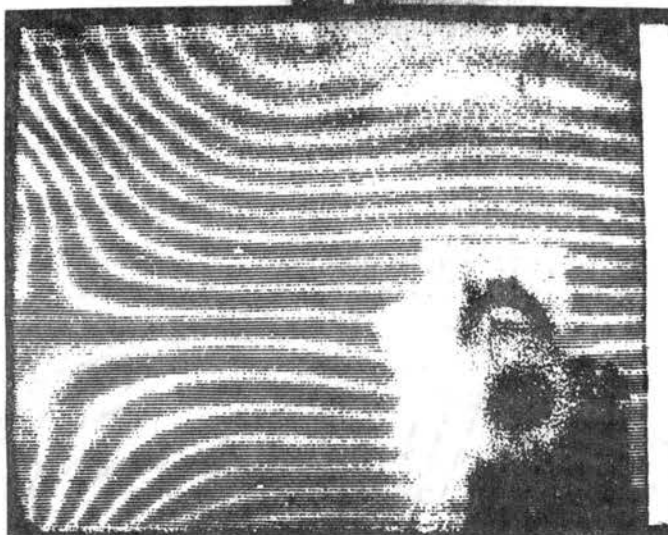


Figure 13. Moiré Fringes in y
Direction at
0.0025 sec.

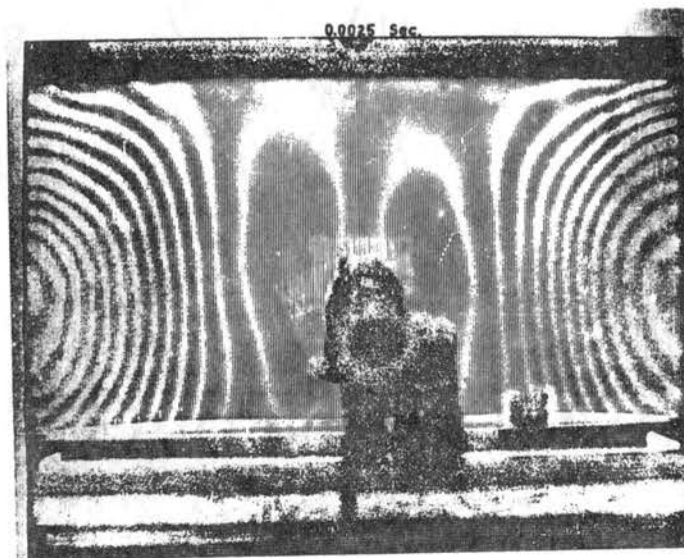


Figure 14. Moiré Fringes in x
Direction at
0.0025 sec.

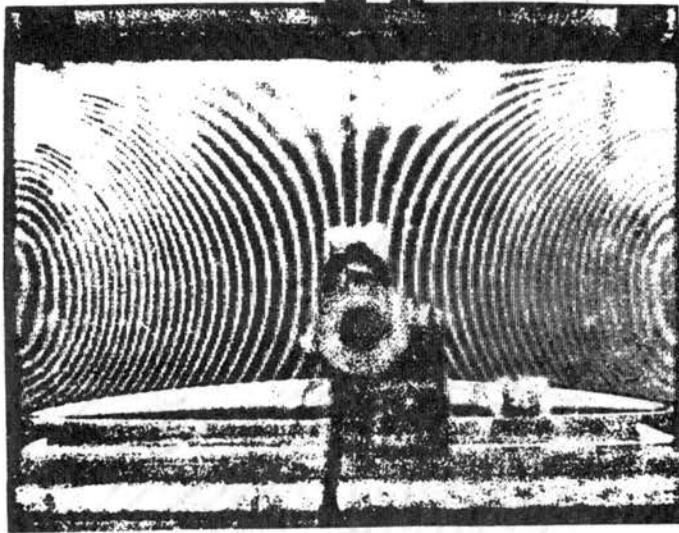


Figure 15. Moiré Fringes in x
Direction at
0.0040 sec.

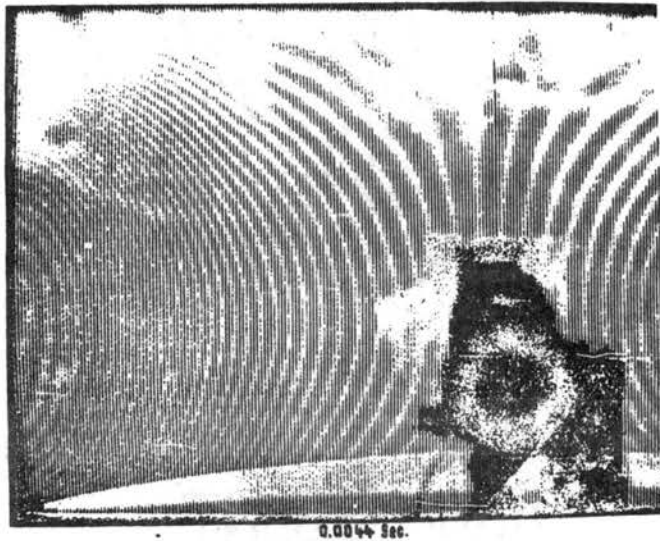


Figure 16. Moiré Fringes in x
Direction at
0.0044 sec.

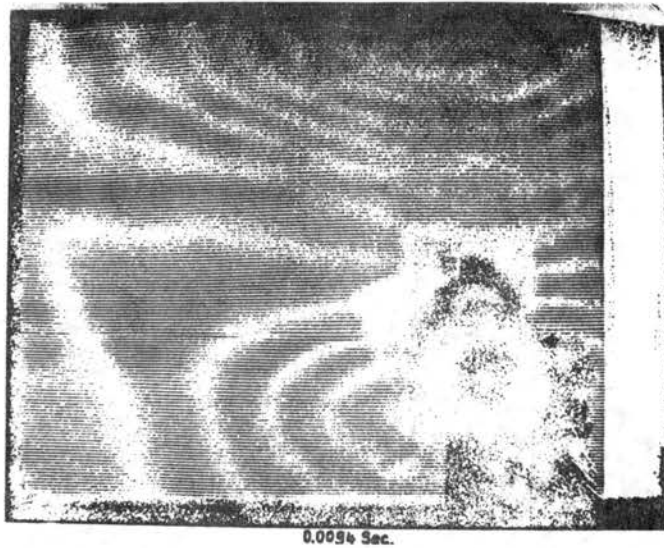


Figure 17. Moiré Fringes in y Direction at 0.0094 sec.

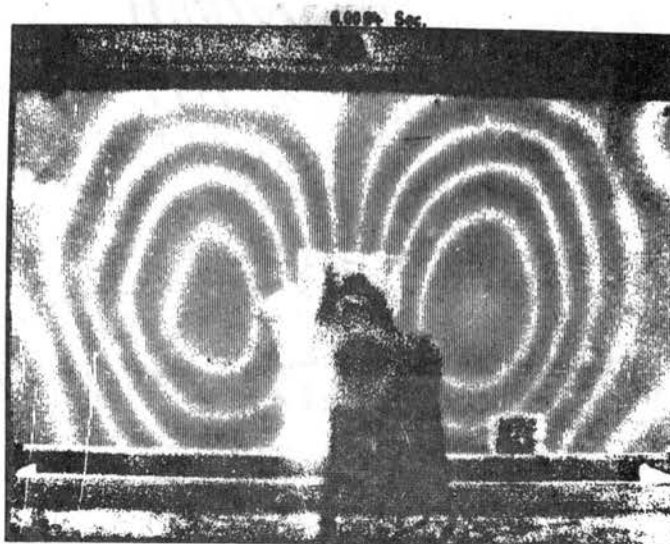


Figure 18. Moiré Fringes in x Direction at 0.0094 sec.

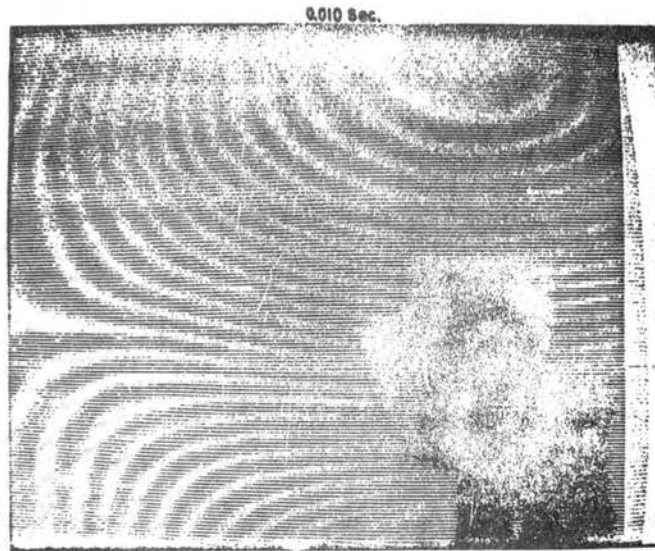


Figure 19. Moiré Fringes in y Direction at 0.010 sec.

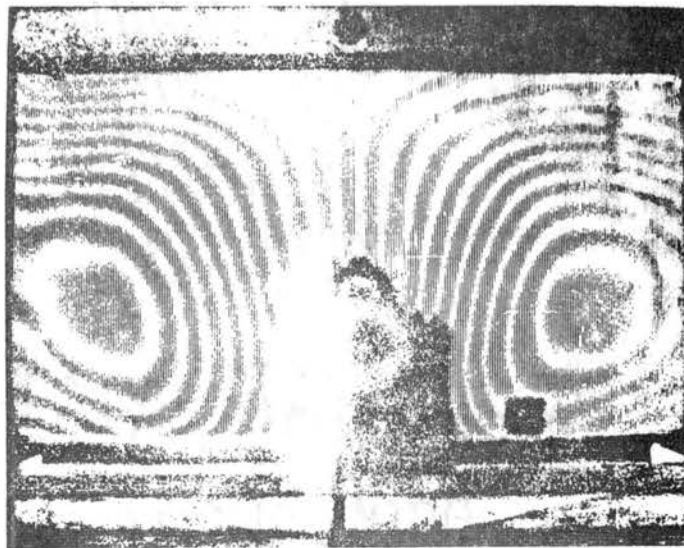


Figure 20. Moiré Fringes in x Direction at 0.010 sec.

mode is clearly displayed. The deflection measured by the Moiré method over one quarter of the plate is shown for two instants of time in Figures 21 and 22.

Strain Data

The strain was measured on the front and back surfaces of the plate (the back surface looks into the plane wave tube) in the x and y directions at the center and at the mid-point of the diagonal connecting the center and the corner. The magnitude of the pressure pulse was varied so as to get data ranging from the almost linear to highly non-linear response. Two photographs of oscilloscope traces of tests in which the maximum center displacement to thickness ratio were 5.6 and 2.6 respectively, are shown in Figures 23 and 24. The traces represent strain in the y direction at the center of the plate on the back surface, the deflection of the center of the plate (inverted), the pressure acting on the plate and the strain in the y direction at the center on the front surface of the plate, in that order from the top of the photographs downward.

The measured strain in the y direction at the center of the front surface of the plate is compared with the values calculated by the finite-difference method, the single mode lumped parameter model of Yamaki and the multimode lumped parameter model in Figures 25 to 30 for maximum deflection to thickness ratios of 5.6, 2.6, and 0.85.

FINITE DIFF. - - - -
EXPT. ————

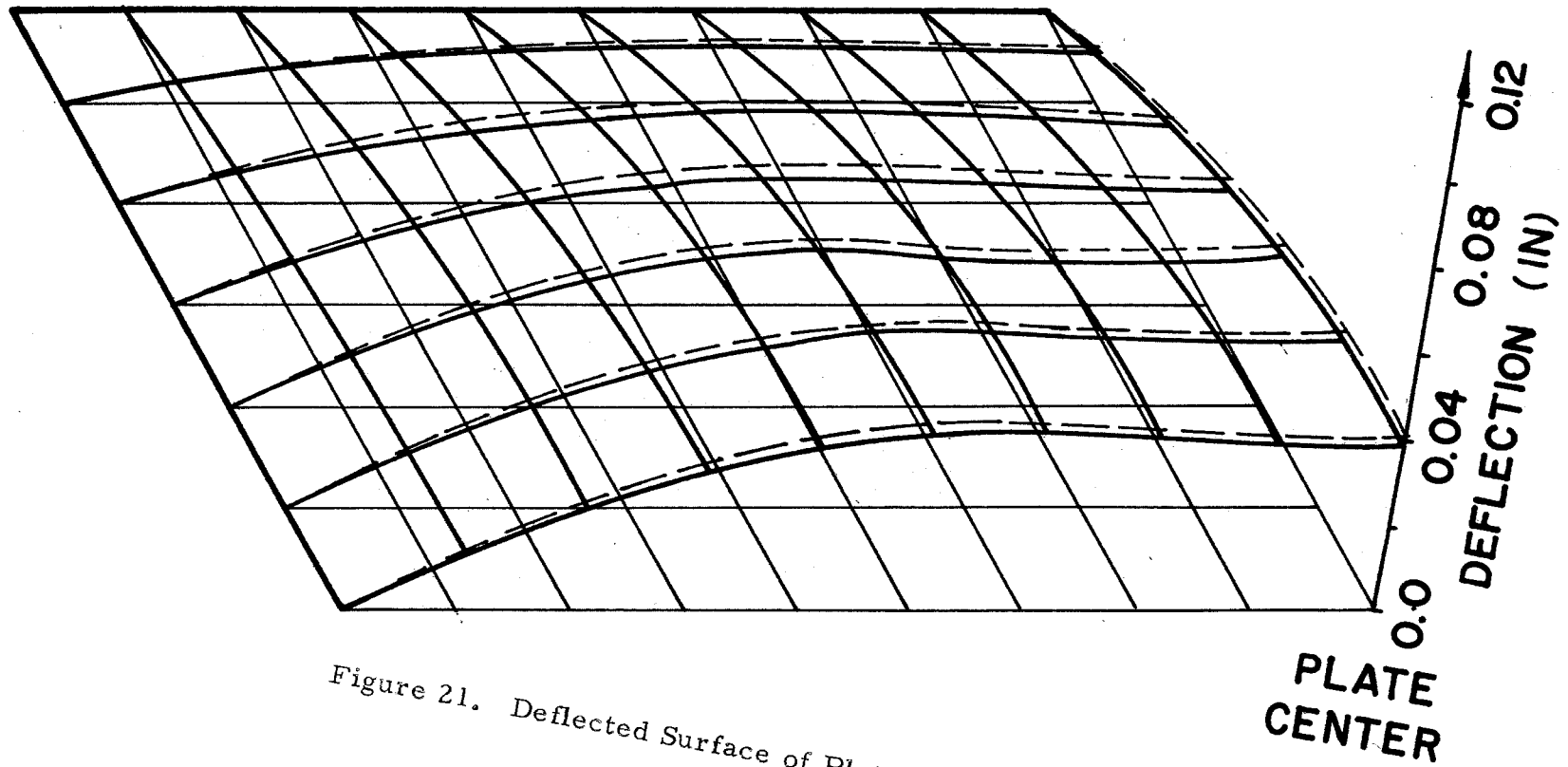


Figure 21. Deflected Surface of Plate at 0.0025 sec.

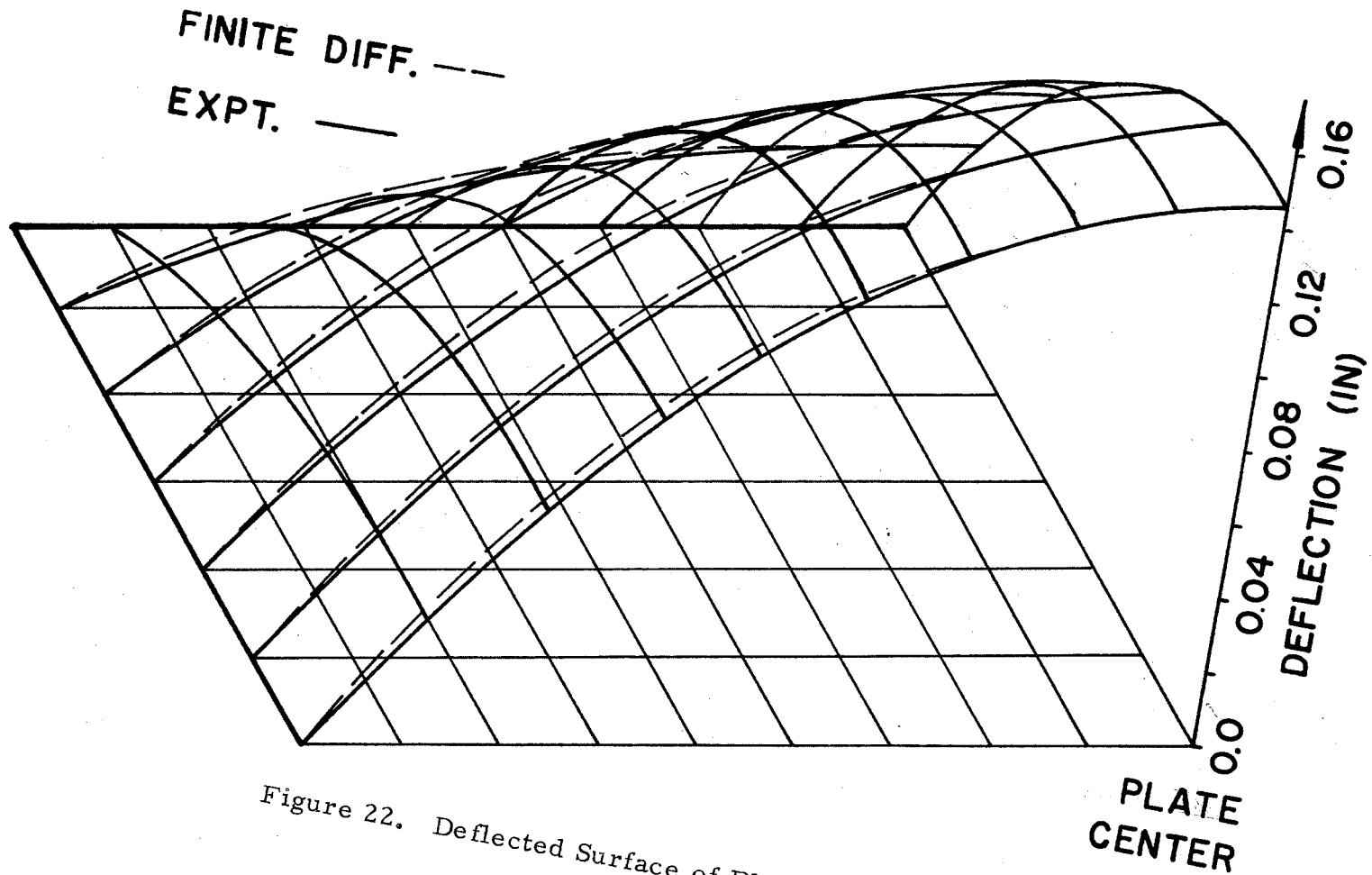


Figure 22. Deflected Surface of Plate at 0.0040 sec.

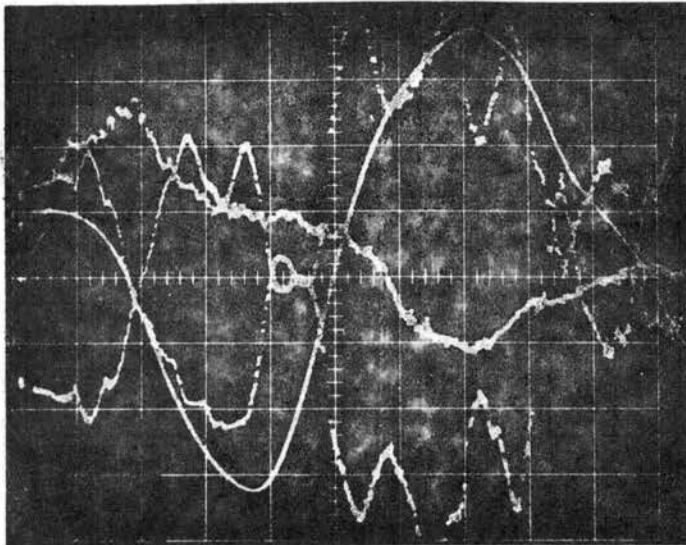


Figure 23. Oscilloscope Traces for Response Corresponding to Max. Center Displacement to Thickness Ratio of 5.6 (1 cm. = 0.002 sec.)

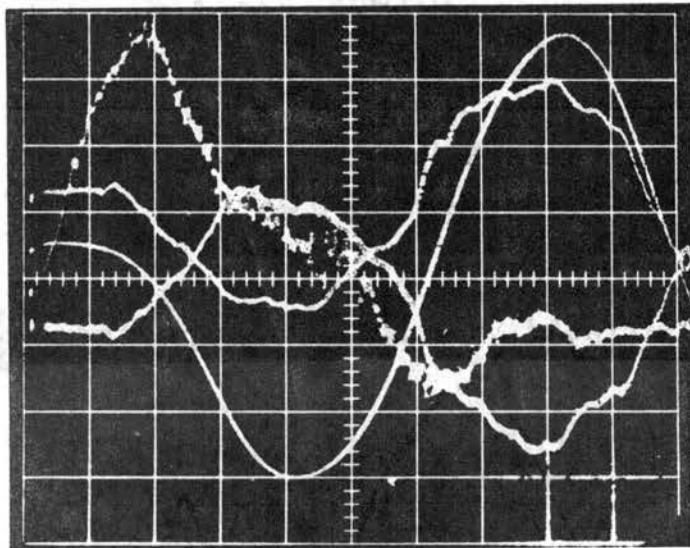


Figure 24. Oscilloscope Traces for Response Corresponding to Max. Center Displacement to Thickness Ratio of 2.6 (1 cm. = 0.002 sec.)

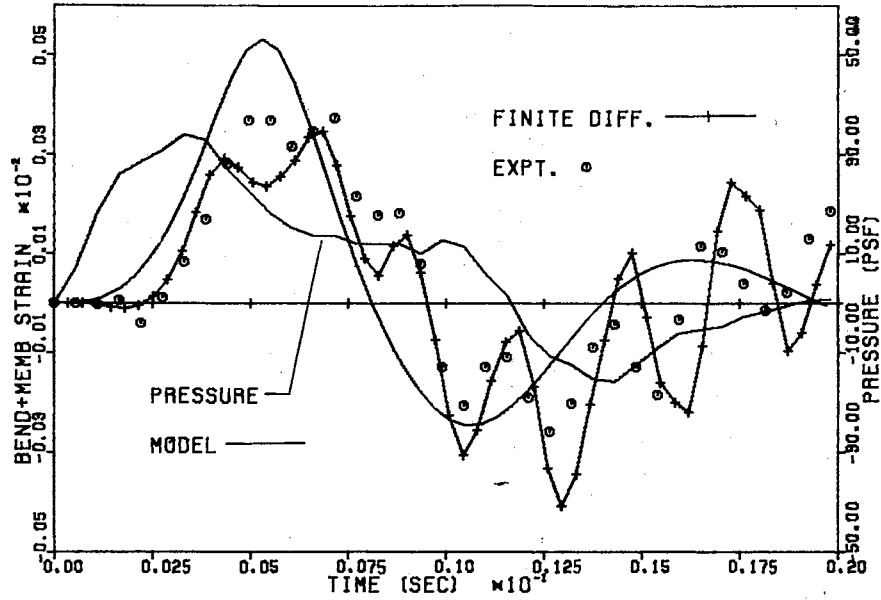


Figure 25. Strain at the Center of the Front Surface in the y Direction for Max. Displacement to Thickness Ratio of 5.6.

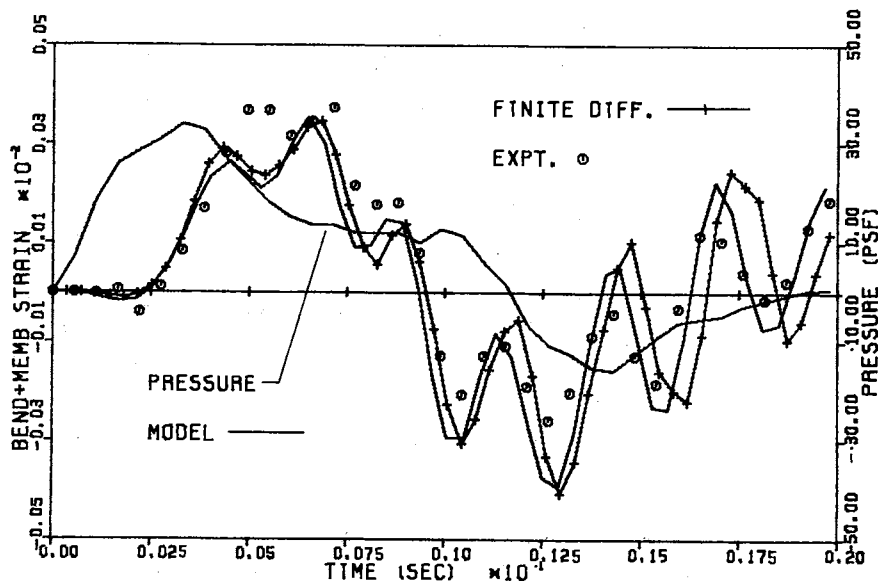


Figure 26. Strain at the Center of the Front Surface in the y Direction for Max. Displacement to Thickness Ratio of 5.6 (Galerkin model, $M = N = 3$, $J = K = 4$)

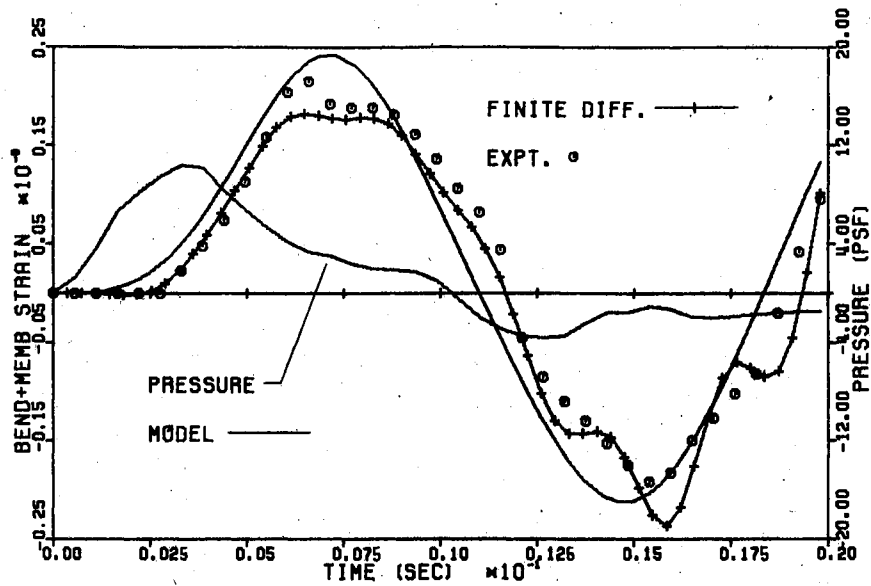


Figure 27. Strain at the Center of the Front Surface in the y Direction for Max. Displacement to Thickness Ratio of 2.6

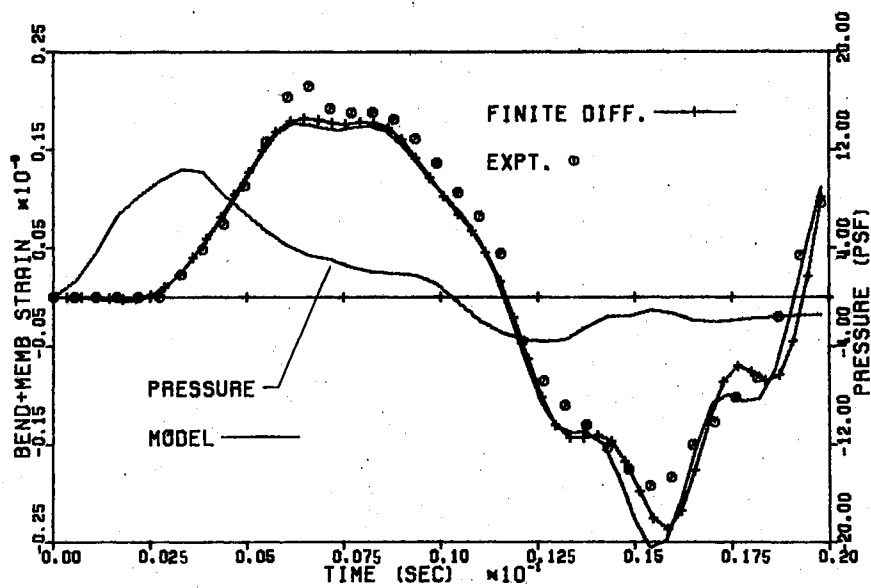


Figure 28. Strain at the Center of the Front Surface in the y Direction for Max. Displacement to Thickness Ratio of 2.6 (Galerkin model, $M=N=3$, $J=K=4$)

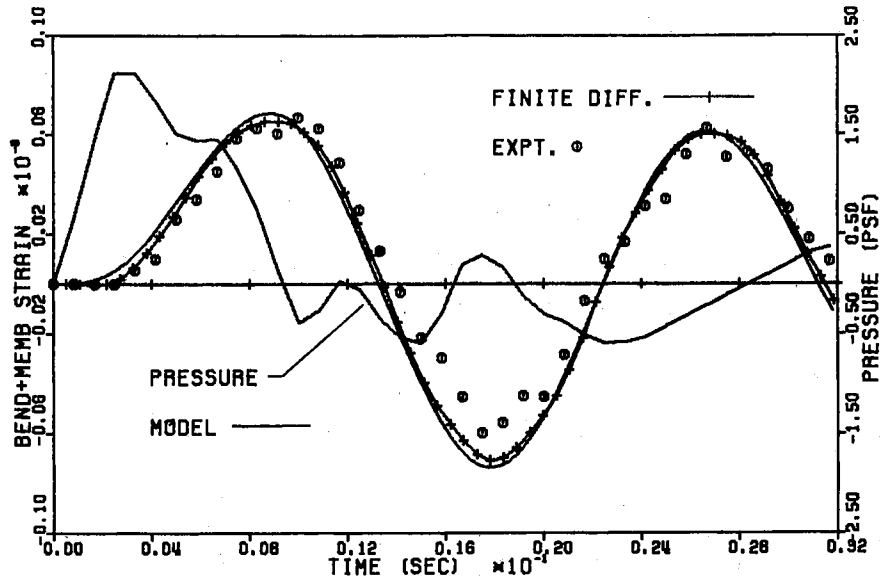


Figure 29. Strain at the Center of the Front Surface in the y Direction for Max. Displacement to Thickness Ratio of 0.85

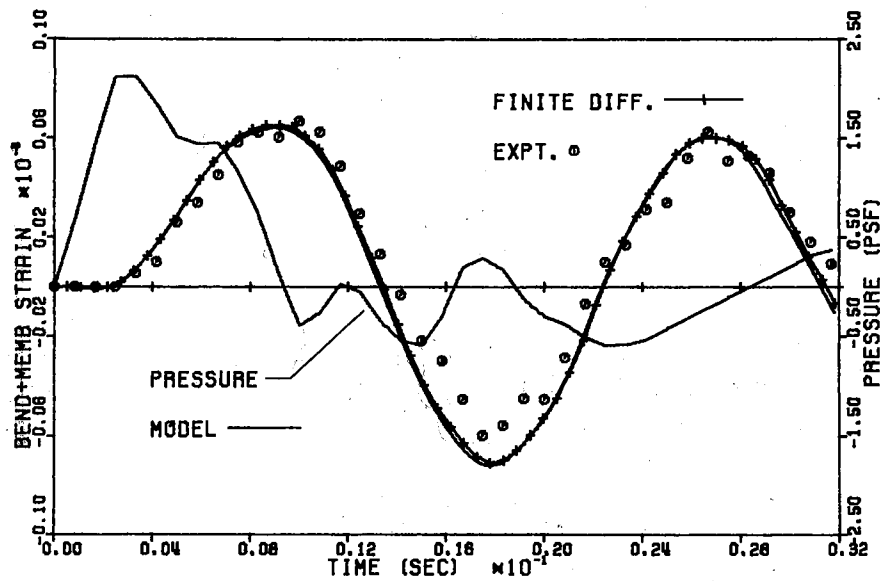


Figure 30. Strain at the Center of the Front Surface in the y Direction for Max. Displacement to Thickness Ratio of 0.85 (Galerkin model, $M = N = 3$, $J = K = 4$)

For all three cases, the density was adjusted empirically to 172.0 lbm/cu. ft. (measured density of glass was 153.0) to account partially for the reactive component of the radiation impedance faced by the front surface of the plate. This corrected value for the density is also obtained by an approximate analysis which is given in Lin (26). The correction for the density was not applied to the face of the plate looking into the plane wave tube because the pressure transducer gives the actual pressure acting on that face. The damping was considered to be zero for all theoretical calculations. The average measured value of the damping ratio was 0.03.

The results shown for the multimode model are for the case, $J = K = 4$, $M = N = 3$ in Equations (13) and (14) for the assumed function. It was found that the results using a smaller number of terms for the stress function, $J = K = 2$, were not much different from the results using $J = K = 4$, but the latter case was closer to the finite-difference data.

In Figures 31 to 36, the measured strains on the back surface of the plate in the x direction at the center (the x axis is oriented along the longer edge of the plate) and in the x and y directions at the quarter diagonal location are compared with the theoretical solutions. As a final example of the strain data obtained in this study, the strain in the y direction on the front surface of the plate is plotted in Figure 37 over one quarter of the plate at about the time of maximum response.

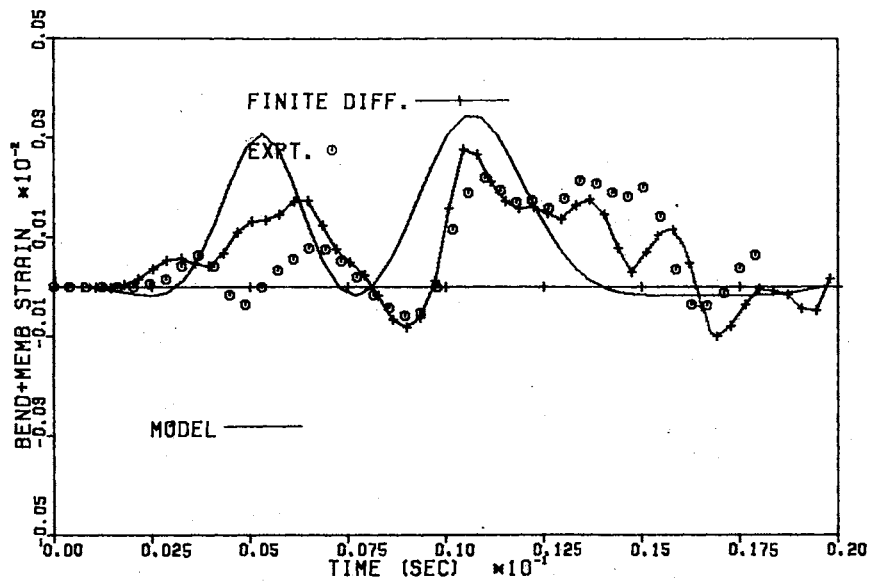


Figure 31. Strain at the Center of the Back Surface in the x Direction for Max. Displacement to Thickness Ratio of 5.6

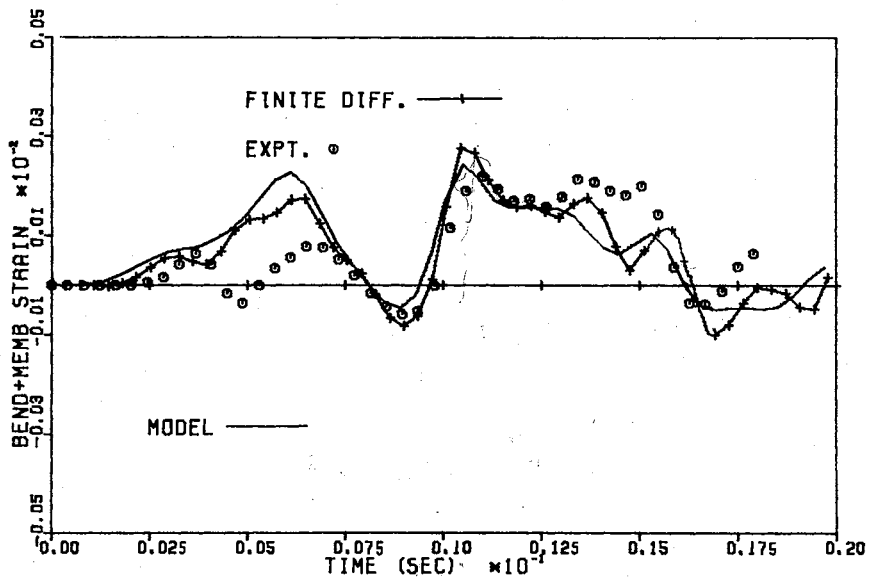


Figure 32. Strain at the Center of the Back Surface in the x Direction for Max. Displacement to Thickness Ratio of 5.6 (Galerkin model, $M = N = 3$, $J = K = 4$)

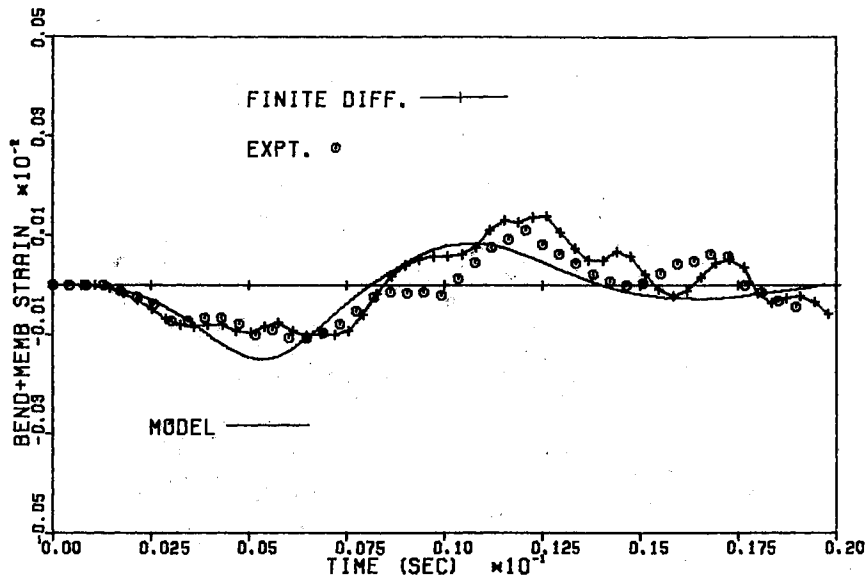


Figure 33. Strain at the Quarter Diagonal Point of the Back Surface in the x Direction for Max. Displacement to Thickness Ratio of 5.6

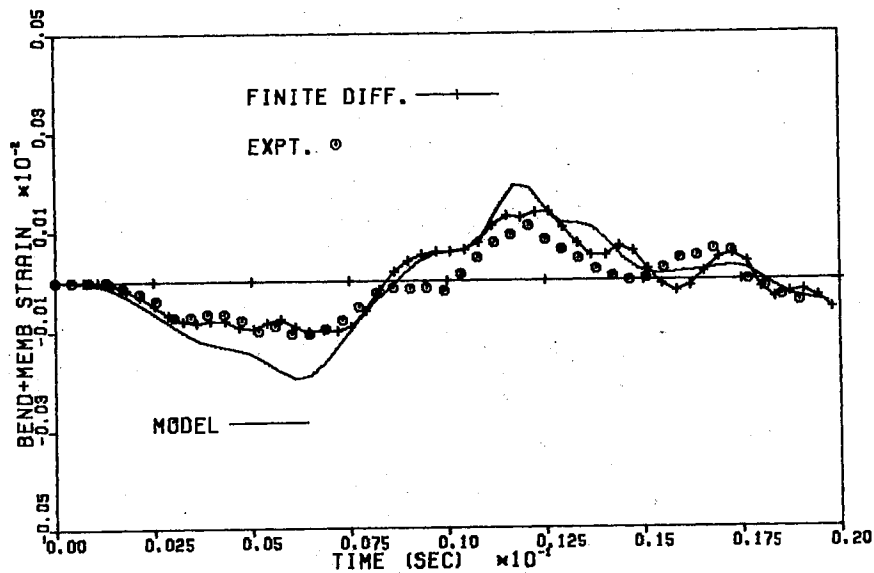


Figure 34. Strain at the Quarter Diagonal Point of the Back Surface in the x Direction for Max. Displacement to Thickness Ratio of 5.6 (Galerkin model, $M = N = 3$, $J = K = 4$)

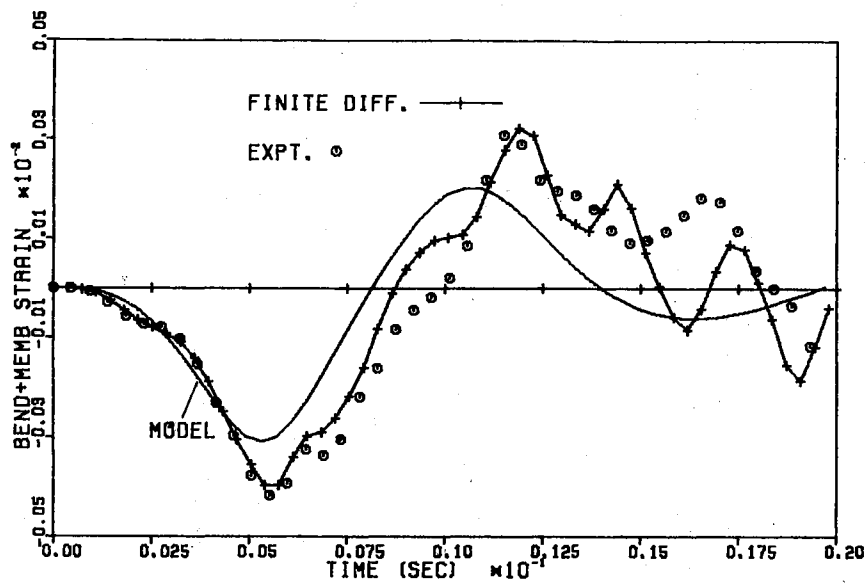


Figure 35. Strain at the Quarter Diagonal Point of the Back Surface in the y Direction for Max. Displacement to Thickness Ratio of 5.6

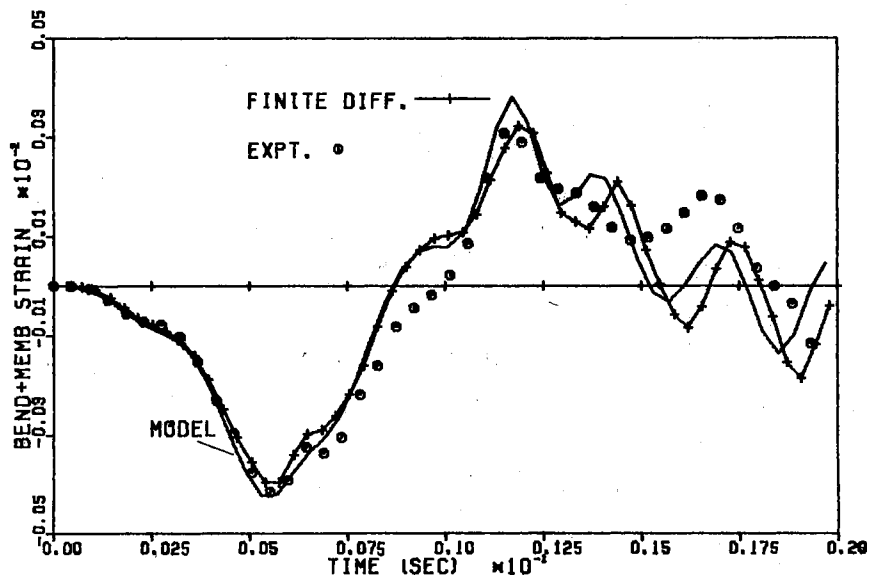


Figure 36. Strain at the quarter Diagonal Point of the Back Surface in the y Direction for Max. Displacement to Thickness Ratio of 5.6 (Galerkin model, $M = N = 3$, $J = K = 4$)

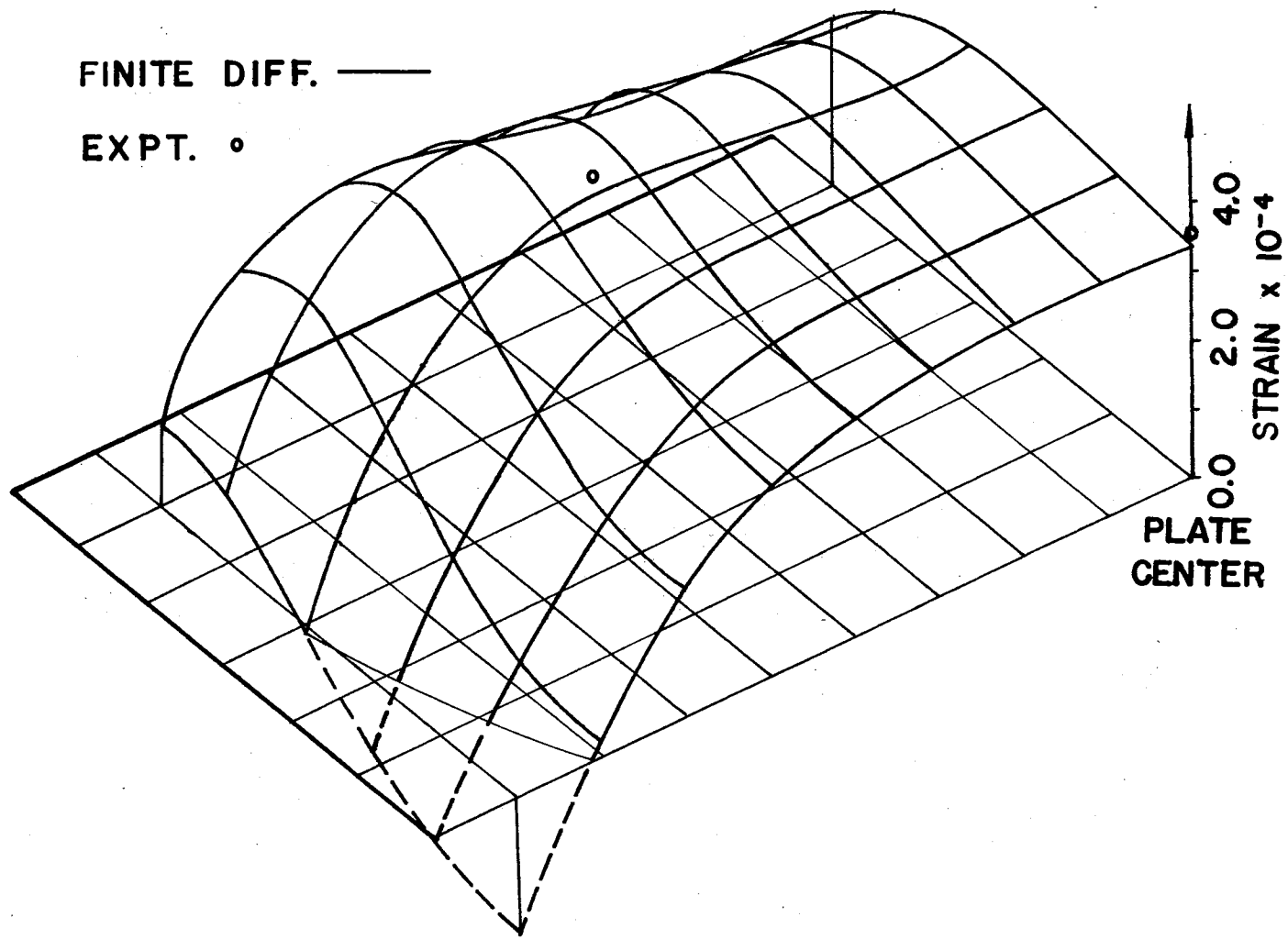


Figure 37. Total Strain in the y Direction on the Front Surface of the Plate at 0.0065 sec.

The following observations may be made about the strain data. The expected error in the strain data is 5%, and this data is the most accurate of the various measurements that were made on the plate. The shapes of the measured and theoretical response curves (especially for the finite-difference and the multimode model) are almost identical for all three relative amplitudes of deflection. For the maximum deflection ratio, the amplitude of the third mode component of strain for the measured data is, at times, only about 45% of the theoretical amplitude. But the mean values are of the same magnitude. It is possible that higher modes are more severely damped than the lower modes. The other possible causes are non-uniformity of the pressure loads and the plate thickness and boundary conditions that are not perfectly symmetrical. The Moiré fringe photographs in Figures 17 and 19 indicate some asymmetry in the fringes in the y direction during the tail end of the response. The strain magnitudes are compared next. The magnitudes of special concern are the peak values. In almost all cases, the measured first maximum strains in the y direction are larger than the finite-difference values--7% larger for the deflection ratio of 5.6, 13% for the 2.6 ratio and 3% for the ratio of 0.85. However, for the second maximum strains, the theoretical values are invariably larger than the measured values. It is possible that this behavior is at least partly due to the low frequency response characteristics of the microphone used to measure the pressure. The

pressure acting on the plate, which is a measured quantity and thus subject to error, is one of the major input quantities for the finite-difference and lumped parameter model computer programs. These programs also require the measured plate dimensions and the material properties. Thus, the theoretical results are also subject to deviations which are dependent on the deviations in the input quantities. It is difficult to give a numerical estimate of the maximum deviation possible in the theoretical results. If the theoretical results are assumed to be subject to no deviations, comparison with the strain data indicates that the finite-difference solution of the Von Kármán equations closely approximates the actual behavior of a thin plate undergoing large deflections up to as much as 5.6 times the plate thickness. The multimode lumped parameter model gives results similar to the finite-difference response. The single mode model is as good as the other two theoretical solutions for a deflection ratio of 0.85. But for deflection ratios of 2.6 and 5.6, the single mode model predicts a much larger strain than either the measured values or the other theoretical solutions.

From Figure 37 it is clear that the maximum strain, for non-linear deflections, does not occur at the center. A large area of the plate is heavily stressed and the maximum strain occurs at a point approximately on the diagonal and closer to the corner than the quarter diagonal position. Since a larger area of the plate is heavily

strained for nonlinear deflections, the probability of failure of a glass plate with a given density of flaws per unit surface area is greater when it is loaded to a specified maximum strain in the nonlinear case than in the linear case where the maximum strain occurs only in a region localized around the center of the plate.

Deflection Response

The measured displacement of the center of the plate is compared with the theoretically predicted values in Figures 38 to 43 for maximum center displacement to plate thickness ratios of 5.6, 2.6, and 0.85. Some of the reasons for the difference between experimental and theoretical values have already been discussed for the strain data. An additional factor contributing to the expected deviation for the deflection data was the inadequate high frequency response of the displacement pickup. The measured data was put through a Fourier transform program, corrected for its frequency response in the frequency domain and reassembled in the time domain by an inverse Fourier transform. The results indicate fair agreement between experiment and theory.

Window-Room-Door Simulation

Photographs of oscilloscope traces obtained during tests on the window-room-door model with the small room and the large room are

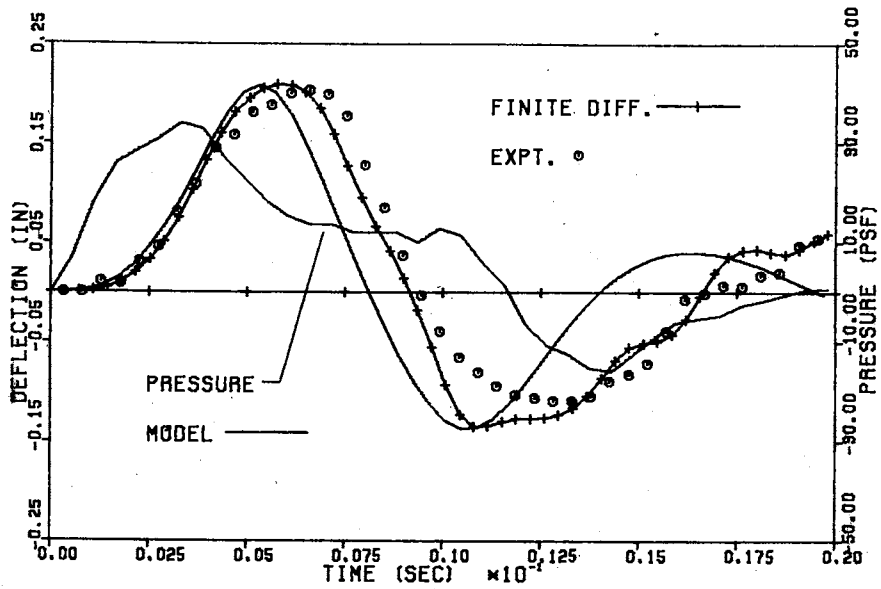


Figure 38. Plate Center Displacement for Maximum Displacement to Thickness Ratio of 5.6

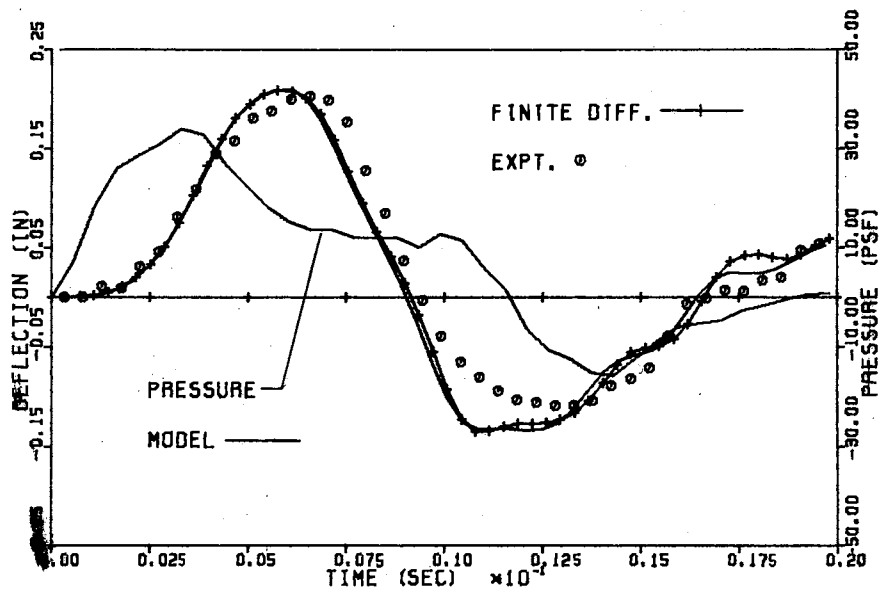


Figure 39. Plate Center Displacement for Maximum Displacement to Thickness Ratio of 5.6 (Galerkin model, $M = N = 3$, $J = K = 4$)

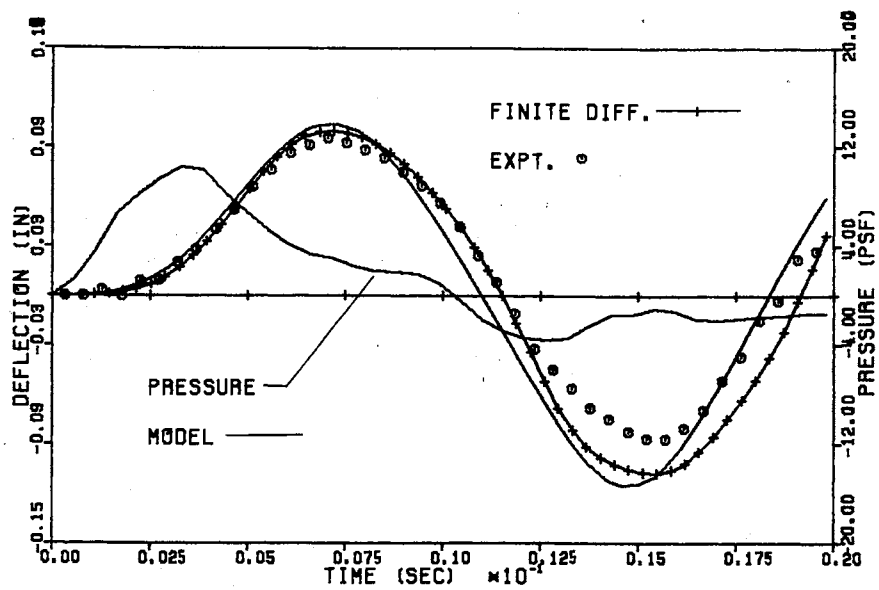


Figure 40. Plate Center Displacement for Maximum Displacement to Thickness Ratio of 2.6

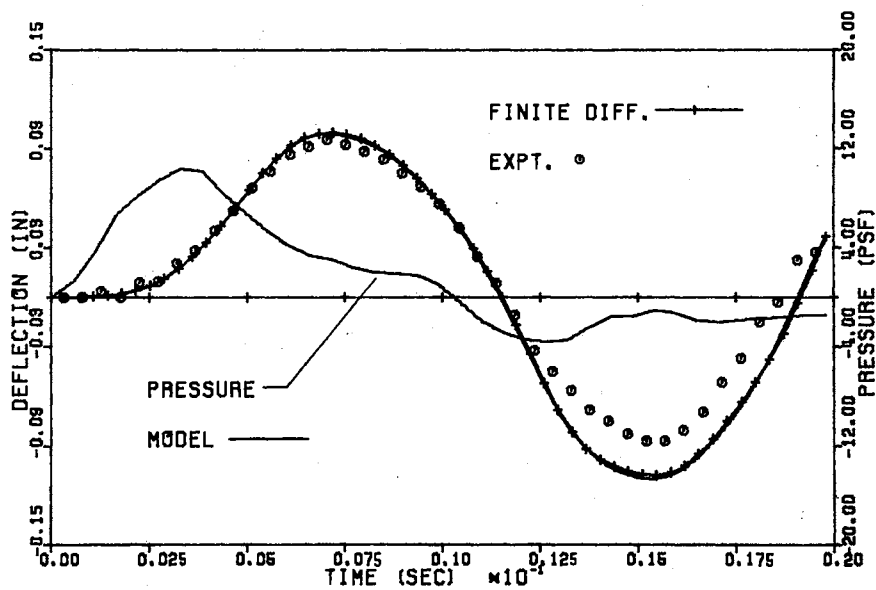


Figure 41. Plate Center Displacement for Maximum Displacement to Thickness Ratio of 2.6 (Galerkin model, $M = N = 3$, $J = K = 4$)

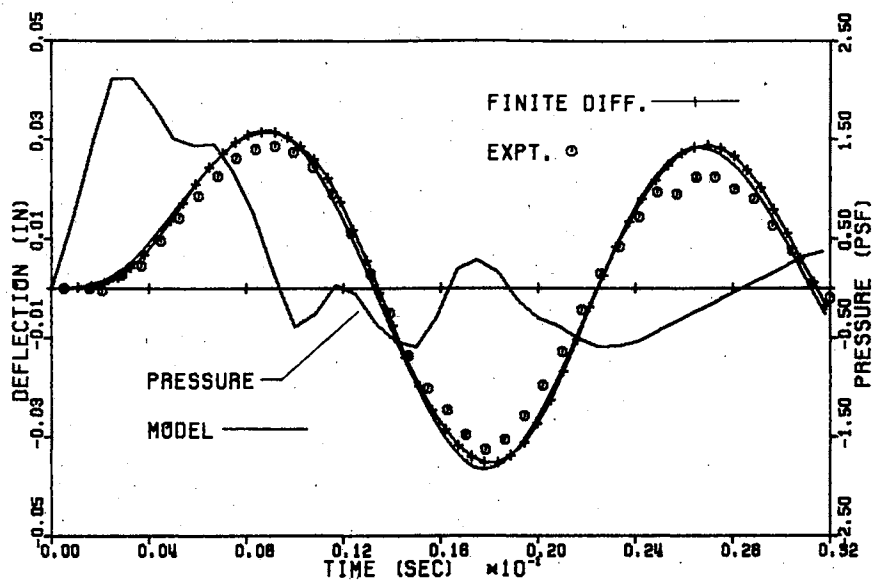


Figure 42. Plate Center Displacement for Maximum Displacement to Thickness Ratio of 0.85

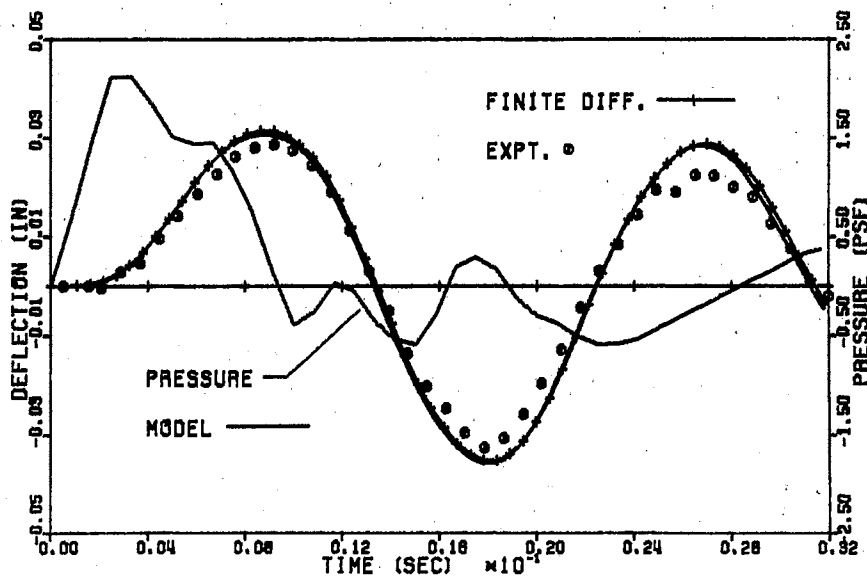


Figure 43. Plate Center Displacement for Maximum Displacement to Thickness Ratio of 0.85 (Galerkin model, $M = N = 3$, $J = K = 4$)

shown in Figures 44 and 45 respectively. In these photographs, the top most trace is strain in the y direction at the center of the front surface, followed by the pressure, center displacement, and y strain at the center of the back surface in that order.

The measured y strain at the center of the front surface of the plate and the theoretically calculated values are plotted in Figures 46 and 47. The lumped parameter model shown in these figures is the fundamental mode model of Yamaki. In the theoretical calculations, the density of the plate was kept at its measured value of 153.0 lbm/cu. ft. and plate damping was neglected. For the given dimensions of the room used in the test and the fundamental frequency of the response, the principal acoustic effect of the displacement of the window was to cause a net change in pressure inside the room that was proportional to the volume displaced by the movement of the plate. The effective length of the doorway was empirically set at 0.67 ft. and a damping factor of 0.05 was used for the door. The maximum center displacement to thickness ratio for both the small room and the large room was 4.2. The center deflection is plotted in Figures 48 and 49. Once again, the important contribution of the third mode to the response at large amplitudes can be readily seen. The agreement between measured and theoretical values is remarkable considering the complicated nature of the system.

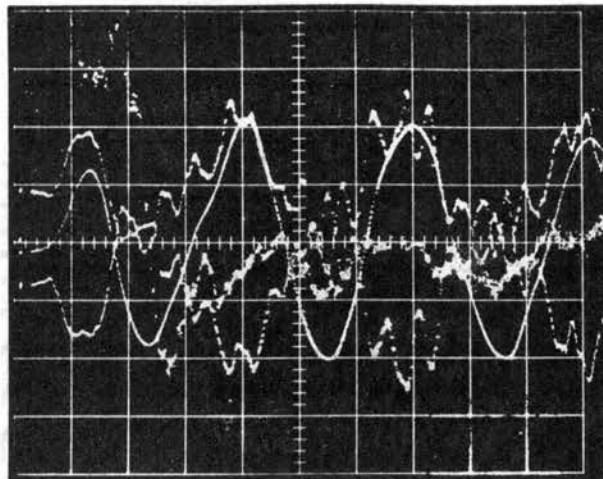


Figure 44. Oscilloscope Traces of
Test on Window-Room-
Door Model With Small
Room (1 cm. =
0.005 sec.)

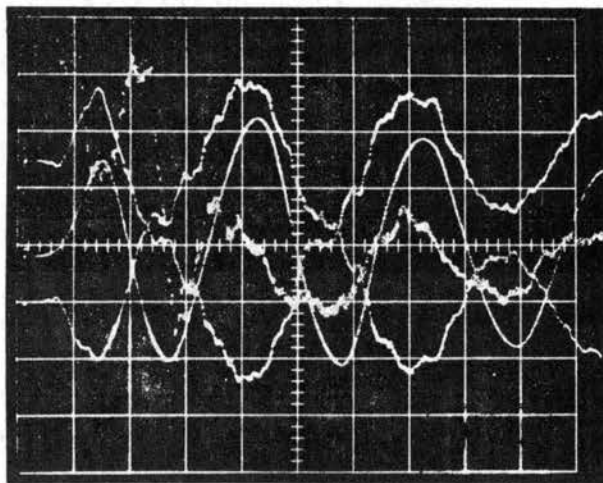


Figure 45. Oscilloscope Traces of
Test on Window-Room-
Door Model With Large
Room (1 cm =
0.005 sec.)

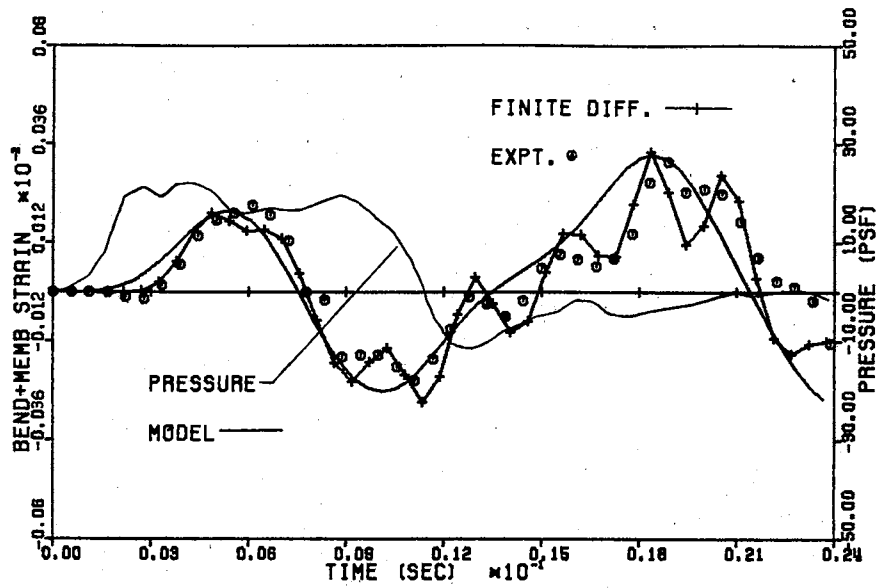


Figure 46. Strain in y Direction at Center of Front Surface of Plate in Window-Room-Door System (Small Room, Volume = 1.8 cu. ft.)

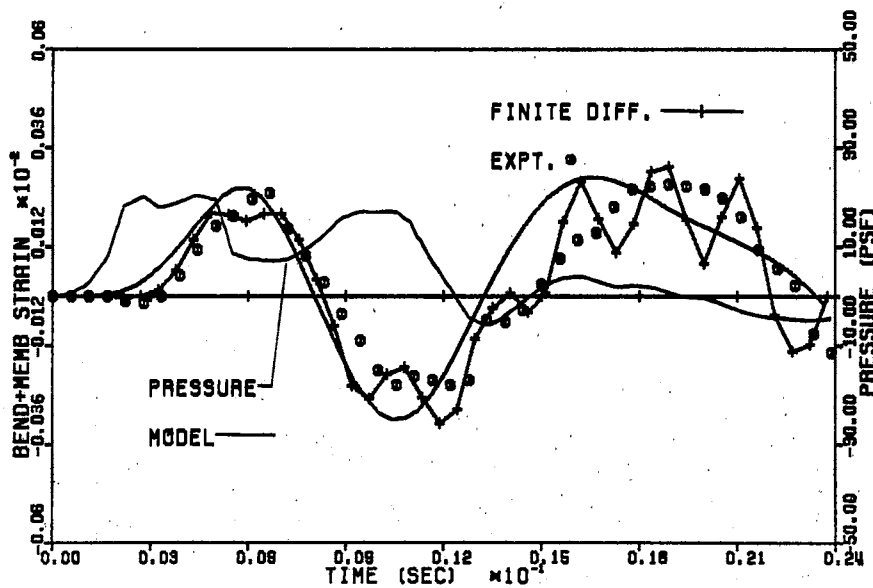


Figure 47. Strain in y Direction at Center of Front Surface of Plate in Window-Room-Door System (Large Room, Volume = 3.66 cu. ft.)

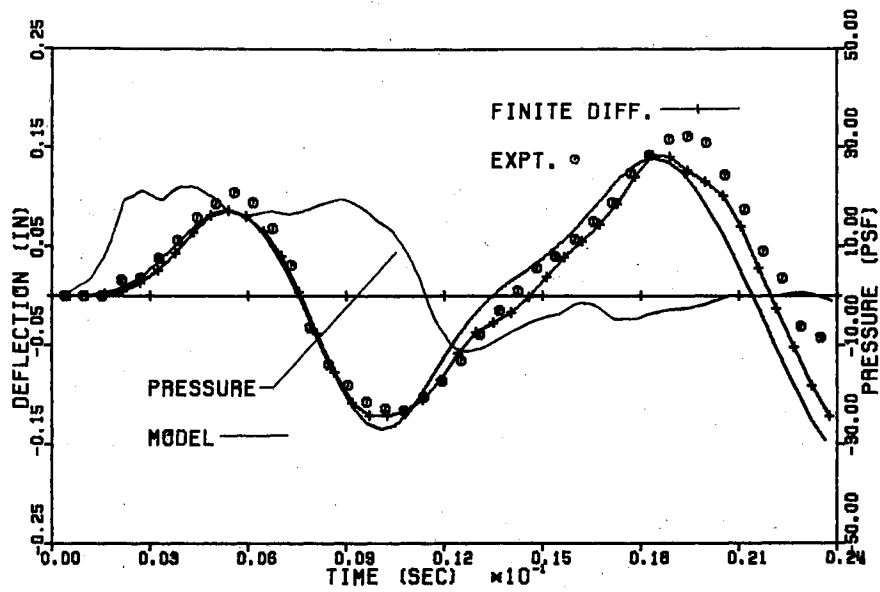


Figure 48. Plate Center Displacement for Window-Room-Door Model With Small Room

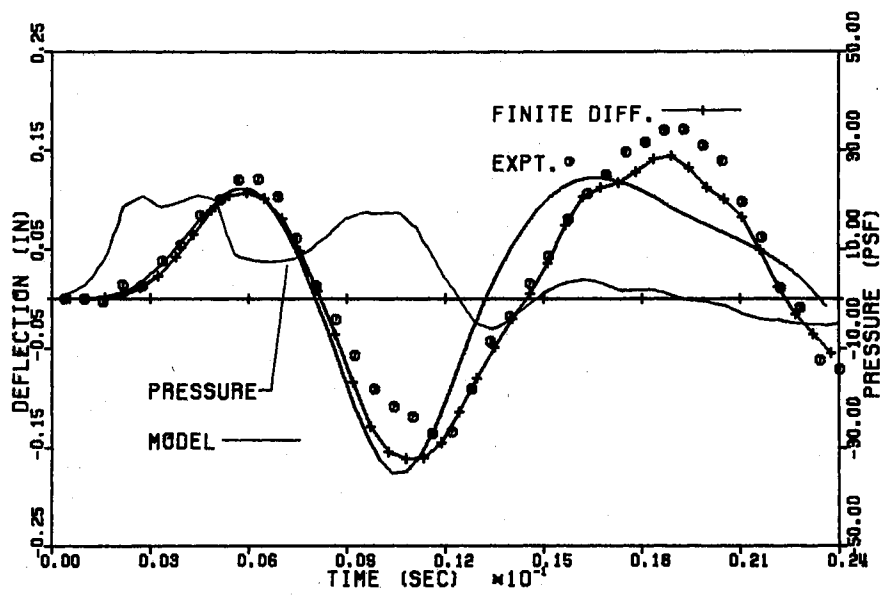


Figure 49. Plate Center Displacement for Window-Room-Door Model With Large Room

CHAPTER VI

SUMMARY, CONCLUSIONS AND RECOMMENDATIONS

An experimental study was made of the nonlinear, transient response of simply supported, thin, rectangular elastic plates subjected to pulse type loads. The reflected Moiré grid technique was used to obtain the deflection response of the plate over its entire surface at several instants during its motion. The strains at the surface of the plate at its center and at a quarter diagonal location were measured during its response.

The results of the experiments were compared with the theoretically predicted values. The theoretical values were obtained from a finite-difference solution, a single mode lumped parameter model, and a multimode, lumped parameter model based on the Von Kármán plate equations. The multimode lumped parameter model was derived as part of the present study, the other two solutions were already available.

The important practical case of a window coupled to a room and an open doorway was simulated experimentally on a small scale. Strain and deflection data at the center of the window was obtained

during its nonlinear response when both the window and the doorway were exposed to pressure pulses. The experimental results were compared with the finite-difference and the single mode lumped parameter model solutions for the plate which were suitably modified to account for the effect of the room and the doorway.

The following results were obtained:

- 1) Close agreement was obtained between the finite-difference solution of the Von Kármán plate equations and the experimentally measured response for maximum center displacement to thickness ratio of 0.85, 2.6 and 5.6.
- 2) The single mode, lumped parameter model for nonlinear plate response was sufficiently accurate at maximum deflection ratios of 0.85 and 2.6. However, at a deflection ratio of 5.6 the maximum strain predicted by the lumped parameter model was about 50% more than the experimental and the finite-difference values.
- 3) The multimode, lumped parameter model gave almost the same results as the finite-difference solution. The contribution of the higher modes increases as the amplitude of plate deflection increases. The presence of membrane stresses at larger deflections causes the shape of the deflected surface to deviate considerably

from a simple sinusoidal shape so that higher mode components are needed to describe the surface.

- 4) The cost of computation for the multimode, lumped parameter model was approximately one sixth the cost of the finite-difference solution.
- 5) At a deflection ratio of 5.6, the higher mode component of the experimentally measured strain was about 45% of the theoretically predicted values. This could be because the higher modes are most sensitive to damping and boundary conditions.
- 6) The reflected Moiré technique provided whole-field data on the deflection of the plate at several instants during its transient motion. The agreement between deflections measured by the Moiré method and the finite-difference values was within 10% except at 0.0094 sec. when the deviation was larger.
- 7) At large nonlinear deflections, a much greater area of the plate was found to be subjected to high stresses as compared to the linear case where the highest stresses occur only in the region around the center. The maximum stresses, for the nonlinear case, were in an area of the plate that was between the quarter diagonal point and the corner. In any predictions on the failure of glass windows

at large deflections, the effect of this stress distribution should be an important factor.

- 8) The finite-difference program for solving the Von Kármán equations was extended by applying it to the study of the transient response of a window coupled to a room and a doorway. Good agreement was obtained between experiment and finite-difference and single mode, lumped parameter solutions at a maximum center deflection to thickness ratio of 4.2.

The major conclusions from this study are:

- 1) The pulse generator and plane wave tube system described in this study is a versatile tool for experimental studies on the transient response of plates and simulated window-room-door systems. Since the energy of the pulse is confined inside the tube it is an efficient way of generating pulses of sufficient strength to cause large deflections or failure in thin glass plates.
- 2) The reflected Moiré technique is a simple and reliable method of recording whole-field deflection data during the transient response of plates and it is applicable to large deflections. It should be particularly helpful when thin glass plates are loaded to failure.

- 3) Comparison with experimental data obtained during this study indicates that the finite-difference solution of the Von Kármán equations accurately represents the behavior of simply supported, thin glass plates undergoing large amplitude transient motion.
- 4) The single mode lumped parameter model is accurate for relatively small deflection to thickness ratios (DT ratio) up to about 1.5. At larger DT ratios, it tends to overpredict the strain. Therefore, it is not advisable to use the single mode model for stress and safety calculations at large deflections.
- 5) At large dynamic deflections, a larger area of the plate is heavily stressed than for the case of linear deflections for which the maximum stresses are localized at the center.
- 6) The multimode lumped parameter model obtained by Galerkin's method gives results comparable to those obtained by the finite-difference technique at much less cost.
- 7) Experimental results obtained in the present study show that the transient response of a window-room-door system subjected to pressure pulses, which cause large deflections, can be simulated accurately by a combination of the finite-

difference model for the window and the lumped parameter representation for the room and open doorway. Useful, but less accurate results are obtained by using the single mode lumped parameter plate model for this case.

The following recommendations are made for further study:

- 1) The finite-difference solution of the Von Kármán equations may be extended to studies on the response of thin plates to steady, sinusoidal pressures. The practical application of such studies would be in the areas of panel flutter and plate response to wind storms and jet noise.
- 2) A more detailed study should be made of multimode lumped parameter models for nonlinear plate behavior. The finite-difference program offers a ready check on the accuracy of such models.
- 3) The failure of glass windows subjected to large amplitude, transient motion may be further investigated taking into account the greater area of the window that is subjected to high stresses as compared to the linear case.
- 4) Further experiments on thin glass plates may be conducted to study the failure criteria governing glass breakage due to pressure pulses.
- 5) In the present study, the Moiré fringe photographs were obtained by repeating the test for each instant of time at

which fringes were desired. A reliable method of obtaining a sequence of photographs during a single test is desirable. Such a method will be of great value in tests in which the glass is loaded to failure.

- 6) The reflected Moiré method gives only the deflection response of the plate. At large amplitudes, the in-plane deformations are also important. The possibility of using in-plane Moiré techniques for determining the in-plane components during nonlinear deformation needs to be investigated.
- 7) The various methods described in this study, both theoretical and experimental, may be extended to the study of nonisotropic plates.

BIBLIOGRAPHY

1. Th. Von Kármán. Encyklopädie der Mathematischen Wissenschaften. Vol. IV, p. 349, 1910.
2. Tadjbakhsh, I., and E. Saibel. "On the Large Elastic Deflections of Plates." ZAMM, Vol. 40 (1960), pp. 259-268.
3. Penning, R. L. "Elastic Stresses and Deflections of Flat Square Plates Under Uniformly Distributed Normal Pressure: A Critical Review." Jl. of Strain Analysis, Vol. 7 (1972), pp. 23-32.
4. Bayles, D. J. "Nonlinear Response of Thin Rectangular Plates Subjected to Pulse Type Loads." (Ph.D. Thesis, Oklahoma State University, May 1970).
5. Yamaki, N. "Influence of Large Amplitudes on Flexural Vibrations of Elastic Plates." ZAMM, Vol. 41 (1961), pp. 501-510.
6. Ventres, C. S., and E. H. Dowell. "Comparison of Theory and Experiment for Nonlinear Flutter of Loaded Plates." AIAA Journal, Vol. 8 (1970), pp. 2022-2030.
7. Farnsworth, C. E., and R. M. Evan-Iwanowski. "Resonance Response of Nonlinear Circular Plates Subjected to Uniform Static Load." JAM, Trans. ASME, Vol. 94 (1970), pp. 1043-1049.
8. Bennett, J. A. "Nonlinear Vibration of Simply Supported Angle Ply Laminated Plates." AIAA Journal, Vol. 9 (1971), pp. 1997-2003.
9. Edge, P. H., and H. H. Hubbard. "Review of Sonic Boom Simulation Devices and Techniques." JASA, Vol. 51 (1972), pp. 722-728.
10. Tomboulian, R. "Research and Development of a Sonic Boom Simulation Device." NASA-CR-1378 (1969).

11. Goodier, J. N., and G. H. Lee. "An Extension of the Photoelastic Method of Stress Measurements to Plates in Transverse Bending." JAM, Trans. ASME, Vol. 63 (1941), pp. A27-A29.
12. Mindlin, R. D. "Discussion of Above Paper." JAM, Trans. ASME, Vol. 63 (1941), pp. A187-A189.
13. Drucker, D. C. "The Photoelastic Analysis of Transverse Bending of Plates in the Standard Transmission Polariscopes." JAM, Trans. ASME, Vol. 64 (1942), pp. A161-A164.
14. Bednar, J. "Experimental Analysis of Plates Using the Method of Model Curing." Exp. Mech., Vol. 7 (1967), pp. 85-90.
15. Ligtenberg, F. K. "The Moire Method--A New Experimental Method for the Determination of Moments in Small Slab Models." Proc. SESA, Vol. 12, No. 2 (1955), pp. 83-98.
16. Nickola, W. E. "The Dynamic Response of Thin Membranes by the Moire Method." Exp. Mech., Vol. 6 (1966), pp. 593-601.
17. Hazell, C. R. "Visualization of Lateral Displacements of Vibrating Plates by the Shadow Moire Method." J. Mech. Engr. Sci., Vol. 11 (1969), pp. 214-219.
18. Theocaris, P. S. Moire Fringes in Strain Analysis. London: Pergamon Press, 1969.
19. Durelli, A. J., and V. J. Parkes. Moire Analysis of Strain. Prentice Hall, 1970.
20. Merchant, D. C., B. A. Wasil, and J. J. Del Veschio, Jr. "Photogrammetric Measurement of Dynamic Displacements." Exp. Mech., Vol. 5 (1965), pp. 332-339.
21. Powell, R. L., and K. A. Stetson. "Interferometric Vibration Analysis by Wave Reconstruction." J. Opt. Soc. Am., Vol. 55 (1965), pp. 1593-1598.
22. Lowery, R. L. "Critical Structural Response to the Sonic Boom." NASA CR-66750 (Dec. 1968).

23. Rajagopal, Ganesh, T. V. Seshadri, and R. L. Lowery.
"Critical Response of Some Multidegree of Freedom
Mechanoacoustical Systems." Presented at the 81st
Meeting of the Acoustical Society of America, Washington,
D. C., (April 20-23, 1971).
24. Clarkson, B. L., and W. H. Mayes. "Sonic-Boom-Induced
Building Structure Responses Including Damage." JASA,
Vol. 51 (1972), pp. 742-757.
25. Bayles, D. J., R. L. Lowery, and D. E. Boyd. "A Nonlinear
Dynamic Lumped-Parameter Model of a Rectangular
Plate." J. of Sound and Vibration, Vol. 21 (1972),
pp. 329-337.
26. Lin, Y. K. Probabilistic Theory of Structural Dynamics.
McGraw Hill (1967), p. 225.

APPENDIX A

The following computer program gives the finite-difference solution to the Von Kármán equations for the transient response of simply supported, thin, elastic plates with no in-plane edge restraints subjected to a uniform pressure pulse. It has the window-room-door system as an option. Its usage is given as part of the listing.

C
 C
 C THIS PROGRAM COMPUTES THE RESPONSE OF THIN, SIMPLY SUPPORTED
 C RECTANGULAR, ELASTIC PLATES SUBJECTED TO SYMMETRIC
 C PRESSURE LOADING. THE VON KARMAN PLATE EQUATIONS
 C ARE SOLVED BY THE METHOD OF FINITE DIFFERENCES
 C MORE DETAILS ABOUT THE PROGRAM CAN BE FOUND IN
 C A THESIS BY D.J. BAYLES-'NONLINEAR DYNAMIC RESPONSE OF
 C THIN RECTANGULAR PLATES SUBJECTED TO PULSE TYPE LOADS'.
 C OKLAHOMA STATE UNIVERSITY, MAY 1970.
 C THE FOLLOWING PROGRAMS AND SUBROUTINES ARE REQUIRED:
 C MAIN,PGM1,DLINT,FDIA,COEFA,AGEA,PGM2
 C JACK BAYLES,CURTIS IKARD AND GANESH RAJAGOPAL D.S.U.
 C
 C THE DATA CARDS SHOULD BE IN THE FOLLOWING SEQUENCE
 C CARD 1 FORMAT(A4) IPGMS
 C IPGMS: INSERT PGM1 IF NEW SET OF DATA IS
 C TO BE CALCULATED
 C INSERT PGM2 IF DATA HAS ALREADY BEEN
 C CALCULATED AND STORED ON DISK AND ONLY
 C SOME PARTICULAR DATA POINTS ARE TO
 C BE OUTPUT. IN THIS CASE SEE
 C 'USAGE-PGM2' WHICH FOLLOWS.
 C
 C CARD 2 FORMAT(3D15.8) TS,PL,TAU
 C TS: STOP TIME FOR THE INTEGRATION (SEC)
 C PL: MAGNITUDE OF N WAVE (PSF)
 C TAU: DURATION OF N WAVE (SEC)
 C IF INPUT PRESSURE IS NOT A N WAVE, PS AND
 C TAU CAN BE LEFT BLANK
 C
 C CARD 3: FORMAT(I4I5) IFTAB,NTAB,IFCDT,IFVOL
 C IFTAB: 0 IF INPUT DATA IS NOT TABULATED
 C 1 IF INPUT DATA IS IN THE FORM OF
 C A TABLE OF NUMBERS.
 C NTAB: NUMBER OF DATA POINTS IN TABLE
 C IFCDT: 0 IF TABLE IS NOT AT UNIFORM TIME
 C INTERVALS
 C 1 IF TABLE IS AT UNIFORM TIME INTERVALS
 C IFVOL: 0 PLATE ALONE
 C 1 WINDOW-ROOM-DOOR SYSTEM
 C
 C CARD 4: FORMAT(D15.8) DTTAB
 C DTTAB: (IFCDT=1) UNIFORM TIME INTERVAL OF
 C TABULATED INPUT DATA.
 C
 C CARD 5: FORMAT(D15.8) TTAB
 C TTAB: (IFTAB=1 AND IFCDT.LE.0) UNITS (SEC)
 C TIMES AT WHICH PRESSURE DATA ARE TABULATED
 C NTAB VALUES ARE REQUIRED IN SEQUENCE, ONE
 C VALUE PER CARD.
 C
 C CARD 6: FORMAT(D15.8) PSCALE
 C PSCALE: MULTIPLYING FACTOR FOR TABULATED
 C PRESSURE VALUES TO CONVERT THEM INTO
 C POUNDS PER SQUARE FOOT UNITS.
 C
 C CARD 7: FORMAT(D15.8) PTAB
 C PTAB: NTAB VALUES FOR THE INPUT PRESSURE

C
 C (IFTAB=1) ONE VALUE PER CARD
 C
 C CARD 8: FORMAT(3D15.8) AX,BY,H
 C AX: LENGTH OF PLATE (FT)
 C BY: WIDTH OF PLATE (FT)
 C H: THICKNESS OF PLATE (IN)
 C
 C CARD 9: FORMAT(3D15.8) E,PR,SW
 C MATERIAL PARAMETERS
 C E: YOUNGS MODULUS (PSI)
 C PR: POISSONS RATIO
 C SW: SPECIFIC WEIGHT (LBF/FT**3)
 C
 C CARD 10: FORMAT(2I5,2D15.8) M,N,DX,DT,
 C M: NUMBER OF GRID POINTS IN X DIRECTION
 C N: NUMBER OF GRID POINTS IN Y DIRECTION
 C DX: GRID LENGTH (FT) MUST BE SAME IN
 C X AND Y DIRECTIONS.
 C DT: INTEGRATION STEP SIZE (SEC) MUST BE
 C LESS THAN CRITICAL VALUE FOR
 C STABILITY. (REFER TO D.J. BAYLES' THESIS)
 C NOTES: M MUST BE GREATER THAN OR EQUAL TO 5
 C ALSO M.LE.N
 C DIMENSIONS HAVE BEEN SET UP FOR
 C A MAXIMUM OF M*N=64 GRID POINTS.
 C
 C INTRODUCE NEXT CARD ONLY IF IFVOL=1
 C CARD 11: FORMAT(4D15.5) EL,AR,VOL,Z
 C EL: EFFECTIVE LENGTH OF DOOR (FT)
 C AR: AREA OF DOOR (FT**2)
 C VOL: VOLUME OF ROOM (FT**3)
 C Z: EFFECTIVE DAMPING FACTOR AT DOOR
 C
 C CARD 11: FORMAT(5I5) NSD,NMULT,NREC,NSREC,IFSOP
 C OUTPUT INFORMATION
 C NSD: NUMBER OF OUTPUT POINTS
 C NMULT: MULTIPLES OF THE TIME INTERVALS AT WHICH DATA IS
 C STORED ON THE DISK AT WHICH STRESS-STRAIN OUTPUT
 C IS DESIRED.
 C NREC: NUMBER OF RECORDS ON DISK
 C NSREC: STARTING RECORD FOR STRESS-STRAIN
 C CALCULATIONS
 C IFSOP: 0 PARTICULAR RECORDS ONLY ARE TO BE
 C OUTPUT. THESE RECORD NUMBERS
 C ARE GIVEN UNDER IVREC. (NEXT)
 C 1 SUCCESSIVE RECORDS SEPARATED
 C IN TIME BY NMULT*DT ARE TO BE
 C OUTPUT
 C
 C NOTES: THIS PROGRAM HAS BEEN SET UP TO STORE
 C A MAXIMUM OF 289 RECORDS ON A DISK. EACH RECORD
 C CONTAINS TIME, DEFLECTION AND STRESS FUNCTION
 C AT EACH GRID POINT AT THAT TIME. THE DATA IS STORED AT
 C 1) EVERY INTEGRATION STEP IF
 C (TS/DT)+1 .E.289
 C 2) EVERY OTHER INTEGRATION STEP IF
 C (TS/DT)+1 .GT.289.AND.LT.594
 C 3) EVERY FIFTH INTEGRATION STEP IF
 C (TS/DT)+1 .GT.594.AND.LT.1188

```

C          4) EVERY TENTH INTEGRATION STEP IF
C          (TS/DT)+1.GT.1100.AND.LT.2376
C          5) PROGRAM QUITS IF (TS/DT)+1.GT.2376
C
C      FOR EACH OF THE CASES ABOVE, THE NUMBER
C      OF RECORDS, NREC, IS THEN
C          1) NREC=(TS/DT)+1
C          2) NREC=(TS/(2*DT))+1
C          3) NREC=(TS/(5*DT))+1
C          4) NREC=(TS/(10*DT))+1
C
C      NMULT IS THE MULTIPLE OF THE TIME INTERVALS
C      BETWEEN RECORDS
C
C      CARD12:  FORMAT(16I5)(IVREC(I),I=1,NSD)
C      REQUIRED ONLY IF IFSOP=0
C      IVREC(I)= THE PARTICULAR NUMBERS OF THE
C      RECORDS WHICH ARE TO BE OUTPUT
C
C      CARD13:  FORMAT(16I5)(IOPV(I),I=1,MN)
C      IOPV(I)= 0 NO PRINT OR PUNCH
C              1 PRINT
C              2 PRINT AND PUNCH
C
C      THIS CONTROLS NATURE OF STRESS, STRAIN,
C      DEFLECTION OUTPUT AT EACH GRID POINT FOR
C      THE SELECTED NSD TIMES AT WHICH OUTPUT
C      IS DESIRED
C
C      PUNCHED OUTPUT FORMAT:
C      FGMAT(5D15.7,I5) EPXB,EPXM,EPYB,EPYM,DEFLECTION,I
C      EPXB:  BENDING STRAIN IN X DIRECTION
C      EPXM:  MEMBRANE STRAIN IN X DIRECTION
C      EPYB:  BENDING STRAIN IN Y DIRECTION
C      EPYM:  MEMBRANE STRAIN IN Y DIRECTION
C      DEFLECTION: DEFLECTION IN INCHES
C      I:     GRID POINT AT WHICH DATA IS OUTPUT.
C
C      THIS PROGRAM ALSO OUTPUTS PRESSURE AND CENTER DEFLECTION
C      AT EACH INTEGRATION STEP AND DEFLECTION PROFILE IN X AND Y
C      DIRECTIONS AT THE CENTER OF THE PLATE AT EVERY TENTH
C      INTEGRATION STEP.
C
C      *USAGE - PGM2*
C          FOR IPGMS IN CARD #1, PGM2 MAY BE
C          INSERTED WHEN DATA HAS ALREADY BEEN
C          PUT ON DISK AND INFORMATION IS TO BE OUTPUT
C          ONLY AT PARTICULAR TIMES. THE
C          FOLLOWING SEQUENCE OF CARDS IS THEN REQUIRED
C
C      CARD 1:  FORMAT(A4)IPGMS
C              IPGMS=PGM2
C      CARD 2:  FORMAT(4D15.8) E,H,PR,DX
C      CARD 3:  FORMAT(2I5)M,N
C      CARD 4:  FORMAT(5I5)NSD,NMULT,NREC,NSREC,IFSOP
C      CARD 5:  FORMAT(16I5)(IVREC(I),I=1,NSD)
C      CARD 6:  FORMAT(16I5)(IOPV(I),I=1,MN)
C              SYMBOLS HAVE SAME MEANING AS BEFORE

```

```

C
C      MAIN
C
C      IMPLICIT REAL*8 (A-H,O-Z)
C
C      COMMON E,H,PR,DX,M,N,ID4
C
C      10 FORMAT (4D15.8)
C      20 FORMAT (A4)
C      30 FORMAT (2I5)
C      699 FORMAT (*1 SKIP A PAGE BETWEEN CASES* )
C
C      DATA IPGM2 /'PGM2'/
C
C      DEFINE A FILE FOR DIRECT ACCESS WITH UP TO 300 RECORDS, EACH WITH
C      A FIXED LENGTH OF 258 STORAGE WORDS. (I,N(64),F(64) = 129 DOUBLE
C      PRECISION WORDS = 258 STORAGE WORDS.)
C
C      DEFINE FILE 4(300,258,U,ID4)
C
C      999 READ (5,20) IPGMS
C          IF (IPGMS .EQ. IPGM2) GO TO 100
C          READ (5,10) TS,PL,TAU
C          ID4=1
C          CALL PGM1 (TS,PL,TAU)
C          GO TO 200
C      100 READ (5,10) E,H,PR,DX
C          READ (5,30) M,N
C      200 CALL PGM2
C          WRITE (6,699)
C          GO TO 999
C      END
C
C
C      SUBROUTINE PGM1 (TS,PL,TAU)
C      IMPLICIT REAL*8 (A-H,C-Z)
C
C      COMMON E,H,PR,DX,M,N,ID4
C
C      DIMENSION W( 64,12),F( 64,12),A( 64, 64),B( 64),C( 64),B8( 64)
C      1 ,DC(1800),P(12)
C      DIMENSION TTAB(100), FTAB(100)
C      DIMENSION POP(11)
C      DIMENSION EX2(12),PI(12)
C
C      KR=64
C
C      INPLT FORMATS.
C      100 FORMAT (3D15.8)
C      101 FORMAT (2I5,2D15.8)
C      500 FORMAT(4I5)
C      501 FORMAT (D15.8)
C
C      CLTPUT FORMATS.

```



```

110 FORMAT (//1X,'TIME = ',F7.5,10X,'ID4 = ',I5)
111 FORMAT (1X,10D13.5)
120 FORMAT (*1 TIME RESPONSE SUBROUTINE SUBPROGRAM (PGM1)*
* //11X,'FROM A MAIN PROGRAM BY JACK BAYLES MAY 1970'
* //11X,'FINAL CHANGES BY ROBERT C IKARD JULY 1971'
* //11X,'BASIC PLATE INPUT DATA IS AS FOLLOWS'
* //11X,'AX (LENGTH ---- X-DIRECTION) =',F16.10,' FEET'
* //11X,'BY (LENGTH ---- Y-DIRECTION) =',F16.10,' FEET'
* //11X,'H (PLATE THICKNESS) =',F16.10,' INCHES'
* //11X,'E (MODULUS) =',D16.8,' PSI'
* //11X,'PR (POISSON'S RATIO) =',F16.10
* //11X,'SW (SPECIFIC WEIGHT) =',F16.10,' PCF / )
121 FORMAT (//11X,'N-WAVE LOAD-TIME PROFILE OPTION'
* //11X,'PL (PRESSURE LEVEL) =',F16.10,' PSF'
* //11X,'TAU (PERIOD) =',F16.10,' SECONDS' )
122 FORMAT (//11X,'TIME RESPONSE CONTROL PARAMETERS'
* //11X,'M (X-DIRECTION NODE POINTS) =',I5
* //11X,'N (Y-DIRECTION NODE POINTS) =',I5
* //11X,'DX (GRID SIZE - EQUAL X,Y) =',F16.12,' FEET'
* //11X,'DT (TIME INCREMENT) =',F16.12,' SECONDS' /// )
600 FORMAT (*1 NUMBER OF TIME STEPS EXCEEDS STORAGE.*
* //2X,'TTIME =',D12.4
* //2X,'PROGRAM HAS ENDED.* )
601 FORMAT (/5X,'TIME-PRESSURE VARIATION DESCRIBED BY TABULAR INPUT'
* //5X,'NUMBER OF TIME-PRESSURE POINTS =',I5
* //5X,'TIME',11X,'PRESSURE' / )
602 FORMAT (1X,D12.5,5X,D12.5)
603 FORMAT ( /1X,'PRESSURE, CENTER DISPLACEMENT AND STRESS FUNCTION FO
*R A SET OF 10 TIME POINTS.* )
604 FORMAT(/1X,
1*Y CENTERLINE DISPLACEMENT AND STRESS FUNCTION AND X CTR LINE DISP FOR
ITIME=',F7.5)
C
C START AT THE FIRST RECCRD ON UNIT 4.
ID4=1
READ(5,500)IFTAB,NTAB,IFCDT,IFVOL
IF (IFTAB .LE. 0) GO TO 87
IF (IFCDT .LE. 0) GO TO 77
READ (5,501) DTTAB
DO 75 I=1,NTAB
75 TTAB(I) = (I-1) * DTTAB
GO TO 78
77 READ (5,501) (TTAB(I),I=1,NTAB)
78 READ (5,501) PSCALE
READ (5,501) (PTAB(I),I=1,NTAB)
DO 59 I=1,NTAB
59 PTAB(I) = PSCALE * PTAB(I)
67 READ (5,100) AX,BY,H,E,PR,SW
WRITE(6,120) AX,BY,H,E,PR,SW
IF (IFTAB .LE. 0) GO TO 88
WRITE (6,601) NTAB
WRITE (6,602) (TTAB(I),PTAB(I),I=1,NTAB)
GO TO 89
88 WRITE(6,121) PL,TAU
89 RO=SW/32.200
D=E*H**3/(12.00*(1.00-PR**2))
READ (5,101) M,N,DX,DT
WRITE(6,122) M,N,DX,DT
TTIME = TS / DT

```

```

IF(TTIME.LE.2376.00) GO TO 15
WRITE(6,600) TTIME
GG TC 90
15 IF(TTIME.GT.1188.00) GO TO 205
IF(TTIME.GT.594.00) GO TO 200
IF(TTIME.GT.289.00) GO TO 201
INCR=1
GO TO 17
201 INCR=2
GO TO 17
200 INCR=5
GO TO 17
205 INCR=10
17 TMFLT=DFLOAT(INCR)
T=C.DO
MN=M*IN
CI=DT**2*D/(RO*H*DX**4)
C2=DT**2/(RO*DX**4)
C3=DT**2*144.00/(RO*H)
C
C SET UP (A) MATRIX
CALL COEFA (A,M,N,KR)
CALL AGEA (A,DC,M,N,KR)
C
C SET UP INITIAL CONDITIONS
C CHECK FOR WINDOW-ROGM-DGOR OPTION
IF(IFVOL-1)300,301,300
301 CONTINUE
READ(5,605)EL,AR,VOL,Z
605 FORMAT(4D15.5)
EL1=EL
EMZ= EL1*AR*1.4*14.7*144./(1100.*1100.)
EK22=1.4*14.7*144./VOL
WRITE(6,606)EL,AR,VOL,EMZ,Z
606 FORMAT(2X,'INPUT FOR ROGM DOOR ETC ',5(2X,D12.5))
MMNAT=1100.*DSQRT(AR/(EL1*VOL))
EMTEM=EMZ/(DT*OT)
ZTEM=Z*MMNAT*EMZ/DT
FACT1=2.*EMTEM/(EMTEM+ZTEM)
FACT2=(ZTEM-EMTEM)/(EMTEM+ZTEM)
FACT3=-AR/(EMTEM+ZTEM)
CTEM=DT*DT/EMZ
EX2(1)=0.00
EX2(2)=-AR*PTAB(1)*DTEM
PI(1)=0.00
300 CONTINUE
DO(3)=1,MN
F(I,1)=0.00
3 W(I,1)=0.00
C
C CALCULATE LOAD AT FIRST TIME STEP
IF (IFTAB .LE. 0) GO TO 37
C
C TABULAR VALUES.
PI(1) = PTAB(1)
GO TO 38
C
C N-WAVE
37 PI(1)=PL

```

```

C
C STARTING FORMULA
38 DO5I=1,MN
5 W(I,2)=-.5DO*C3*P(1)
POP(1) = P(1)
6 CONTINUE

C
C CALCULATE LOAD FOR NEXT 10 TIME STEPS
IF (IFTAB .LE. 0) GO TO 70

C
C TABULAR VALUES.
IF (T .GT. TTAB(NTAB)) GO TO 8
DO 56 J=2,11
T = T + DT
CALL DLINT1 (TTAB,T,PTAB,PINT,NTAB)
P(J) = PINT
IF (T .LE. TTAB(NTAB)) GO TO 56
P(J) = 0.00
56 CONTINUE
GO TO 10

C
C N-WAVE
7C IF(T.GT.TAU) GO TO 8
DO7J=2,11
T=T+DT
P(J)=PL*(1.00-2.00*T/TAU)
IF(T.LE.TAU) GO TO 7
P(J)=0.00
7 CONTINUE
GO TO 10
8 DO9J=2,11
T=T+DT
9 P(J)=0.00
10 CONTINUE

C
C CALCULATE W & F FOR 10 TIME STEPS
CALL FDIA(M,N,MN,W,F,A,B,C,BB,DC,P,C1,C2,C3,E,KR,EK22,DTEM,
1 AR,EX2,P1,DX,FACT1,FACT2,FACT3,IFVOL)
TT = T - 10.00 * DT
WRITE (6,110) TT,1D4
DO 479 I=2,11
479 POP(I) = P(I)
WRITE (6,603)
WRITE (6,111) (POP(I),I=1,10)
POP(1) = P(11)
WRITE(6,111) (W(MN,J),J=1,10)
WRITE(6,111) (F(MN,J),J=1,10)
TMM = TT + 9.00 * DT
WRITE (6,604) TMM
WRITE(6,111) (W(I,10),I=M,MN,M)
WRITE(6,111) (F(I,10),I=M,MN,M)
NCAT=MN-M+1
WRITE(6,111)(W(I,10),I=NCAT,MN)
IF(IFVOL-11302,303,302)
303 CONTINUE
EX2(1)=EX2(11)
EX2(2)=EX2(12)
P1(1)=P1(11)
302 CONTINUE

```

```

TW=TT
DO 20 J=1,10,INCR
WRITE (4*104) TW,(W(1,J),I=1,MN),(F(1,J),I=1,MN)
20 TW = TW + IMFLT * DT
DO7I=1,MN
F(1,1)=F(1,11)
W(1,1)=W(1,11)
71 W(1,2)=W(1,12)
IF (TT .LT. TS) GO TO 6
GO TO 199
9C CALL EXIT
199 RETURN
END

```

```

C
C
C
C SUBROUTINE FDIA(M,N,MN,W,F,A,B,C,BB,DC,P,C1,C2,C3,E,KR,EK22,DTEM,
1 AR,EX2,P1,DX,FACT1,FACT2,FACT3,IFVOL)
IMPLICIT REAL*8 (A-H,O-Z)
DIMENSION W(KR,1),F(KR,1),A(KR,1),B(1),C(1),BB(1),DC(1),P(1)
DIMENSION EX2(1),P1(1)
C SET UP CONSTANTS ONE TIME ONLY
1 IF(MN,1).NE.0.) GO TO 2
M1=M+1
M2=2*M
M3=3*M
M4=4*M
MNM=MN-M
LT=(A-2)*M+1
LN=N-2
LM=M-1
LLN=N-3
LLM=M-2
LLT=LT+2
LLS=MNM-2
M21=M2+1
LS=(N-3)*M+1
LST=(N-2)*M
2 CONTINUE
CO70J=2,11

C
C USE LINEAR TERMS ONLY FOR VERY SMALL W
C
IF(W(MN,J)*W(MN,J).GT.0.0001D0)GO TO 10
DO3I=1,MN
F(I,J)=0.00
3 BB(I)=0.00
GO TO 50
10 CONTINUE

C
C CALCULATE CONSTANT VECTOR FOR A F=C (SS GR C)
C(1)=(W(M+2,J)**2/10.00-(-2.00*W(1,J)+W(2,J))*(-2.00*W(1,J)+
1 W(M+1,J)))*E

```

```

C(M) = (-2.00*W(M-1,J) - 2.00*W(M,J)) * (W(M2,J) - 2.00*W(M,J)) * E
C(MN) = (-2.00*W(MN-1,J) - 2.00*W(MN,J)) * (2.00*W(MNM,J) - 2.00*W(MN,J)) * E
1  ) * E
K=MNM+1
C(K) = (-2.00*W(K,J) + W(K+1,J)) * (2.00*W(K-M,J) - 2.00*W(K,J)) * E
DO11I=2,LM
K=I+M
C(I) = ((-W(K-1,J) + W(K+1,J)) ** 2 / 16.00 - (W(I-1,J) - 2.00*W(I,J) + W(I+1,J))
1  ) * (-2.00*W(I,J) + W(K,J)) * E
K=MNM+1

```

```

11 C(K) = (-W(K-1,J) - 2.00*W(K,J) + W(K+1,J)) * (2.00*W(K-M,J) - 2.00*W(K,J)) * E
1  ) * E
DO12I=M1,LT,M
IM=I+M
IL=I-M

```

```

12 C(I) = ((W(IM+1,J) - W(IL+1,J)) ** 2 / 16.00 - (2.00*W(I,J) + W(I+1,J)) *
1  (W(IL,J) - 2.00*W(I,J) + W(IM,J))) * E
DO13I=M2,MNM,M
IM=I+M
IL=I-M

```

```

13 C(I) = (-2.00*W(I-1,J) - 2.00*W(I,J)) * (W(IL,J) - 2.00*W(I,J) + W(IM,J))
1  ) * E
DO14K=1,LM
KM=K+M
DO14L=2,LM
I=KM+L
IM=I+M
IL=I-M

```

```

14 C(I) = ((W(IL-1,J) - W(IM-1,J)) + W(IM+1,J) - W(IL+1,J)) ** 2 / 16.00 - (W(I-1,J)
1  - 2.00*W(I,J) + W(I+1,J)) * (W(IL,J) - 2.00*W(I,J) + W(IM,J)) * E

```

PERFORM GAUSS ELIMINATION ON C(I)

```

21 KK=0
L=2*M+1
K=1
22 I=K+1
23 KK=KK+1
C(I) = C(I) - DC(KK)*C(K)
IF(I-L) 24,25,40
24 I=I+1
GOTO23
25 IF(L.LT.MN) L=L+1
26 IF(K-MN+1) 27,31,40
27 K=K+1
GGTC22

```

PERFORM BACK SUBSTITUTION FOR F(I)

```

31 LL=MN-M2
L=MN
F(L,J) = C(L) / A(L,L)
I=MN-1
32 IF(I.LT.LL) L=L-1
K=I+1
S=0.00
33 S=S+A(I,K)*F(K,J)
IF(K-L) 34,35,40
34 K=K+1

```

```

GGT033
35 F(I,J) = (C(I) - S) / A(I,I)
IF(I-1) 40,40,36
36 I=I-1
GGTC32
40 CONTINUE

```

CALCULATE NONLINEAR TERMS FOR SS OR C

```

BB(I) = (-2.00*F(1,J) + F(M+1,J)) * (-2.00*W(1,J) + W(2,J)) + (-2.00*F(1,J) +
1  F(2,J)) * (-2.00*W(1,J) + W(M+1,J)) - (F(M+2,J) * W(M+2,J)) / 8.00
BB(M) = (-2.00*F(M,J) + F(M2,J)) * (2.00*W(M-1,J) - 2.00*W(M,J)) + (2.00*
1  F(M-1,J) - 2.00*F(M,J)) * (-2.00*W(M,J) + W(M2,J))
BB(MN) = (2.00*F(MNM,J) - 2.00*F(MN,J)) * (2.00*W(MN-1,J) - 2.00*W(MN,J)) +
1  (2.00*F(MN-1,J) - 2.00*F(MN,J)) * (2.00*W(MNM,J) - 2.00*W(MN,J))
K=MNM+1

```

```

BB(K) = (2.00*F(K-M,J) - 2.00*F(K,J)) * (-2.00*W(K,J) + W(K+1,J)) +
1  (-2.00*F(K,J) + F(K+1,J)) * (2.00*W(K-M,J) - 2.00*W(K,J))
DO41I=2,LM
K=I+M

```

```

BB(I) = (-2.00*F(I,J) + F(K,J)) * (W(I-1,J) - 2.00*W(I,J) + W(I+1,J)) +
1  (F(I-1,J) - 2.00*F(I,J) + F(I+1,J)) * (-2.00*W(I,J) + W(K,J)) -
2  (-F(K-1,J) + F(K+1,J)) * (-W(K-1,J) + W(K+1,J)) / 8.00
K=MNM+1

```

```

41 BB(K) = (2.00*F(K-M,J) - 2.00*F(K,J)) * (W(K-1,J) - 2.00*W(K,J) + W(K+1,J)) +
1  (F(K-1,J) - 2.00*F(K,J) + F(K+1,J)) * (2.00*W(K-M,J) - 2.00*W(K,J))
DO42I=M1,LT,M
IM=I+M
IL=I-M

```

```

42 BB(I) = (F(IL,J) - 2.00*F(I,J) + F(IM,J)) * (-2.00*W(I,J) + W(I+1,J)) +
1  (-2.00*F(I,J) + F(I+1,J)) * (W(IL,J) - 2.00*W(I,J) + W(IM,J)) -
2  (F(IM-1,J) - F(IL+1,J)) * (W(IM+1,J) - W(IL+1,J)) / 8.00
DO43I=M2,MNM,M
IM=I+M
IL=I-M

```

```

43 BB(I) = (F(IL,J) - 2.00*F(I,J) + F(IM,J)) * (2.00*W(I-1,J) - 2.00*W(I,J)) +
1  (2.00*F(I-1,J) - 2.00*F(I,J)) * (W(IL,J) - 2.00*W(I,J) + W(IM,J))
DO44K=1,LM
KM=K+M
DO44L=2,LM
I=KM+L
IM=I+M
IL=I-M

```

```

44 BB(I) = (F(IL,J) - 2.00*F(I,J) + F(IM,J)) * (W(I-1,J) - 2.00*W(I,J) + W(I+1,J))
1  + (F(I-1,J) - 2.00*F(I,J) + F(I+1,J)) * (W(IL,J) - 2.00*W(I,J) + W(IM,J)) -
2  (F(IL-1,J) - F(IM-1,J) + F(IM+1,J) - F(IL+1,J)) *
3  (W(IL-1,J) - W(IM-1,J) + W(IM+1,J) - W(IL+1,J)) / 8.00
50 CONTINUE

```

CALCULATE DEL FOURTH W FOR SIMPLY SUPPORTED

```

B(1) = 16.00*W(1,J) - 8.00*(W(2,J) + W(M1,J)) + 2.00*W(M1+1,J) + W(3,J) +
1  W(M2+1,J)
B(2) = 19.00*W(2,J) - 8.00*(W(1,J) + W(3,J) + W(M+2,J)) + 2.00*W(M1,J) +
1  W(M+3,J) + W(4,J) + W(M2+2,J)
B(M1) = 19.00*W(M1,J) - 8.00*(W(M+2,J) + W(M2+1,J) + W(1,J)) + 2.00*
1  (W(M2+2,J) + W(2,J)) + W(M+3,J) + W(M3+1,J)
B(M+2) = 20.00*W(M+2,J) - 8.00*(W(M1,J) + W(M+3,J) + W(M2+2,J) + W(2,J)) +
1  2.00*(W(M2+1,J) + W(M2+3,J) + W(1,J) + W(3,J)) + W(M+4,J) + W(M3+2,J)

```

```

B(M-1)=20.DO*W(M-1,J)-8.DO*(W(M-2,J)+W(M,J)+W(M-1,J))+2.DO*
1 (W(M-2,J)+W(M2,J))+W(M-3,J)+W(M3-1,J)
B(M)=19.DO*W(M,J)-8.DO*(2.DO*W(M-1,J)+W(M2,J))+4.DO*W(M-1,J)+
1 2.DO*W(M-2,J)+W(M3,J)
B(M-1)=21.DO*W(M-1,J)-8.DO*(W(M-2,J)+W(M2,J)+W(M-1,J)+W(M-1,J)
1 )+2.DO*W(M-2,J)+W(M3,J)+W(M-2,J)+W(M,J)+W(M-3,J)+W(M4-1,J)
B(M2)=20.DO*W(M2,J)-8.DO*(2.DO*W(M-1,J)+W(M3,J)+W(M,J))+4.DO*
1 (W(M-1,J)+W(M-1,J))+2.DO*W(M-2,J)+W(M4,J)
K=LT
B(K)=20.DO*W(K,J)-8.DO*(W(K+1,J)+W(K+M,J)+W(K-M,J))+2.DO*
1 (W(K+M1,J)+W(K-LM,J))+W(K+2,J)+W(K-M2,J)
K=K+1
B(K)=21.DO*W(K,J)-8.DO*(W(K-1,J)+W(K+1,J)+W(K+M,J)+W(K-M,J))+2.DO*
1 (W(K+LM,J)+W(K+M1,J)+W(K-M1,J)+W(K-LM,J))+W(K+2,J)+W(K-M2,J)
K=MNM+1
B(K)=19.DO*W(K,J)-8.DO*(W(K+1,J)+2.DO*W(K-M,J))+4.DO*W(K-LM,J)+
1 W(K+2,J)+2.DO*W(K-M2,J)
K=K+1
B(K)=20.DO*W(K,J)-8.DO*(W(K-1,J)+W(K+1,J)+2.DO*W(K-M,J))+4.DO*
1 (W(K-M1,J)+W(K-LM,J))+W(K+2,J)+2.DO*W(K-M2,J)
K=MNM-1
B(K)=22.DO*W(K,J)-8.DO*(W(K-1,J)+W(K+1,J)+W(K+M,J)+W(K-M,J))+2.DO*
1 (W(K+LM,J)+W(K+M1,J)+W(K-M1,J)+W(K-LM,J))+W(K-2,J)+W(K-M2,J)
K=K+1
B(K)=21.DO*W(K,J)-8.DO*(2.DO*W(K-1,J)+W(K+M,J)+W(K-M,J))+4.DO*
1 (W(K+LM,J)+W(K-M1,J))+2.DO*W(K-2,J)+W(K-M2,J)
K=MN-1
B(K)=21.DO*W(K,J)-8.DO*(W(K-1,J)+W(K+1,J)+2.DO*W(K-M,J))+4.DO*
1 (W(K-M1,J)+W(K-LM,J))+W(K-2,J)+2.DO*W(K-M2,J)
B(MN)=20.DO*W(MN,J)-16.DO*(W(K,J)+W(MNM,J))+8.DO*W(MN-M1,J)+
1 2.DO*(W(MN-2,J)+W(MN-M2,J))
DO51 I=3,LLM
B(I)=19.DO*W(I,J)-8.DO*(W(I-1,J)+W(I+1,J)+W(I+M,J))+2.DO*
1 (W(I+LM,J)+W(I+M1,J)+W(I-2,J)+W(I+2,J)+W(I+M2,J)
K=I+M
51 B(K)=20.DO*W(K,J)-8.DO*(W(K-1,J)+W(K+1,J)+W(K+M,J)+W(K-M,J))+2.DO*
1 (W(K+LM,J)+W(K+M1,J)+W(K-M1,J)+W(K-LM,J))+W(K-2,J)+W(K+2,J)+
2 W(K+M2,J)
DO52 I=LLT,LLS
B(I)=21.DO*W(I,J)-8.DO*(W(I-1,J)+W(I+1,J)+W(I+M,J)+W(I-M,J))+2.DO*
1 (W(I+LM,J)+W(I+M1,J)+W(I-M1,J)+W(I-LM,J))+W(I-2,J)+W(I+2,J)+
2 W(I-M2,J)
K=I+M
52 B(K)=20.DO*W(K,J)-8.DO*(W(K-1,J)+W(K+1,J)+2.DO*W(K-M,J))+4.DO*
1 (W(K-M1,J)+W(K-LM,J))+W(K-2,J)+W(K+2,J)+2.DO*W(K-M2,J)
DO53 I=M21,LS,M
B(I)=19.DO*W(I,J)-8.DO*(W(I+1,J)+W(I+M,J)+W(I-M,J))+2.DO*
1 (W(I+M1,J)+W(I-LM,J))+W(I+2,J)+W(I+M2,J)+W(I-M2,J)
K=I+1
53 B(K)=20.DO*W(K,J)-8.DO*(W(K-1,J)+W(K+1,J)+W(K+M,J)+W(K-M,J))+2.DO*
1 (W(K+LM,J)+W(K+M1,J)+W(K-M1,J)+W(K-LM,J))+W(K+2,J)+W(K+M2,J)+
2 W(K-M2,J)
DO54 I=M3,LST,M
B(I)=20.DO*W(I,J)-8.DO*(2.DO*W(I-1,J)+W(I+M,J)+W(I-M,J))+4.DO*
1 (W(I+LM,J)+W(I-M1,J))+2.DO*W(I-2,J)+W(I+M2,J)+W(I-M2,J)
K=I-1
54 B(K)=21.DO*W(K,J)-8.DO*(W(K-1,J)+W(K+1,J)+W(K-M,J)+W(K+M,J))+2.DO*
1 (W(K+LM,J)+W(K+M1,J)+W(K-M1,J)+W(K-LM,J))+W(K-2,J)+W(K+M2,J)+
2 W(K-M2,J)

```

```

DO55K=2,LLN
KM=K*M
DO55 L=3,LLM
I=K+L
55 B(I)=20.DO*W(I,J)-8.DO*(W(I-1,J)+W(I+1,J)+W(I+M,J)+W(I-M,J))+2.DO*
1 (W(I+LM,J)+W(I+M1,J)+W(I-M1,J)+W(I-LM,J))+W(I-2,J)+W(I+2,J)+
2 W(I+M2,J)+W(I-M2,J)
C
IF(IFVOL-1)100,101,100
101 CONTINUE
C
THE VOLUME DISPLACED BY PLATE DEFLECTION IS CALCULATED NEXT.
C
VOL=W(1,J)*DX*DX/3.
DO 71 I=1,LM
VCL=VOL+W(I,J)+W(I+1,J))*DX*DX/4.
71 CONTINUE
DO 72 I=1,LT,M
VOL=VOL+W(I,J)+W(I+M,J))*DX*DX*0.25
72 CONTINUE
NV=N-1
DO 73 I=1,NV
L1=(I-1)*M+1
W1=W(L1,J)
W3=W(L1+M,J)
DO 73 K=1,LM
L2=L1+K-1
W2=W(L2+1,J)
W4=W(L2+M+1,J)
VOL=VOL+0.25*DX*DX*(W1+W2+W3+W4)
W1=W2
W3=W4
73 CONTINUE
VOL=VOL/3.
ETVOL=AR*EX2(J)-VOL
P1(J)=EK22*ETVOL
PJ=P1(J)+P1(J)
EX2(J+1)=FACT1*EX2(J)+FACT2*EX2(J-1)+FACT3*PJ
C
CALCULATE W(I,J+1)
C
DO6CI=1,MN
60 W(I,J+1)=2.*W(I,J)-W(I,J-1)-C1*B(I)+C2*BB(I)+C3*PJ
GO TO 70
100 CONTINUE
C
CALCULATE DEFLECTION FOR PLATE
DO 102 I=1,MN
102 W(I,J+1)=2.DO*W(I,J)-W(I,J-1)-C1*B(I)+C2*BB(I)+C3*PJ
70 CONTINUE
RETURN
END
C
C
C
SUBROUTINE COEFA (A,M,N,KR)
IMPLICIT REAL*8 (A-H,C-Z)
DIMENSION A(KR,1)
C
SET UP (A) MATRIX FOR STRESS FREE EDGES
C
(A)F=C, SIMPLY SUPPORTED OR CLAMPED

```

```

MN=M*N
DO11=1,MN
DO1J=1,MN
1 A(I,J)=0.00
DO2K=1,MN
2 A(K,K)=20.00
A(1,1)=22.00
L=M-2
DO3K=2,L
3 A(K,K)=21.00
A(M-1,M-1)=22.00
A(M,M)=21.00
L=MN-3*M
DO4K=M,L,M
A(K+1,K+1)=21.00
KK=K+M-1
4 A(KK,KK)=21.00
L1=(N-2)*M+2
A(L1-1,L1-1)=22.00
L=L1+M-1
DO5K=L1,L
5 A(K,K)=21.00
A(MN-M-1,MN-M-1)=22.00
A(MN-1,MN-1)=21.00
DO6K=2,MN
A(K,K-1)=-8.00
6 A(K-1,K)=-8.00
MNM=MN-M
DO7K=M,MNM,M
A(K+1,K)=0.00
7 A(K,K+1)=0.00
DO8K=3,MN
A(K,K-2)=1.00
8 A(K-2,K)=1.00
DO9K=M,MNM,M
A(K+1,K-1)=0.00
A(K+2,K)=0.00
A(K-1,K+1)=0.00
9 A(K,K+2)=0.00
DO10K=M,MNM,M
A(K,K-1)=-16.00
10 A(K,K-2)=2.00
M1=M+1
DO11K=M1,MN
KM=K-M
A(K,KM)=-8.00
A(KM,K)=-8.00
A(K-1,KM)=2.00
11 A(KM,K-1)=2.00
MN1=MN-1
DO12K=M1,MN1
A(K+1,K-M)=2.00
12 A(K-M,K+1)=2.00
MN1=MN+1
DO13K=M1,MN1,M
KM=K-M
A(K-1,KM)=0.00
13 A(KM,K-1)=0.00
M2=2*M

```

```

DO14K=M2,MNM,M
KM=K-M
A(K+1,KM)=0.00
14 A(KM,K+1)=0.00
M21=M2+1
DO15K=M21,MN
KM2=K-M2
A(K,KM2)=1.00
15 A(KM2,K)=1.00
DO16K=M2,MNM,M
A(K,K-M-1)=4.00
16 A(K-M,K-1)=4.00
L=MN-M+1
DO17K=L,MN
KM=K-M
A(K,KM)=-16.00
A(K,KM+1)=4.00
A(K,KM-1)=4.00
17 A(K,KM-M)=2.00
A(L,MN-M2)=0.00
A(MN,MN-M-1)=8.00
A(MN,L)=0.00
RETURN
END

```

C
C
C
C

```

SUBROUTINE AGEA (A,DC,M,N,KR)
IMPLICIT REAL*8 (A-H,O-Z)
DIMENSION A(KR,1),DC(1)
C PERFORM GAUSS ELIMINATION ON (A) MATRIX AND
C SET UP (DC) VECTOR FOR USE ON (C) VECTOR
C FOR STRESS FREE EDGES, SIMPLY SUPPORTED OR CLAMPED
MN=M*N
K=1
KK=C
1 I=K+1
L=2*M+K
IF(L.GT.MN) L=MN
2 KK=KK+1
DC(KK)=A(I,K)/A(K,K)
A(I,K)=0.
J=K+1
3 A(I,J)=A(I,J)-DC(KK)*A(K,J)
IF(J-L)4,5,30
4 J=J+1
GOTC3
5 IF(I-L)6,7,30
6 I=I+1
GOTC2
7 IF(K-MN+1)8,30,30
8 K=K+1
GOTC1
30 RETURN
END

```

C
C
C

```

C
SUBROUTINE DLINT1 (T,TH,X,XW,N)
REAL*8 T,TH,X,XW
DIMENSION T(1),X(1)
C
C LINEAR INTERPOLATION ROUTINE. EXTRAPOLATION IS VALID.
C RESTRICTION TO SINGLE VALUED DEPENDENT VARIABLE.
C (TEST IS IF ABSOLUTE VALUE OF DIFFERENCE OF TWO SUCCEEDING
C VALUES OF THE INDEPENDENT VARIABLE (T) IS .GT. 1.0-10).
C IN OTHER WORDS, ALL T(I),I=1,N MUST BE DISTINCT.
C
C ***ARGUMENTS***
C T = INPUT VECTOR OF INDEPENDENT VARIABLE. SIZE(N)
C TH = INPUT VALUE AT WHICH INTERPOLATED VALUE IS WANTED.
C X = INPUT VECTOR OF DEPENDENT VARIABLE (CORRES. TO T). SIZE(N)
C XW = OUTPUT INTERPOLATED VALUE.
C N = INPUT NUMBER OF PAIRS OF DATA POINTS.
C
600 FORMAT ('1 ERROR IN SUBROUTINE DLINT1'
* //2X,'SINGLE VALUED DEPENDENT VARIABLE IS ASSUMED'
* //2X,'T(1) = ',D12.5,5X,'T(I+1) = ',D12.5
* //2X,'PROGRAM HAS ENDED.' )
C
DO 10 I=1,N
IF (TH .LE. T(I+1) .OR. (I+1) .EQ. N) GO TO 20
10 CONTINUE
20 IF ( T(I+1) - T(I) ) .GT. 1.0-10) GO TO 30
WRITE (6,600) T(I),T(I+1)
CALL EXIT
30 XW = X(I) + (TH-T(I)) * (X(I+1)-X(I)) / (T(I+1)-T(I))
RETURN
END
C
SUBROUTINE PGM2
REAL*8 E,H,PR,DXI,SBC,SMC,TBC,THC,WXX,WYY,W,F,T,
* SIGXB,SIGXM,SIGYB,SIGYM,XYB,XYM,
* SXBMT,SXMMT,SYBMT,SYMHT,XYBMT,XYMMT
REAL*8 DX
REAL*8 CS1,CS2,CS3,CS4,CS5,CS6,
* CMT1,CMT2,CMT3,CMT4,CMT5,CMT6
REAL*8 DNST,DNSB,PNT,PNB,SST,SSB,ST,SB,
* PNTMT,PNBMT,SSTMT,SSBMT
REAL*8 STRAIN,S1,S2,S3,S4
C
COMMON E,H,PR,DX,M,N,IDA
DXI = 12.00 * DX
C
SONIC BOOM PROJECT. ROBERT CURTIS IKARD
PROGRAM TO CALCULATE STRESS DISTRIBUTIONS FOR THE FINITE DIFFERENCE
METHOD OF NONLINER PLATE DYNAMIC RESPONSE - CASE IA.
C
DIMENSION M( 64), F( 64), SIGXB( 64), SIGXM( 64), SIGYB( 64),
* SIGYM( 64), TXYB( 64), TXYM( 64), SXBMT( 64,4),
* SXHMT( 64,4), SYBMT( 64,4), SYHMT( 64,4),

```

DLINT1

```

* TXYBMT( 64,4), TXYHMT( 64,4), IVREC(300)
DIMENSION CS1( 64), CS2( 64), CS3( 64), CS4( 64), CS5( 64),
* CS6( 64), CMT1( 64,4), CMT2( 64,4), CMT3( 64,4),
* CMT4( 64,4), CMT5( 64,4), CMT6( 64,4)
DIMENSION PNT( 64), PNB( 64), SST( 64), SSB( 64),
* PNTMT( 64,4), PNBMT( 64,4),
* SSTMT( 64,4), SSBMT( 64,4)
DIMENSION STRAIN( 64,4), S1( 64,4), S2( 64,4),
* S3( 64,4), S4( 64,4), IDPV( 64)
C
C INPUT FORMATS.
501 FORMAT (16I5)
C
C OUTPUT FORMATS.
600 FORMAT ('1 STRESS DISTRIBUTION FOR FINITE DIFFERENCE METHOD OF NON
* LINEAR PLATE DYNAMIC RESPONSE - CASE IA'
* //2X,'FINAL REVISIONS BY ROBERT C IKARD JULY 1971'
* //2X,'BENDING STRESS IS CALCULATED AT Z = +H/2'
* ///2X,'STRESS COMPONENTS ARE PROPORTIONAL AS FOLLOWS,'
* //2X,'SIGMA X,Y BENDING PR TO',D12.4,' * FUNCTIONS OF W'
* //2X,'SIGMA X,Y MEMBRANE PR TO',D12.4,' * FUNCTIONS OF F'
* //2X,'TAU XY BENDING PR TO',D12.4,' * FUNCTIONS OF W'
* //2X,'TAU XY MEMBRANE PR TO',D12.4,' * FUNCTIONS OF F' )
601 FORMAT (1X,'STRESS DISTRIBUTION FOR TIME =',F12.0,6X,'ID4 =',I5,
* 7X,'DEFLECT ON CENTER OF PLATE =',D12.4
* //2X,'GRID POINT',4X,'X-DIRECTION NORMAL STRESS',9X,'Y-DIRECT ID
* N NORMAL STRESS',14X,'SHEARING STRESS'
* //4X,'NUMBER ',3(4X,'BENDING(PSI) MEMBRANE(PSI)',2X) / )
602 FORMAT (5X,I3,3(6X,D12.4,4X,D12.4))
603 FORMAT (1X)
604 FORMAT ('1',32X,'MAXIMUM-MINIMUM SUMMARY OF' )
605 FORMAT (37X,'BENDING COMPONENT' )
606 FORMAT (37X,'MEMBRANE COMPONENT' )
607 FORMAT (32X,'OF STRESS IN THE X-DIRECTION' //)
608 FORMAT (32X,'OF STRESS IN THE Y-DIRECTION' //)
609 FORMAT (37X,'OF SHEARING STRESS' //)
610 FORMAT (10X,'GRID POINT',5X,'TIME OF',26X,'TIME OF'
* //2X,'NUMBER',5X,'MAX STRESS',5X,'MAX STRESS',
* 7X,'MIN STRESS',5X,'MIN STRESS' //)
611 FORMAT (13X,I3,Z(5X,F12.6,4X,D12.4))
615 FORMAT (//2X,'THE FOLLOWING RECORDS ARE TO BE PROCESSED BY DIRECT
* ACCESS' // (2X,20I5))
620 FORMAT (//2X,'FOLLOWING INTEGER PARAMETERS WERE SPECIFIED',
* //2X,'M =',I3, //2X,'N =',I3,
* //2X,'NSD =',I3, //2X,'NMULT =',I3,
* //2X,'NREL =',I3, //2X,'NSREC =',I3,
* //2X,'FOLLOWING DOUBLE PRECISION PARAMETERS WERE SPECIFIED',
* //2X,'E =',D12.4, //2X,'H =',D12.4,
* //2X,'PR =',D12.4, //2X,'DXI =',D12.4,' INCHES' )
621 FORMAT (//2X,'GRID POINT',5X,'COMBINED X NORMAL STRESS',10X,'CUMB
* INED Y NORMAL STRESS',10X,'COMBINED SHEARING STRESS'
* //4X,'NUMBER',2X,3(5X,'AT + H/2',8X,'AT - H/2',5X) / )
622 FORMAT (32X,'COMBINED ( +H/2 ) COMPONENTS' )
623 FORMAT (32X,'COMBINED ( -H/2 ) COMPONENTS' )
624 FORMAT (//2X,'GRID POINT',5X,'PRINCIPLE NORMAL STRESS',
* 10X,'MAXIMUM SHEARING STRESS'
* //4X,'NUMBER',2X,2(5X,'AT + H/2',8X,'AT - H/2',5X) / )
625 FORMAT (5X,I3,2(6X,D12.4,4X,D12.4))
626 FORMAT (29X,'PRINCIPLE NORMAL STRESS AT Z=+H/2' // )

```

```

627 FORMAT (29X,'PRINCIPLE NORMAL STRESS AT Z=-H/2' // )
628 FORMAT (31X,'MAXIMUM SHEAR STRESS AT Z=+H/2' // )
629 FORMAT (31X,'MAXIMUM SHEAR STRESS AT Z=-H/2' // )
630 FORMAT (///2X,'GRID POINT',4X,'X-DIRECTION NORMAL STRAIN',9X,'Y-DI
*RECTION NORMAL STRAIN'
* /4X,'NUMBER',2(4X,' BENDING MEMBRANE ',2X) / )
631 FORMAT (5F15.7,15)
637 FORMAT (32X,'OF STRAIN IN THE X-DIRECTION' //)
638 FORMAT (32X,'OF STRAIN IN THE Y-DIRECTION' //)
640 FORMAT (10X,'GRID POINT',5X,'TIME OF',26X,'TIME OF'
/12X,'NUMBER',5X,'MAX STRAIN',5X,'MAX STRAIN',
* 7X,'MIN STRAIN',5X,'MIN STRAIN' //)
689 FORMAT (/// (10X,8D12.4))
C
C START THE PROGRAM.
C READ (5,501) NSD,NMULT,NREC,NSREC,IFSOP
C
C IF NMULT .NE. 0,
C CALCULATE STRESSES FOR NREC CONSECUTIVE TIMES, BUT OUTPUT ONLY
C THOSE RECORDS NSREC, NSREC + NMULT, NSREC + 2*NMULT,....
C IN MULTIPLES OF NMULT, STARTING WITH NSREC.
C
C IF NMULT .EQ. 0,
C READ IN SPECIFIC LOCATION OF RECORDS DESIRED, CALCULATE STRESSES
C ONLY AT THOSE TIMES AND OUTPUT.
C
C IN THE 1ST CASE (NMULT .NE. 0), NREC CONSECUTIVE VALUES CALCULATED,
C ONLY NSD STRESS DISTRIBUTIONS OUTPUT.
C
C IN THE 2ND CASE (NMULT .EQ. 0), NSD STRESS DISTRIBUTIONS CALCULATED
C AND OUTPUT.
C
C IN ANY CASE, NSD RECORDS WILL BE OUTPUT (PRINTED).
C **NOTE** AT LEAST 1 PAGE OF OUTPUT RESULTS FOR EACH RECORD PROCESSED,
C THEREFORE, RUNS WITH NSD MORE THAN 40 RESULTS IN EXCESSIVE
C OUTPUT BEING PRINTED. (SEE OSU COMPUTER CENTER USERS GUIDE)
C
C IF (NMULT .GT. 0) GO TO 5
C READ (5,501) (IVREC(I),I=1,NSD)
C GO TO 7
C 5 IVREC(I)=NSREC
C DO 6 I=2,NSD
C 6 IVREC(I) = IVREC(I-1) + NMULT
C 7 CONTINUE
C
C CALCULATE INTEGERS NEEDED.
C MN=M*N
C NMI=M-1
C MML=M-1
C
C DEFINE INTEGER OUTPUT CONTROL VECTOR, PRINT ALL IF (IFSOP .LE. 0).
C OTHERWISE, READ IN CONTROL VECTOR. METHOD OF CONTROL IS AS FOLLOWS.
C
C IOPV(I) = 0 DON'T PRINT OR PUNCH DATA FOR ITH NODE.
C IOPV(I) = 1 PRINT DATA FOR ITH NODE POINT.
C IOPV(I) = 2 PRINT DATA AND PUNCH STRAINS FOR ITH NODE.
C
C MAX - MIN SUMMARIES WILL BE PRINTED FOR ALL POINTS.
C

```

```

DO 8 I=1,MN
8 IOPV(I) = 1
IF (IFSOP .LE. 0) GO TO 9
READ (5,501) (IOPV(I),I=1,MN)
C
C DEFINE CONSTANTS NEEDED IN STRESS CALCULATION LOOP AND OUTPUT THEM.
9 SBC = -E*H/(2.00*(1.00-PR*PR)*DXI*DXI)
SMC = 1.00/(DXI*DXI)
TBC = -E*H/(2.00*(1.00+PR)*4.00*DXI*DXI)
TMC = -1.00/(4.00*DXI*DXI)
WRITE (6,600) SBC,SMC,TBC,TMC
C
C WRITE OUT INPUT DATA.
C WRITE (6,620) M,N,NSD,NMULT,NREC,NSREC,E,H,PR,DXI
C IF (NMULT .EQ. 0) WRITE (6,615) (IVREC(I),I=1,NSD)
C
C ZERC OUT MAXMIN-TIME MATRICES.
DO 10 I=1,MN
DO 10 J=1,4
SXBM(T(I,J))=0.00
SXM(T(I,J))=0.00
SYBM(T(I,J))=0.00
SYM(T(I,J))=0.00
TXBM(T(I,J))=0.00
TXM(T(I,J))=0.00
CMT1(I,J)=0.00
CMT2(I,J)=0.00
CMT3(I,J)=0.00
CMT4(I,J)=0.00
CMT5(I,J)=0.00
CMT6(I,J)=0.00
PNTMT(I,J) = 0.00
PNBMT(I,J) = 0.00
SSTMT(I,J) = 0.00
SSBMT(I,J) = 0.00
S1(I,J) = 0.00
S2(I,J) = 0.00
S3(I,J) = 0.00
10 S4(I,J) = 0.00
C
C STRESS CALCULATION LOOP.
ID4=NSREC
NTIME=NREC
IF (NMULT .EQ. 0) NTIME=NSD
KOUT=1
DO 300 LCOUNT=1,NTIME
IF (NMULT .EQ. 0) ID4 = IVREC(LCOUNT)
READ (4*ID4) T,(W(I),I=1,MN),(F(J),J=1,MN)
C
C STRESS AT I=1,J=1 CORNER. (1)
IJ=1
IR=IJ+1
IA=IJ+M
IAR=IJ+M+1
WXX = -2.00*W(IJ) + W(IR)
WYY = -2.00*W(IJ) + W(IA)
SIGXB(IJ) = SBC*(WXX + PR*WYY)
SIGYB(IJ) = SBC*(WYY + PR*WXX)
SIGXB(IJ) = SMC*(-2.00*F(IJ) + F(IA))

```

```

SIGYM(IJ) = SMC*( -2.00*F(IJ) + F(IR))
TXYB(IJ) = TBC*W(IAR)
TXYM(IJ) = TMC*F(IAR)
CS1(IJ) = SIGXB(IJ) + SIGXM(IJ)
CS2(IJ) = -SIGXB(IJ) + SIGXM(IJ)
CS3(IJ) = SIGYB(IJ) + SIGYM(IJ)
CS4(IJ) = -SIGYB(IJ) + SIGYM(IJ)
CS5(IJ) = TXYB(IJ) + TXYM(IJ)
CS6(IJ) = -TXYB(IJ) + TXYM(IJ)
DNST = (CS1(IJ) - CS3(IJ)) / 2.00
DNSB = (CS2(IJ) - CS4(IJ)) / 2.00
ST = CS5(IJ)
SB = CS6(IJ)
SST(IJ) = DSQRT(DNST*DNST + ST*ST)
SSB(IJ) = DSQRT(DNSB*DNSB + SB*SB)
PNT(IJ) = (CS1(IJ) + CS3(IJ)) / 2.00 + SST(IJ)
PNB(IJ) = (CS2(IJ) + CS4(IJ)) / 2.00 + SSB(IJ)
STRAIN(IJ,1) = (SIGXB(IJ) - PR*SIGYB(IJ)) / E
STRAIN(IJ,2) = (SIGXM(IJ) - PR*SIGYM(IJ)) / E
STRAIN(IJ,3) = (SIGYB(IJ) - PR*SIGXB(IJ)) / E
STRAIN(IJ,4) = (SIGYM(IJ) - PR*SIGXM(IJ)) / E
C
C STRESS ALONG J=1 SIDE (I=2,M-1) (2)
DO 20 I=2,MM1
IJ=I
IR=IJ+1
IL=IJ-1
IA=IJ+M
IAL=IJ+M-1
IAR=IJ+M+1
WXX = W(IL) -2.00*W(IJ) + W(IR)
WYY = -2.00*W(IJ) + W(IA)
SIGXB(IJ) = SBC*(WXX + PR*WYY)
SIGYB(IJ) = SBC*(WYY + PR*WXX)
SIGXM(IJ) = SMC*( -2.00*F(IJ) + F(IA))
SIGYM(IJ) = SMC*(F(IL) -2.00*F(IJ) + F(IR))
TXYB(IJ) = TBC*( -W(IAL) + W(IAR) )
TXYM(IJ) = TMC*( -F(IAL) + F(IAR) )
CS1(IJ) = SIGXB(IJ) + SIGXM(IJ)
CS2(IJ) = -SIGXB(IJ) + SIGXM(IJ)
CS3(IJ) = SIGYB(IJ) + SIGYM(IJ)
CS4(IJ) = -SIGYB(IJ) + SIGYM(IJ)
CS5(IJ) = TXYB(IJ) + TXYM(IJ)
CS6(IJ) = -TXYB(IJ) + TXYM(IJ)
DNST = (CS1(IJ) - CS3(IJ)) / 2.00
DNSB = (CS2(IJ) - CS4(IJ)) / 2.00
ST = CS5(IJ)
SB = CS6(IJ)
SST(IJ) = DSQRT(DNST*DNST + ST*ST)
SSB(IJ) = DSQRT(DNSB*DNSB + SB*SB)
PNT(IJ) = (CS1(IJ) + CS3(IJ)) / 2.00 + SST(IJ)
PNB(IJ) = (CS2(IJ) + CS4(IJ)) / 2.00 + SSB(IJ)
STRAIN(IJ,1) = (SIGXB(IJ) - PR*SIGYB(IJ)) / E
STRAIN(IJ,2) = (SIGXM(IJ) - PR*SIGYM(IJ)) / E
STRAIN(IJ,3) = (SIGYB(IJ) - PR*SIGXB(IJ)) / E
20 STRAIN(IJ,4) = (SIGYM(IJ) - PR*SIGXM(IJ)) / E
C
C STRESS AT I=M,J=1 CORNER (3)
IJ=M

```

```

IL=IJ-1
IA=IJ+M
WXX = 2.00*(W(IL) - W(IJ))
WYY = -2.00*W(IJ) + W(IA)
SIGXB(IJ) = SBC*(WXX + PR*WYY)
SIGYB(IJ) = SBC*(WYY + PR*WXX)
SIGXM(IJ) = SMC*( -2.00*F(IJ) + F(IA))
SIGYM(IJ) = 2.00*SMC*(F(IL) - F(IJ))
TXYB(IJ) = 0.00
TXYM(IJ) = 0.00
CS1(IJ) = SIGXB(IJ) + SIGXM(IJ)
CS2(IJ) = -SIGXB(IJ) + SIGXM(IJ)
CS3(IJ) = SIGYB(IJ) + SIGYM(IJ)
CS4(IJ) = -SIGYB(IJ) + SIGYM(IJ)
CS5(IJ) = TXYB(IJ) + TXYM(IJ)
CS6(IJ) = -TXYB(IJ) + TXYM(IJ)
DNST = (CS1(IJ) - CS3(IJ)) / 2.00
DNSB = (CS2(IJ) - CS4(IJ)) / 2.00
ST = CS5(IJ)
SB = CS6(IJ)
SST(IJ) = DSQRT(DNST*DNST + ST*ST)
SSB(IJ) = DSQRT(DNSB*DNSB + SB*SB)
PNT(IJ) = (CS1(IJ) + CS3(IJ)) / 2.00 + SST(IJ)
PNB(IJ) = (CS2(IJ) + CS4(IJ)) / 2.00 + SSB(IJ)
STRAIN(IJ,1) = (SIGXB(IJ) - PR*SIGYB(IJ)) / E
STRAIN(IJ,2) = (SIGXM(IJ) - PR*SIGYM(IJ)) / E
STRAIN(IJ,3) = (SIGYB(IJ) - PR*SIGXB(IJ)) / E
STRAIN(IJ,4) = (SIGYM(IJ) - PR*SIGXM(IJ)) / E
C
C STRESS ALONG I=1 SIDE (J=2,N-1) (4)
DO 30 J=2,NN1
IJ=1+M*(J-1)
IR=IJ+1
IB=IJ-M
IA=IJ+M
IAR=IJ+M+1
IBR=IJ-M+1
WXX = -2.00*W(IJ) + W(IR)
WYY = W(IB) -2.00*W(IJ) + W(IA)
SIGXB(IJ) = SBC*(WXX + PR*WYY)
SIGYB(IJ) = SBC*(WYY + PR*WXX)
SIGXM(IJ) = SMC*(F(IB) -2.00*F(IJ) + F(IA))
SIGYM(IJ) = SMC*( -2.00*F(IJ) + F(IR))
TXYB(IJ) = TBC*( W(IAR) - W(IBR))
TXYM(IJ) = TMC*( F(IAR) - F(IBR))
CS1(IJ) = SIGXB(IJ) + SIGXM(IJ)
CS2(IJ) = -SIGXB(IJ) + SIGXM(IJ)
CS3(IJ) = SIGYB(IJ) + SIGYM(IJ)
CS4(IJ) = -SIGYB(IJ) + SIGYM(IJ)
CS5(IJ) = TXYB(IJ) + TXYM(IJ)
CS6(IJ) = -TXYB(IJ) + TXYM(IJ)
DNST = (CS1(IJ) - CS3(IJ)) / 2.00
DNSB = (CS2(IJ) - CS4(IJ)) / 2.00
ST = CS5(IJ)
SB = CS6(IJ)
SST(IJ) = DSQRT(DNST*DNST + ST*ST)
SSB(IJ) = DSQRT(DNSB*DNSB + SB*SB)
PNT(IJ) = (CS1(IJ) + CS3(IJ)) / 2.00 + SST(IJ)
PNB(IJ) = (CS2(IJ) + CS4(IJ)) / 2.00 + SSB(IJ)

```



```

    STRAIN(IJ,1) = (SIGXB(IJ) - PR*SIGYB(IJ)) / E
    STRAIN(IJ,2) = (SIGXM(IJ) - PR*SIGYM(IJ)) / E
    STRAIN(IJ,3) = (SIGYB(IJ) - PR*SIGXB(IJ)) / E
30 STRAIN(IJ,4) = (SIGYM(IJ) - PR*SIGXM(IJ)) / E
C
C STRESS ALONG I=M SIDE (J=2,N-1) (5)
  DO 40 J=2,NM1
    IJ=M+M*(J-1)
    IL=IJ-1
    IB=IJ-M
    IA=IJ+M
    WXX = 2.00*(W(IL) - W(IJ))
    WYY = W(IB) - 2.00*W(IJ) + W(IA)
    SIGXB(IJ) = SBC*(WXX + PR*WYY)
    SIGYB(IJ) = SBC*(WYY + PR*WXX)
    SIGXM(IJ) = SMC*(F(IB) - 2.00*F(IJ) + F(IA))
    SIGYM(IJ) = 2.00*SMC*(F(IL) - F(IJ))
    TXYB(IJ) = 0.00
    TXYM(IJ) = 0.00
    CS1(IJ) = SIGXB(IJ) + SIGXM(IJ)
    CS2(IJ) = -SIGXB(IJ) + SIGXM(IJ)
    CS3(IJ) = SIGYB(IJ) + SIGYM(IJ)
    CS4(IJ) = -SIGYB(IJ) + SIGYM(IJ)
    CS5(IJ) = TXYB(IJ) + TXYM(IJ)
    CS6(IJ) = -TXYB(IJ) + TXYM(IJ)
    DNST = (CS1(IJ) - CS3(IJ)) / 2.00
    DNSB = (CS2(IJ) - CS4(IJ)) / 2.00
    ST = CS5(IJ)
    SB = CS6(IJ)
    SST(IJ) = DSQRT(DNST*DNST + ST*ST)
    SSB(IJ) = DSQRT(DNSB*DNSB + SB*SB)
    PNT(IJ) = (CS1(IJ) + CS3(IJ)) / 2.00 + SST(IJ)
    PNB(IJ) = (CS2(IJ) + CS4(IJ)) / 2.00 + SSB(IJ)
    STRAIN(IJ,1) = (SIGXB(IJ) - PR*SIGYB(IJ)) / E
    STRAIN(IJ,2) = (SIGXM(IJ) - PR*SIGYM(IJ)) / E
    STRAIN(IJ,3) = (SIGYB(IJ) - PR*SIGXB(IJ)) / E
40 STRAIN(IJ,4) = (SIGYM(IJ) - PR*SIGXM(IJ)) / E
C
C STRESS AT I=1,J=N CORNER (6)
  IJ=1+M*(N-1)
  IR=IJ+1
  IB=IJ-M
  WXX = -2.00*W(IJ) + W(IR)
  WYY = 2.00*(W(IB) - W(IJ))
  SIGXB(IJ) = SBC*(WXX + PR*WYY)
  SIGYB(IJ) = SBC*(WYY + PR*WXX)
  SIGXM(IJ) = 2.00*SMC*(F(IB) - F(IJ))
  SIGYM(IJ) = SMC*(-2.00*F(IJ) + F(IR))
  TXYB(IJ) = 0.00
  TXYM(IJ) = 0.00
  CS1(IJ) = SIGXB(IJ) + SIGXM(IJ)
  CS2(IJ) = -SIGXB(IJ) + SIGXM(IJ)
  CS3(IJ) = SIGYB(IJ) + SIGYM(IJ)
  CS4(IJ) = -SIGYB(IJ) + SIGYM(IJ)
  CS5(IJ) = TXYB(IJ) + TXYM(IJ)
  CS6(IJ) = -TXYB(IJ) + TXYM(IJ)
  DNST = (CS1(IJ) - CS3(IJ)) / 2.00
  DNSB = (CS2(IJ) - CS4(IJ)) / 2.00
  ST = CS5(IJ)

```

```

    SB = CS6(IJ)
    SST(IJ) = DSQRT(DNST*DNST + ST*ST)
    SSB(IJ) = DSQRT(DNSB*DNSB + SB*SB)
    PNT(IJ) = (CS1(IJ) + CS3(IJ)) / 2.00 + SST(IJ)
    PNB(IJ) = (CS2(IJ) + CS4(IJ)) / 2.00 + SSB(IJ)
    STRAIN(IJ,1) = (SIGXB(IJ) - PR*SIGYB(IJ)) / E
    STRAIN(IJ,2) = (SIGXM(IJ) - PR*SIGYM(IJ)) / E
    STRAIN(IJ,3) = (SIGYB(IJ) - PR*SIGXB(IJ)) / E
    STRAIN(IJ,4) = (SIGYM(IJ) - PR*SIGXM(IJ)) / E
C
C STRESS ALONG J=N SIDE (I=2,M-1) (7)
  DO 50 I=2,MM1
    IJ=1+M*(N-1)
    IR=IJ+1
    IL=IJ-1
    IB=IJ-M
    WXX = W(IL) - 2.00*W(IJ) + W(IR)
    WYY = 2.00*(W(IB) - W(IJ))
    SIGXB(IJ) = SBC*(WXX + PR*WYY)
    SIGYB(IJ) = SBC*(WYY + PR*WXX)
    SIGXM(IJ) = 2.00*SMC*(F(IB) - F(IJ))
    SIGYM(IJ) = SMC*(F(IL) - 2.00*F(IJ) + F(IR))
    TXYB(IJ) = 0.00
    TXYM(IJ) = 0.00
    CS1(IJ) = SIGXB(IJ) + SIGXM(IJ)
    CS2(IJ) = -SIGXB(IJ) + SIGXM(IJ)
    CS3(IJ) = SIGYB(IJ) + SIGYM(IJ)
    CS4(IJ) = -SIGYB(IJ) + SIGYM(IJ)
    CS5(IJ) = TXYB(IJ) + TXYM(IJ)
    CS6(IJ) = -TXYB(IJ) + TXYM(IJ)
    DNST = (CS1(IJ) - CS3(IJ)) / 2.00
    DNSB = (CS2(IJ) - CS4(IJ)) / 2.00
    ST = CS5(IJ)
    SB = CS6(IJ)
    SST(IJ) = DSQRT(DNST*DNST + ST*ST)
    SSB(IJ) = DSQRT(DNSB*DNSB + SB*SB)
    PNT(IJ) = (CS1(IJ) + CS3(IJ)) / 2.00 + SST(IJ)
    PNB(IJ) = (CS2(IJ) + CS4(IJ)) / 2.00 + SSB(IJ)
    STRAIN(IJ,1) = (SIGXB(IJ) - PR*SIGYB(IJ)) / E
    STRAIN(IJ,2) = (SIGXM(IJ) - PR*SIGYM(IJ)) / E
    STRAIN(IJ,3) = (SIGYB(IJ) - PR*SIGXB(IJ)) / E
50 STRAIN(IJ,4) = (SIGYM(IJ) - PR*SIGXM(IJ)) / E
C
C STRESS AT I=M,J=N CORNER (8)
  IJ=MN
  IL=IJ-1
  IB=IJ-M
  WXX = 2.00*(W(IL) - W(IJ))
  WYY = 2.00*(W(IB) - W(IJ))
  SIGXB(IJ) = SBC*(WXX + PR*WYY)
  SIGYB(IJ) = SBC*(WYY + PR*WXX)
  SIGXM(IJ) = 2.00*SMC*(F(IB) - F(IJ))
  SIGYM(IJ) = 2.00*SMC*(F(IL) - F(IJ))
  TXYB(IJ) = 0.00
  TXYM(IJ) = 0.00
  CS1(IJ) = SIGXB(IJ) + SIGXM(IJ)
  CS2(IJ) = -SIGXB(IJ) + SIGXM(IJ)
  CS3(IJ) = SIGYB(IJ) + SIGYM(IJ)
  CS4(IJ) = -SIGYB(IJ) + SIGYM(IJ)

```

```

CS5(IJ) = TXYB(IJ) + TXYM(IJ)
CS6(IJ) = -TXYB(IJ) + TXYM(IJ)
DNST = (CS1(IJ) - CS3(IJ)) / 2.00
DMSB = (CS2(IJ) - CS4(IJ)) / 2.00
ST = CS5(IJ)
SB = CS6(IJ)
SST(IJ) = DSQRT(DNST*DNST + ST*ST)
SSB(IJ) = DSQRT(DMSB*DMSB + SB*SB)
PNT(IJ) = (CS1(IJ) + CS3(IJ)) / 2.00 + SST(IJ)
PNB(IJ) = (CS2(IJ) + CS4(IJ)) / 2.00 + SSB(IJ)
STRAIN(IJ,1) = (SIGXB(IJ) - PR*SIGYB(IJ)) / E
STRAIN(IJ,2) = (SIGXM(IJ) - PR*SIGYM(IJ)) / E
STRAIN(IJ,3) = (SIGYB(IJ) - PR*SIGXB(IJ)) / E
STRAIN(IJ,4) = (SIGYM(IJ) - PR*SIGXM(IJ)) / E
C
C STRESS AT INTERIOR POINTS (GENERAL CASE) (9)
DO 60 J=2,MN1
DO 60 I=2,MN1
IJ=I+M*(J-1)
IR=IJ+1
IL=IJ-1
IB=IJ-M
IA=IJ+M
IBL=IJ-M-1
IAL=IJ+M-1
IAR=IJ+M+1
IBR=IJ-M+1
WXX = W(IL) - 2.00*W(IJ) + W(IR)
WYY = W(IB) - 2.00*W(IJ) + W(IA)
SIGXB(IJ) = SBC*(WXX + PR*WYY)
SIGYB(IJ) = SBC*(WYY + PR*WXX)
SIGXM(IJ) = SMC*(F(IL) - 2.00*F(IJ) + F(IA))
SIGYM(IJ) = SMC*(F(IL) - 2.00*F(IJ) + F(IA))
TXYB(IJ) = TBC*(W(IL) - W(IAL) + W(IAR) - W(IBR))
TXYM(IJ) = TMC*(F(IL) - F(IAL) + F(IAR) - F(IBR))
CS1(IJ) = SIGXB(IJ) + SIGXM(IJ)
CS2(IJ) = -SIGYB(IJ) + SIGYM(IJ)
CS3(IJ) = SIGYB(IJ) + SIGYM(IJ)
CS4(IJ) = -SIGXB(IJ) + SIGXM(IJ)
CS5(IJ) = TXYB(IJ) + TXYM(IJ)
CS6(IJ) = -TXYB(IJ) + TXYM(IJ)
DNST = (CS1(IJ) - CS3(IJ)) / 2.00
DMSB = (CS2(IJ) - CS4(IJ)) / 2.00
ST = CS5(IJ)
SB = CS6(IJ)
SST(IJ) = DSQRT(DNST*DNST + ST*ST)
SSB(IJ) = DSQRT(DMSB*DMSB + SB*SB)
PNT(IJ) = (CS1(IJ) + CS3(IJ)) / 2.00 + SST(IJ)
PNB(IJ) = (CS2(IJ) + CS4(IJ)) / 2.00 + SSB(IJ)
STRAIN(IJ,1) = (SIGXB(IJ) - PR*SIGYB(IJ)) / E
STRAIN(IJ,2) = (SIGXM(IJ) - PR*SIGYM(IJ)) / E
STRAIN(IJ,3) = (SIGYB(IJ) - PR*SIGXB(IJ)) / E
60 STRAIN(IJ,4) = (SIGYM(IJ) - PR*SIGXM(IJ)) / E
C
C ALL STRESS VALUES COMPUTED. OUTPUT HEADING AND SPACE BETWEEN ROWS.
NM4=104-1
IF (NM4 .NE. IVREC(KOUT)) GO TO 90
WRITE (6,601) I,NI,MI
DO 80 J=1,N

```

```

DO 70 I=1,M
IJ=I+M*(J-1)
IF (IOPV(IJ) .LE. 0) GO TO 70
WRITE (6,602) IJ,SIGXB(IJ),SIGXM(IJ),SIGYB(IJ),SIGYM(IJ),
* TXYB(IJ),TXYM(IJ)
70 CONTINUE
80 CONTINUE
WRITE (6,689) (W(I),I=1,MN)
WRITE (6,689) (F(I),I=1,MN)
WRITE (6,621)
DO 87 J=1,N
DO 83 I=1,M
IJ=I+M*(J-1)
IF (IOPV(IJ) .LE. 0) GO TO 83
WRITE (6,602) IJ,CS1(IJ),CS2(IJ),CS3(IJ),CS4(IJ),CS5(IJ),CS6(IJ)
83 CONTINUE
87 WRITE (6,603)
C
C WRITE OUT PRINCIPAL NORMAL AND MAXIMUM SHEAR STRESSES.
WRITE (6,624)
DO 89 J=1,N
DO 88 I=1,M
IJ=I+M*(J-1)
IF (IOPV(IJ) .LE. 0) GO TO 88
WRITE (6,625) IJ,PNT(IJ),PNB(IJ),SST(IJ),SSB(IJ)
88 CONTINUE
89 WRITE (6,603)
C
C WRITE OUT STRAINS.
WRITE (6,630)
DO 92 J=1,N
DO 91 I=1,M
IJ=I+M*(J-1)
IF (IOPV(IJ) .GT. 0) WRITE (6,625) IJ,(STRAIN(IJ,K),K=1,4)
IF (IOPV(IJ) .GT. 1) WRITE (7,631) (STRAIN(IJ,K),K=1,4),W(MN),IJ
91 CONTINUE
92 WRITE (6,603)
KOUT=KOUT+1
90 CONTINUE
C
C
C CHECK FOR MAXIMUM AND MINIMUM VALUES.
DO 200 I=1,M
DO 200 J=1,N
IJ=I+M*(J-1)
IF (SIGXB(IJ) .LE. SXBMT(IJ,2)) GO TO 105
SXBMT(IJ,2) = SIGXB(IJ)
SXBMT(IJ,1) = T
105 IF (SIGXB(IJ) .GE. SXBMT(IJ,4)) GO TO 110
SXBMT(IJ,4) = SIGXB(IJ)
SXBMT(IJ,3) = T
110 IF (SIGXM(IJ) .LE. SXMNT(IJ,2)) GO TO 115
SXMNT(IJ,2) = SIGXM(IJ)
SXMNT(IJ,1) = T
115 IF (SIGXM(IJ) .GE. SXMNT(IJ,4)) GO TO 120
SXMNT(IJ,4) = SIGXM(IJ)
SXMNT(IJ,3) = T
120 IF (SIGYB(IJ) .LE. SYBMT(IJ,2)) GO TO 125
SYBMT(IJ,2) = SIGYB(IJ)
SYBMT(IJ,1) = T

```

```

125 IF (SIGYB(IJ) .GE. SYBMT(IJ,4)) GO TO 130
SYBMT(IJ,4) = SIGYB(IJ)
SYBMT(IJ,3) = T
130 IF (SIGYM(IJ) .LE. SYMMT(IJ,2)) GO TO 135
SYMMT(IJ,2) = SIGYM(IJ)
SYMMT(IJ,1) = T
135 IF (SIGYM(IJ) .GE. SYMMT(IJ,4)) GO TO 140
SYMMT(IJ,4) = SIGYM(IJ)
SYMMT(IJ,3) = T
140 IF (TXYB(IJ) .LE. TXYBMT(IJ,2)) GO TO 145
TXYBMT(IJ,2) = TXYB(IJ)
TXYBMT(IJ,1) = T
145 IF (TXYB(IJ) .GE. TXYBMT(IJ,4)) GO TO 150
TXYBMT(IJ,4) = TXYB(IJ)
TXYBMT(IJ,3) = T
150 IF (TXYM(IJ) .LE. TXYMNT(IJ,2)) GO TO 155
TXYMNT(IJ,2) = TXYM(IJ)
TXYMNT(IJ,1) = T
155 IF (TXYM(IJ) .GE. TXYMNT(IJ,4)) GO TO 160
TXYMNT(IJ,4) = TXYM(IJ)
TXYMNT(IJ,3) = T
160 IF (CS1(IJ) .LE. CMT1(IJ,2)) GO TO 162
CMT1(IJ,2) = CS1(IJ)
CMT1(IJ,1) = T
162 IF (CS1(IJ) .GE. CMT1(IJ,4)) GO TO 164
CMT1(IJ,4) = CS1(IJ)
CMT1(IJ,3) = T
164 IF (CS2(IJ) .LE. CMT2(IJ,2)) GO TO 166
CMT2(IJ,2) = CS2(IJ)
CMT2(IJ,1) = T
166 IF (CS2(IJ) .GE. CMT2(IJ,4)) GO TO 168
CMT2(IJ,4) = CS2(IJ)
CMT2(IJ,3) = T
168 IF (CS3(IJ) .LE. CMT3(IJ,2)) GO TO 170
CMT3(IJ,2) = CS3(IJ)
CMT3(IJ,1) = T
170 IF (CS3(IJ) .GE. CMT3(IJ,4)) GO TO 172
CMT3(IJ,4) = CS3(IJ)
CMT3(IJ,3) = T
172 IF (CS4(IJ) .LE. CMT4(IJ,2)) GO TO 174
CMT4(IJ,2) = CS4(IJ)
CMT4(IJ,1) = T
174 IF (CS4(IJ) .GE. CMT4(IJ,4)) GO TO 176
CMT4(IJ,4) = CS4(IJ)
CMT4(IJ,3) = T
176 IF (CS5(IJ) .LE. CMT5(IJ,2)) GO TO 178
CMT5(IJ,2) = CS5(IJ)
CMT5(IJ,1) = T
178 IF (CS5(IJ) .GE. CMT5(IJ,4)) GO TO 180
CMT5(IJ,4) = CS5(IJ)
CMT5(IJ,3) = T
180 IF (CS6(IJ) .LE. CMT6(IJ,2)) GO TO 182
CMT6(IJ,2) = CS6(IJ)
CMT6(IJ,1) = T
182 IF (CS6(IJ) .GE. CMT6(IJ,4)) GO TO 184
CMT6(IJ,4) = CS6(IJ)
CMT6(IJ,3) = T
184 IF (PNT(IJ) .LE. PNTMT(IJ,2)) GO TO 186
PNTMT(IJ,2) = PNT(IJ)

```

```

PNTMT(IJ,1) = T
186 IF (PNT(IJ) .GE. PNTMT(IJ,4)) GO TO 188
PNTMT(IJ,4) = PNT(IJ)
PNTMT(IJ,3) = T
188 IF (PNB(IJ) .LE. PNBMT(IJ,2)) GO TO 190
PNBMT(IJ,2) = PNB(IJ)
PNBMT(IJ,1) = T
190 IF (PNB(IJ) .GE. PNBMT(IJ,4)) GO TO 192
PNBMT(IJ,4) = PNB(IJ)
PNBMT(IJ,3) = T
192 IF (SST(IJ) .LE. SSTMT(IJ,2)) GO TO 194
SSTMT(IJ,2) = SST(IJ)
SSTMT(IJ,1) = T
194 IF (SST(IJ) .GE. SSTMT(IJ,4)) GO TO 196
SSTMT(IJ,4) = SST(IJ)
SSTMT(IJ,3) = T
196 IF (SSB(IJ) .LE. SSBMT(IJ,2)) GO TO 198
SSBMT(IJ,2) = SSB(IJ)
SSBMT(IJ,1) = T
198 IF (SSB(IJ) .GE. SSBMT(IJ,4)) GO TO 199
SSBMT(IJ,4) = SSB(IJ)
SSBMT(IJ,3) = T
199 IF (STRAIN(IJ,1) .LE. S1(IJ,2)) GO TO 210
S1(IJ,2) = STRAIN(IJ,1)
S1(IJ,1) = T
210 IF (STRAIN(IJ,1) .GE. S1(IJ,4)) GO TO 220
S1(IJ,4) = STRAIN(IJ,1)
S1(IJ,3) = T
220 IF (STRAIN(IJ,2) .LE. S2(IJ,2)) GO TO 230
S2(IJ,2) = STRAIN(IJ,2)
S2(IJ,1) = T
230 IF (STRAIN(IJ,2) .GE. S2(IJ,4)) GO TO 240
S2(IJ,4) = STRAIN(IJ,2)
S2(IJ,3) = T
240 IF (STRAIN(IJ,3) .LE. S3(IJ,2)) GO TO 250
S3(IJ,2) = STRAIN(IJ,3)
S3(IJ,1) = T
250 IF (STRAIN(IJ,3) .GE. S3(IJ,4)) GO TO 260
S3(IJ,4) = STRAIN(IJ,3)
S3(IJ,3) = T
260 IF (STRAIN(IJ,4) .LE. S4(IJ,2)) GO TO 270
S4(IJ,2) = STRAIN(IJ,4)
S4(IJ,1) = T
270 IF (STRAIN(IJ,4) .GE. S4(IJ,4)) GO TO 200
S4(IJ,4) = STRAIN(IJ,4)
S4(IJ,3) = T
200 CONTINUE
300 CONTINUE
C
C WRITE OUT MAXIMUM - MINIMUM SUMMARIES.
WRITE (6,604)
WRITE (6,605)
WRITE (6,607)
WRITE (6,610)
DO 310 L=1,MN
310 WRITE (6,611) L, (SXBMT(L,J),J=1,4)
WRITE (6,604)
WRITE (6,606)
WRITE (6,607)

```

```

WRITE (6,610)
DO 320 L=1,MN
320 WRITE (6,611) L,(SXMMT(L,J),J=1,4)
WRITE (6,604)
WRITE (6,605)
WRITE (6,608)
WRITE (6,610)
DO 330 L=1,MN
330 WRITE (6,611) L,(SYBMT(L,J),J=1,4)
WRITE (6,604)
WRITE (6,606)
WRITE (6,608)
WRITE (6,610)
DO 340 L=1,MN
340 WRITE (6,611) L,(SYMHT(L,J),J=1,4)
WRITE (6,604)
WRITE (6,605)
WRITE (6,609)
WRITE (6,610)
DO 350 L=1,MN
350 WRITE (6,611) L,(TXBMT(L,J),J=1,4)
WRITE (6,604)
WRITE (6,606)
WRITE (6,609)
WRITE (6,610)
DO 360 L=1,MN
360 WRITE (6,611) L,(TXYMT(L,J),J=1,4)
C
C WRITE OUT COMBINED STRESS MAX-MIN SUMMARIES.
WRITE (6,604)
WRITE (6,622)
WRITE (6,607)
WRITE (6,610)
DO 370 L=1,MN
370 WRITE (6,611) L,(CMT1 (L,J),J=1,4)
WRITE (6,604)
WRITE (6,623)
WRITE (6,607)
WRITE (6,610)
DO 380 L=1,MN
380 WRITE (6,611) L,(CMT2 (L,J),J=1,4)
WRITE (6,604)
WRITE (6,622)
WRITE (6,608)
WRITE (6,610)
DO 390 L=1,MN
390 WRITE (6,611) L,(CMT3 (L,J),J=1,4)
WRITE (6,604)
WRITE (6,623)
WRITE (6,608)
WRITE (6,610)
DO 400 L=1,MN
400 WRITE (6,611) L,(CMT4 (L,J),J=1,4)
WRITE (6,604)
WRITE (6,622)
WRITE (6,609)
WRITE (6,610)
DO 410 L=1,MN
410 WRITE (6,611) L,(CMT5 (L,J),J=1,4)

```

```

WRITE (6,604)
WRITE (6,623)
WRITE (6,609)
WRITE (6,610)
DO 420 L=1,MN
420 WRITE (6,611) L,(CMT6 (L,J),J=1,4)
C
C WRITE OUT PRINCIPAL AND SHEAR STRESS MAX-MIN SUMMARIES.
WRITE (6,604)
WRITE (6,626)
WRITE (6,610)
DO 430 L=1,MN
430 WRITE (6,611) L,(PNTMT(L,J),J=1,4)
WRITE (6,604)
WRITE (6,627)
WRITE (6,610)
DO 440 L=1,MN
440 WRITE (6,611) L,(PNBMT(L,J),J=1,4)
WRITE (6,604)
WRITE (6,628)
WRITE (6,610)
DO 450 L=1,MN
450 WRITE (6,611) L,(SSTMT(L,J),J=1,4)
WRITE (6,604)
WRITE (6,629)
WRITE (6,610)
DO 460 L=1,MN
460 WRITE (6,611) L,(SSBMT(L,J),J=1,4)
C
C WRITE OUT COMPONENT STRAIN SUMMARIES.
WRITE (6,604)
WRITE (6,605)
WRITE (6,637)
WRITE (6,640)
DO 465 L=1,MN
465 WRITE (6,611) L,(S1(L,J),J=1,4)
WRITE (6,604)
WRITE (6,606)
WRITE (6,637)
WRITE (6,640)
DO 470 L=1,MN
470 WRITE (6,611) L,(S2(L,J),J=1,4)
WRITE (6,604)
WRITE (6,605)
WRITE (6,638)
WRITE (6,640)
DO 475 L=1,MN
475 WRITE (6,611) L,(S3(L,J),J=1,4)
WRITE (6,604)
WRITE (6,606)
WRITE (6,638)
WRITE (6,640)
DO 480 L=1,MN
480 WRITE (6,611) L,(S4(L,J),J=1,4)
RETURN
END

```

APPENDIX B

The following computer program uses a single mode, lumped parameter model for a simply supported plate based on the results of either Yamaki (5) or Bayles (25). The transient response is obtained by numerical integration of the model differential equation using Subroutine DHPCG which is available as part of the IBM System/360 Scientific Subroutine Package, Version III. This program has the window-room-door system as an option. Its usage is given as part of the listing.


```

X1=XX(I)
Y1=YY(I)
SX=DSIN(3.1416DO*X1/A)
SY=DSIN(3.1416DO*Y1/B)
SIGXB(I)=SIGB*((SX/(A*A)))+(PR*SY/(B*B))
SIGYB(I)=SIGB*((SY/(B*B)))+(PR*SX/(A*A))
EPSXB(I)=(SIGXB(I)-PR*SIGYB(I))/E
EPSYB(I)=(SIGYB(I)-PR*SIGXB(I))/E
IF(NYMAK-1)109,110,109
110 CONTINUE
C USE YAMAKI'S MODEL
X1=0.5DO*A-XX(I)
Y1=0.5DO*B-YY(I)
P01=P01-(1.00/(32.00*B2))
SIGXM(I)=P01*DCOS(PB*2.00*Y1)
P10=P10-(B2/32.00)
SIGYM(I)=P10*DCOS(PA*2.00*X1)
L=N/2
DO 106 NP=1,L
NSQ=-1**NP
PBE=NP*3.1416DO/BETA
DPP=DEXP(PBE)
DPM=DEXP(-PBE)
SINHNP=(DPP-DPM)*0.5DO
COSHNP=(DPP+DPM)*0.5DO
DO 107 NQ=1,L
NSP=-1**NQ
ACOF=NP *NSP*SINHNP/SINHNP/(SINHNP*COSHNP+PBE)
QBE=NQ*3.1416DO*BETA
CATCH=4.00*BETA/(3.1416DO*((NP*NP+B2*NQ*NQ)**2))
DQM=DEXP(-QBE)
DCP=DEXP(QBE)
SINHNP=(-DQM+DQP)*0.5DO
COSHNP=(DQM+DQP)*0.5DO
BCGF=NQ*NSQ*SINHNP*SINHNP/(SINHNP*COSHNP+QBE)
PUSH=DCOS(2.00*NP*PA*X1)*DCOS(2.00*NQ*PB*Y1)*CATCH*(ACOF*X(NP)+
1 BCGF*X(L+NQ))
SIGXM(I)=SIGXM(I)+PUSH*NQ*NQ
SIGYM(I)=SIGYM(I)+PUSH*NP*NP
107 CONTINUE
106 CONTINUE
SIGXM(I)=SIGXM(I)*E**4.00*PB*PB
SIGYM(I)=SIGYM(I)*E**4.00*PA*PA
EPSXM(I)=(SIGXM(I)-PR*SIGYM(I))/E
EPSYM(I)=(SIGYM(I)-PR*SIGXM(I))/E
GO TO 111
105 CONTINUE
C USE BAYLES'S MODEL
EP2=EP
SIGXM(I)=SIGX*SX*DX*DCOS(6.2832DO*Y1/B)
SIGYM(I)=SIGY*DY*DX*DCOS(6.2832DO*X1/A)*SY*SY
EPSXM(I)=(SIGXM(I)-PR*SIGYM(I))/E
EPSYM(I)=(SIGYM(I)-PR*SIGXM(I))/E
111 CONTINUE
7 CONTINUE
EKS=EK1PNL
PRR=1.-PR*PR
EP1=12.*PRR/((C1+2.)*{6.*C1+4.})
NC=0

```

```

DAMP=2.*EM1*OMEGP*Z
EK1PNL=(EP2/EP)*EKS
PRMT(1)=0.00
PRMT(2)=(ND-1)*DT
PRMT(4)=0.001
PRMT(5)=0.00
Y(1)=0.00
Y(2)=0.00
DERY(1)=0.5
DERY(2)=0.5
NDIM=2
C WRITE OUT INPUT DATA
WRITE(6,4)A,B,H,E,PR,RQ,Z
4 FGMAT(1H1,10X,'INPUT DATA FOR PLATE',/,5X,'A=',D12.5,2X,'B=',
4 D12.5,2X,'H=',D12.5,/,5X,'E=',D12.5,1X,'PR=',D12.5,1X,'RQ=',
5 D12.5,2X,'Z=',D12.5,/)
WRITE(6,5)EM1,DAMP,EK1,EK1PNL,C3
5 FGMAT(5X,'SYSTEM DIFFERENTIAL EQUATION',/,5X,
1 D12.5,'*DDX+',D12.5,'*DX+',D12.5,'*X+',D12.5,'**X*3=',D12.5,'*P(
2)',/)
WRITE(6,101)EP,EP1,EP2
101 FGMAT(10X,'EP=',D12.5,5X,'EP1=',D12.5,5X,'EP2=',D12.5,/)
WRITE(6,6)OMEGP,OMEG31,OMEG13,PER100,PER31,PER13
6 FGMAT(5X,'NATURAL FREQUENCIES (LINEAR)',/,5X,'OMEGP=',D12.5,
7 2X,'OMEG31=',D12.5,2X,'OMEG13=',D12.5,/,5X,'PER100=',D12.5,
8 2X,'PER10031=',D12.5,2X,'PER10013=',D12.5,/)
WRITE(6,40)(I,XX(I),YY(I),I=1,NSTRAN)
40 FGMAT(/,5X,'STRAIN IS CALCULATED AT THE FOLLOWING POINTS',2(/,10
1X,12,5X,D12.5,5X,D12.5),/)
WRITE(6,8)DT,PRMT(3), NSTRAN,PSCALE
8 FGMAT(5X,'OTHER INPUT DATA',/,5X,'DT=',D12.5,2X,'PRMT(3)='
9 ,D12.5,2X,/,5X,'NSTRAN=',12,5X,'PRESSURE SCALE
2FACTR=',D12.5,/,/,5X,'INPUT PRESSURE DATA',/,5X,'I',9X,'P(I)'
8,/)
WRITE(6,9)(I,P(I),I=1,ND)
9 FGMAT(1X,15,5X,D12.5)
C
C THE FOLLOWING BLOCK OF CARDS ARE FOR ROOM WINDOW DOOR RESPONSE
IF(IFRQDM-1)609,610,609
610 CONTINUE
READ(5,605)EL,AR,VOL,DAMP1
605 FGMAT(4D15.8)
EL1=EL+1.45*DSQRT(AR/3.1416)
EL1=EL
EM2=EL1*AR*1.4*14.7*144./((1100.*1100.))
EK22=1.4*14.7*144./VOL
WRITE(6,606)EL,EL1,AR,VOL,EM2,DAMP1
606 FGMAT(1X,/,11X,'INPUT DATA ON ROOM AND DOOR',
*/11X,'LENGTH OF DOOR',/,F16.10,'FEET'
*/11X,'EFFECTIVE LENGTH OF DOOR',/,F16.10,'FEET'
*/11X,'AREA OF DOOR',/,F16.10,'FT**2'
*/11X,'VOLUME OF ROOM',/,F16.10,'FT**3'
*/11X,'EFFECTIVE MASS OF AIR IN DOOR',/,F16.10,'SLUGS'
*/11X,'EFFECTIVE DAMPING FACTOR',/,F16.10,'DIMENSIONLESS'/)
EK2=EK22
EK21=EK2*AR*C3/EM2
EK22=-EK2*AR*AR/EM2
C6=-AR/EM2

```



```

TFC=-1.00**J*4.00*G*TF
DO 3 M=1,L
3 A(M,J)=-1.00**M**2/(G**2+M**2)**2*TFC
DO 4 J=1,L
G=J*BETA
ANG=PI*G
EXN=DEXP(-ANG)
HSIN=(EX-EXN)*0.500
HCOS=(EX+EXN)*0.500
TF=HSIN**2/(PI*(HSIN*HCOS+ANG))
TFC=-1**J*4*G*TF
DO 4 M=1,L
4 A(M+L,J+L)=-1**M**2/(G**2+M**2)**2*TFC
DO 5 I=1,N
5 C(I)=0.00
C(I)=1.00/32.00
C(L+1)=BETA**2/32.00
CALL BANDGE (A,C,X,N,L)
ANG=PI*BETA
EX=DEXP(-ANG)
EXN=DEXP(-ANG)
HSIN=(EX-EXN)*0.500
HCOS=(EX+EXN)*0.500
CPB=HSIN**2/(PI*(HSIN*HCOS+ANG))
ANG=PI/BETA
EX=DEXP(-ANG)
EXN=DEXP(-ANG)
HSIN=(EX-EXN)*0.500
HCOS=(EX+EXN)*0.500
CPCB=HSIN**2/(PI*(HSIN*HCOS+ANG))
B2=BETA*BETA
P01=2.00/BETA**3*CPB*X(L+1)
P10=2*BETA*CPCB*X(1)
D(K)=-2*.00*B2/(1.00+B2)**2*(P01+P10-(B2+1./B2)/32.00)
PR=PRO
PRC=1-PR*PR
EP2=D(K)*PRC
WRITE(6,10)N,EP2,BETA
10 FORMAT (/,10X,'NONLINEAR PARAMETER FOR PLATE BY YAMAKIS METHOD',//
1,5X,'NUMBER OF TERMS N=',I2,5X,'EP=',D12.5,5X,'BETA=',F4.2,/)
RETURN
END

```

C
C
C
C

```

SUBROUTINE BANDGE (A,C,X,N,M)
IMPLICIT REAL*8 (A-H,O-Z)
DIMENSION A(16,16),C(16),X(16)
K=1
1 I=K+1
L=M*K
IF(L.GT.N) L=N
2 D=A(I,K)/A(K,K)
A(I,K)=0.00
J=K+1
3 A(I,J)=A(I,J)-D*A(K,J)
IF(J-L)4,5,20

```

```

4 J=J+1
GO TO 3
5 C(I)=C(I)-D*C(K)
IF(I-L)6,7,20
6 I=I+1
GO TO 2
7 IF(K=N+1)8,11,20
8 K=K+1
GO TO 1
11 LL=N-M
L=N
X(N)=C(N)/A(N,N)
I=N-1
12 IF(I.LT.LL)L=L-1
J=I+1
S=0.00
13 S=S+A(I,J)*X(J)
IF(J-L)14,15,20
14 J=J+1
GO TO 13
15 X(I)=(C(I)-S)/A(I,I)
IF(I-L)20,20,16
16 I=I-1
GO TO 12
20 RETURN
END
//GC.SYSPUNCH DO SYSOUT=6
//GO.SYSIN DO *
//

```

APPENDIX C

The following computer program generates and numerically integrates a multimode, lumped parameter model for a simply supported rectangular plate based on the Von Kármán equations. Its usage is given as a part of the listing.


```

C READ ALL THE NECESSARY COEFFICIENT MATRICES IN.
C FIRST FCOEFF
C 22 CONTINUE
DO 23 I=1,JM1
C 23 READ(5,111){FCOEFF(I,J),I,J,J=1,JM1}
C SECOND COEFF
C
C DO 24 NUV=1,4
DO 24 NPQ=1,4
DO 24 NRS=1,4
C 24 READ(5,109){COEFW(NUV,NPQ,NRS,NMN),NUV,NPQ,NRS,NMN,NMN=1,4}
GO TO 25
C 21 CONTINUE
DO 16 M=1,JL
DO 16 N=1,KL
DO 16 J=1,JL
DO 16 K=1,KL
JJ=JL*(N-1)+M
KK=JL*(K-1)+J
FF(JJ,KK)={({PA*J}*PA*J+PB*K*PB*K)**2}*C2JSQ(J,M,A)+C2JSQ(K,N,B)
1B)-({PA*J}*PA*J+PB*K*PB*K)**2}*C2JSQ(J,M,A)*0.5DO*B-({PB*K}*PB*K)**2}*C2JSQ(K,N,B)
2*0.5DO*A
C 16 CONTINUE
WRITE(6,105)
FORMAT(5X,'FF IS GIVEN BELOW')
DO 103 I=1,JM1
WRITE(6,102){FF(I,J),J=1,JM1}
C 102 FORMAT(5X,8(2X,D10.3),/,10X,8(2X,D10.3))
C 103 CONTINUE
DO 113 I=1,JM1
DO 113 J=1,JM1
C 113 FFF(I,J)=FF(I,J)
CALL MATINV(0,DET)
WRITE(6,106)
C 106 FORMAT(5X,'FF INVERSE IS GIVEN BELOW')
DO 104 I=1,JM1
WRITE(6,102){FF(I,J),J=1,JM1}
C 104 CONTINUE
CHECK ON INVERSION
DO 114 I=1,JM1
DO 114 J=1,JM1
COEF(I,J)=0.DO
DO 114 K=1,JM1
C 114 COEF(I,J)=COEF(I,J)+FF(I,K)*FFF(K,J)
WRITE(6,115)
C 115 FORMAT(2X,'IDENTITY MATRIX SHOULD BE BELOW')
DO 116 I=1,JM1
C 116 WRITE(6,102){COEF(I,J),J=1,JM1}
CONTINUE TO CALCULATE PARAMETERS
DO 17 J=1,JL
DO 17 K=1,KL
JJ=JL*(K-1)+J
DO 17 NP=1,NL,2
DO 17 NQ=1,ML,2
NPQ=(ML+1)*(NP-1)/4+((NQ+1)/2)
DC 17 NR=1,NL,2
DO 17 NS=1,ML,2
NRS=(ML+1)*(NR-1)/4+((NS+1)/2)

```

```

NPQRS=4*(NRS-1)+NPQ
COEF(JJ,NPQRS)=E*36. *(PA*NP*PA*NR*PB*NQ*PB*NS+CCSQ(NP,NR,J,A)
1*CCSQ(NQ,NS,K,B)-PA*NP*PA*NP*PB*NS*PB*NS+SSSQ(NP,NR,J,A)+SSSQ(NQ,NS,
2S,K,B))
C 17 CONTINUE
C CALCULATE FCOEFF=FF INVERSE*COEFF
C
C DO 107 I=1,JM1
DO 107 NPQRS=1,JM1
FCOEFF(I,NPQRS)=0.DO
DO 107 K=1,JM1
C 107 FCOEFF(I,NPQRS)=FF(I,K)*COEF(K,NPQRS)+FCOEFF(I,NPQRS)
C
DO 108 NU=1,NL,2
DO 108 NV=1,ML,2
NUV=NU-1+((NV+1)/2)
DO 108 M=1,ML,2
DC 108 N=1,NL,2
NMN=M-1+((N+1)/2)
DO 108 J=1,NP2
LEFT=(J-1)/NP1
NRS=LEFT+1
NPQ=J-NP1*LEFT
COEFW(NUV,NPQ,NRS,NMN)=0.DO
DO 108 I=1,JM1
LEFT=(I-1)/JL
KK=LEFT+1
JJ=I-JL*LEFT
C 108 CCOEFW(NUV,NPQ,NRS,NMN)=COEFW(NUV,NPQ,NRS,NMN)+FCOEFF(I,J)*(KK*KK*
1M**M*SSSQ(M,NU,JJ,A)*CSS(KK,N,NV,B)+JJ*JJ*N*N*CSS(JJ,M,NU,A)*
2SSSQ(NV,KK,B)+JJ*KK*M*N*SCS(M,NU,JJ,A)*SCS(N,NV,KK,B))*BRAT
DO 112 I=1,JM1
WRITE(7,111){FCOEFF(I,J),I,J,J=1,JM1}
WRITE(6,111){FCOEFF(I,J),I,J,J=1,JM1}
C 111 FORMAT(4(1X,D15.8,2I2))
C 112 CONTINUE
DO 110 NUV=1,NP1
DO 110 NPQ=1,NP1
DO 110 NRS=1,NP1
WRITE(6,109){COEFW(NUV,NPQ,NRS,NMN),NUV,NPQ,NRS,NMN,NMN=1,4}
WRITE(7,109){COEFW(NUV,NPQ,NRS,NMN),NUV,NPQ,NRS,NMN,NMN=1,4}
C 109 FORMAT(4(1X,D15.8,4I1))
C 110 CONTINUE
C 25 CONTINUE
PB=3.1416*PB
PA=PA*3.1416
C SET UP PARAMETERS FOR STRESS CALCULATIONS
BEND=E*H*0.5*3.1416*3.1416/((1-PR*PR)*12.)
DO 7 I=1,NSTRAN
X1=XX(I)
Y1=YY(I)
DO 19 M=1,ML,2
DO 19 N=1,NL,2
DS=DS IN(M*PA*X1)*DS IN(N*PB*Y1)
SIGXB(I,M,N)=BEND*((M/A)*(M/A)+PR*(N/B)*(N/B))*DS
SIGYB(I,M,N)=BEND*((M/A)*(M/A)+PR*(N/B)*(N/B))*DS
C 19 CONTINUE
DO 20 J=1,JL

```

```

      DG 20 K=1,KL
      SIGXM(I,J,K)=2.*PB*PB**K*(DSIN(I*PA*X1)**2)*DCOS(2.*PB*K*Y1)
      SIGYM(I,J,K)=2.*PA*PA*J*(DSIN(K*PB*Y1)**2)*DCOS(2.*PA*J*X1)
20  CONTINUE
7   CONTINUE
121 CONTINUE
C   PARAMETERS NEEDED FOR DHPG
      PRMT(1)=0.DO
      PRMT(2)=(ND-1)*DT
      PRMT(4)=0.001DO
      PRMT(5)=0.DO
C   SET UP INITIAL CONDITIONS
      NDIM=2*NP1
      DO 18 I=1,NDIM
        Y(I)=0.DO
18  DERY(I)=1.DO/NDIM
C   WRITE OUT INPUT DATA
      WRITE(6,*)A,B,H,E,PR,RO,Z
4   FORMAT(1H1,10X,'INPUT DATA FOR PLATE',//,5X,'A=',D12.5,2X,'B=',
        D12.5,2X,'H=',D12.5,/,5X,'E=',D12.5,1X,'PR=',D12.5,1X,'RO=',
        D12.5,2X,'Z=',D12.5,/)
      WRITE(6,5)EM1
5   FORMAT(5X,'EFFECTIVE MASS OF PLATE=',D12.5)
      WRITE(6,12)I1,XX(I1,YY(I1),I=1,NSTRAN)
12  FORMAT(5X,'STRESSES AND STRAINS ARE COMPUTED AT THE FOLLOWING LOC
        IATIONS',/2(15X,11,D12.5,2X,D12.5,/)
      WRITE(6,8)DT,PRMT(3),TFRING,NSTRAN,PSCALE
8   FORMAT(5X,'OTHER INPUT DATA',//,5X,'DT=',D12.5,2X,'PRMT(3)='
        ,D12.5,2X,'TFRING=',D12.5,/,5X,'NSTRAIN=',12,5X,'PRESSURE SCALE
        2FACTR=',D12.5,/,/,5X,'INPUT PRESSURE DATA',//,5X,'I',9X,'P(I)'
        ,/)
      WRITE(6,9)(I,P(I),I=1,ND)
9   FORMAT(1X,15,5X,D12.5)
      WRITE(6,11)NL,ML,JL,KL
11  FORMAT(2X,'LARGEST MODE CONSIDERED',//,5X,'DEFLECT ION=',12,
        1,'',12,/,5X,'STRESS',12,'',12)
      WRITE(6,10)
10  FORMAT(1H1,5X,'OUTPUT DATA',//,7X,'TIME',6X,'DEFLECT ION',6X,
        1,'EPSUMX',7X,'EPSUMY',/)
      CALL DHPG(PRMT,Y,DERY,NDIM,IHLF,FCT,OUTP,AUX)
12C CONTINUE
      STCP
      END
C
C
C
      SUBROUTINE OUTP(X,Y,DERY,IHLF,NDIM,PRMT)
      IMPLICIT REAL*8(A-H,O-Z)
      DIMENSION AUX(16,8),DERY(8),Y(8),PRMT(5)
      COMMON COEFF(4,4,4,4),
1     SIGXB(2,3,3),SIGYB(2,3,3),SIGXM(2,16,16),
2     SIGYM(2,16,16),FF(16,16),FFF(16,16),
        *FCOEFF(16,16),COEF(16,16),
3     FWW(3,3),AEFF(3,3),FFW(16),FWW(4),P(100),XX(3),YY(3),FW(16)
      PR,E,DT,BRAT,NRL,NL,ML,JML,NC,NMULT,JL,KL,NPL,NPZ,NSTRAN
C   OUTPUT ONLY AT MULTIPLES OF PRMT(3)
      IF(X.LT.NC*NMULT*PRMT(3)) RETURN
      NC=NC+1

```

```

C   COMPUTE CENTER DEFLECTION
C
C   CHECK IF ONLY SINGLE MODE MODEL IS TO BE USED
C
      IF(ML-1)5,6,5
6   CONTINUE
      FW(1)=Y(1)
C   FOLLOWING THREE CARDS ONLY FOR USING SAME FORMAT
      Y(3)=0.DO
      Y(5)=0.DO
      Y(7)=0.DO
      W(1,1)=Y(1)
      Y2=12.DO*Y(1)
      GO TO 7
5   CONTINUE
      Y2=12.*(Y(1)-Y(3)-Y(5)+Y(7))
      FW(1)=Y(1)
      FW(2)=Y(3)
      FW(3)=Y(5)
      FW(4)=Y(7)
      W(1,1)=Y(1)
      W(1,3)=Y(3)
      W(3,1)=Y(5)
      W(3,3)=Y(7)
7   CONTINUE
C   COMPUTE STRESSES AND STRAINS
C   GENERATE STRESS FUNCTION ELEMENTS.
C
      DO 9 I=1,JM1
        LEFT=(I-1)/JL
        KK=LEFT+1
        JJ=I-JL*LEFT
        FFF(JJ,KK)=0.DO
      DO 9 J=1,JM1
        LEFT=(J-1)/NP1
        NRS=LEFT+1
        NPQ=J-NP1*LEFT
9     FFF(JJ,KK)=FFF(JJ,KK)+FCUEFF(I,J)*FW(NPQ)*FW(NRS)
      DG 1 I=1,NSTRAN
      SXB=0.DO
      SYB=0.DO
      DO 2 M=1,NL,2
      DO 2 N=1,NL,2
        SXB=SXB+SIGXB(I,M,N)*W(M,N)
        SYB=SYB+SIGYB(I,M,N)*W(M,N)
2   CONTINUE
      SXM=0.DO
      SYM=0.DO
      DO 8 J=1,JL
      DO 8 K=1,KL
        SXM=SXM+SIGXM(I,J,K)*FFF(J,K)
        SYM=SYM+SIGYM(I,J,K)*FFF(J,K)
8   CONTINUE
      SXM=SXM/144.DO
      SYM=SYM/144.DO
      EPXB=(SXB-PR*SXB)/E
      EPYB=(SYB-PR*SXB)/E
      EPXM=(SXM-PR*SYM)/E
      EPYM=(SYM-PR*SXM)/E

```

```

EPSUMX=EPXB*EPXM
EPSUMY=EPYB*EPMY
WRITE(7,4)X,EPXB,EPXM,EPYB,EPMY,Y2,I
4  FORMAT(6F13.7,I2)
WRITE(6,3)X,Y2,EPSUMX,EPSUMY
3  FORMAT(1X,4(2X,D11.4))
WRITE(6,10)Y(1),Y(3),Y(5),Y(7),SXB,SYB,SXM,SYM
10  FORMAT(10X,8(2X,D11.4),/)
1  CCNTINUE
IF(X.GE.PRMT(2)) PRMT(5)=1.
RETURN
END

C
C
C
C
C
SUBROUTINE FCT(X,Y,DERY)
IMPLICIT REAL*8(A-H,O-Z)
DIMENSION AUX(16,8),DERY(8),Y(8),PRMT(5)
COMMON COEFW(4,4,4,4),
1 SIGXB(2,3,3),SIGYB(2,3,3),SIGXM(2,16,16),
1 SIGYM(2,16,16),FF(16,16),FFF(16,16),
* FCOEFF(16,16), COEF(16,16),
2 FWW(3,3),AEFF(3,3), FFW(16), FWWW(4), P(100),XX(3),YY(3),FW(16)
3,PR,E ,DT,BRAT ,NRI,NL,ML,JMI ,NC,NMULT,JL,KL,NPI ,NPZ
DEFINITIONS Y(1)=W(1,1) ITS DERIVATIVE=Y(2)
Y(3)=W(1,3) ITS DERIVATIVE=Y(4)
Y(5)=W(3,1) ITS DERIVATIVE=Y(6)
Y(7)=W(3,3) ITS DERIVATIVE=Y(8)
CALCULATE PRESSURE BY LINEAR INTERPGLATION
IP=X/DT+1
FR=X/DT-IP+1
PRESS=P(IP)+FR*(P(IP+1)-P(IP))
CHECK IF ONLY SINGLE MODE MODEL IS TO BE USED
IF(ML-1)1,2,1
1  CCNTINUE
DERY(1)=Y(2)
DERY(3)=Y(4)
DERY(5)=Y(6)
DERY(7)=Y(8)
FW(1)=Y(1)
FW(2)=Y(3)
FW(3)=Y(5)
FW(4)=Y(7)
C
GENERATE NONLINEAR TERMS FOR THE DIFF EQUATIONS
DO 30 I=1,NP1
FWW(I)=0.00
DO 30 J=1,NP1
DO 30 K=1,NP1
DO 30 L=1,NP1
30  FWWW(I)=FWWW(I)+COEFW(I,J,K,L)*FW(K)*FW(J)*FW(L)
DERY(2)=AEFF(1,1)*PRESS-WNA(1,1)*Y(1)+FWWW(1)
DERY(4)=AEFF(1,3)*PRESS-WNA(1,3)*Y(3)+FWWW(2)
DERY(6)=AEFF(3,1)*PRESS-WNA(3,1)*Y(5)+FWWW(3)
DERY(8)=AEFF(3,3)*PRESS-WNA(3,3)*Y(7)+FWWW(4)
GO TO 3

```

```

2  DERY(1)=Y(2)
DERY(2)=AEFF(1,1)*PRESS-WNA(1,1)*Y(1)+COEFW(1,1,1,1)*Y(1)*Y(1)
1*Y(1)
3  CCNTINUE
RETURN
END

```

C
C
C
C

```

FUNCTION SCS(M,N,J,AB)
J2=2*J
IF (M-N)1,2,1
1  IF((M-N).NE.J2.AND.(M-N).NE.J2.AND.(N-M).NE.J2) GO TO 3
IF((M-N).EQ.J2) GO TO 5
4  SCS=AB*0.2500
RETURN
5  SCS=-0.2500*AB
RETURN
2  IF(M-J)3,4,3
3  SCS=0.000
RETURN
END

```

C
C
C

```

FUNCTION C2JSQ(L,J,L,AB)
IMPLICIT REAL*8(A-H,O-Z)
IF(J-L)1,2,1
1  C2JSQ=0.00
RETURN
2  C2JSQ=-AB*0.2500
RETURN
END

```

C
C
C

```

FUNCTION CCSQ(M,N,J,AB)
IMPLICIT REAL*8(A-H,O-Z)
J2=2*J
IF(M-N)1,2,1
1  IF((M-N).NE.J2.AND.(M-N).NE.J2.AND.(N-M).NE.J2) GO TO 3
CCSQ=-0.12500*AB
RETURN
2  IF(M.NE.J) GC TC 4
CCSQ=0.12500*AB
RETURN
4  CCSQ=0.2500*AB
RETURN
3  CCSQ=0.00
RETURN
END

```

C
C
C

```

FUNCTION SSSQ(M,N,J,AB)
IMPLICIT REAL*8(A-H,O-Z)
J2=2*J
IF(M-N)1,2,1

```



```

A(ICCL,ICOL)=1.
DO 205 L=1,N
205 A(ICOL,L)=A(ICOL,L)/PIVOT(I)
   IF(M) 347,347,66
   DO 52 L=1,M
   52 B(ICOL,L)=B(ICOL,L)/PIVOT(I)
C FOLLOWING 10 STATEMENTS TO REDUCE NON-PIVOT ROWS
347 DO 135 LI=1,N
   IF(LI-ICOL) 21,135,21
   21 T=A(LI,ICOL)
   A(LI,ICOL)=0.
   DO 89 L=1,N
   89 A(LI,L)=A(LI,L)-A(ICOL,L)*T
   IF(M) 135,135,18
   18 DO 68 L=1,M
   68 B(LI,L)=B(LI,L)-B(ICOL,L)*T
135 CONTINUE
C FOLLOWING 11 STATEMENTS TO INTERCHANGE COLUMNS
222 DO 3 I=1,N
   L=N-I+1
   IF (INDEX(L,1)-INDEX(L,2)) 19,3,19
   19 JROW=INDEX(L,1)
   JCCL=INDEX(L,2)
   DO 549 K=1,N
   T=A(K,JROW)
   A(K,JROW)=A(K,JCCL)
   A(K,JCCL)=T
549 CONTINUE
3 CONTINUE
E1 RETURN
END
//GC.SYSPUNCH DD SYSOUT=B
//GO.SYSIN DD *
//

```


VITA }
}

Ganesh Rajagopal

Candidate for the Degree of

Doctor of Philosophy

Thesis: THE NONLINEAR TRANSIENT RESPONSE OF THIN
RECTANGULAR PLATES

Major Field: Mechanical Engineering

Biographical:

Personal Data: Born September 10, 1943, in Madras, India,
the son of T. N. Rajagopalan and Janaki.

Education: Graduated from the Lawrence School, Lovedale,
India, in 1958; received the degree of Bachelor of
Technology in Mechanical Engineering from the Indian
Institute of Technology, Madras, India, in July, 1964;
received the Master of Engineering degree in Mechanical
Engineering from the Indian Institute of Science,
Bangalore, India, in August 1966; completed the require-
ments for the degree of Doctor of Philosophy from
Oklahoma State University in July 1972.

Professional Experience: Lecturer in Mechanical Engineering
at the Indian Institute of Science, Bangalore, India, from
August, 1966 to July, 1969; Graduate Research and
Teaching Assistant at Oklahoma State University from
September, 1969 to May, 1972.